EXAMINING THE SOURCES AND TRANSPORT OF REACTIVE NITROGEN EMISSIONS USING STABLE ISOTOPES TECHNIQUES

by

Joseph David Felix

Bachelor of Science, Indiana University of Pennsylvania, 2004

Master of Science, University of North Carolina Wilmington, 2008

Submitted to the Graduate Faculty of the

Kenneth P. Dietrich School of Arts and Sciences in partial fulfillment

of the requirements for the degree of

Doctor of Philosophy in Geology and Planetary Science

University of Pittsburgh

2012

UNIVERSITY OF PITTSBURGH

KENNETH P. DIETRICH OF ARTS AND SCIENCES

This dissertation was presented

by

Joseph David Felix

It was defended on

November 20, 2012

and approved by

Emily Elliott, PhD, Assistant Professor

Daniel Bain, PhD, Assistant Professor

Mark Abbott, PhD, Associate Professor

Brian Stewart, PhD, Associate Professor

Peter Adams, PhD, Associate Professor

Dissertation Advisor: Emily Elliott, PhD, Assistant Professor

EXAMINING THE SOURCES AND TRANSPORT OF REACTIVE NITROGEN EMISSIONS USING STABLE ISOTOPES TECHNIQUES

Joseph David Felix, PhD

University of Pittsburgh, 2012

Reactive nitrogen (Nr) emissions (i.e., NO_x, HNO_3, and NH_3) from the transportation and electricity-generating sectors are declining due to increasingly stringent air quality regulations and development of new emission reduction technologies. In comparison, Nr emissions from the agricultural sector are increasing and are largely unregulated in the US. Identifying Nr emission sources and quantifying Nr source contributions are important initial steps for reducing nitrogen inputs to the environment and have become of particular concern to air quality managers, modelers, and epidemiologists.

Stable isotope techniques are an emerging tool used to aid in the quantification of Nr emission sources and transport. This work presents a comprehensive inventory of the isotopic compositions of reactive Nr sources. The inventory reveals distinct differences between the isotopic compositions of fossil fuel and agricultural Nr emission sources. Equipped with these isotopic signatures of Nr sources, the isotopic ratios of ambient Nr were used to trace the transport and deposition of emissions across landscapes including dairy farms, a concentrated animal feeding operation, tallgrass prairies, conventionally managed cornfields, barrier island dunes, and urban systems. The isotopic composition of ambient Nr was used in conjunction with source signatures and isotope mixing models to quantify source contributions to ambient Nr concentrations.

After assessing the effectiveness of using isotopic ratios to trace Nr emissions across landscapes, investigations were scaled up to examine Nr regional transport. In collaboration with the National Atmospheric Deposition Program's Ammonia Monitoring Network, monthly NH_3 emission were collected at nine sites across the U.S and analyzed for isotopic composition. Resulting NH_3 isotopic composition showed spatial and temporal trends associated with primary regional NH_3 sources. To further investigate regional transport of Nr emissions, nitrate isotopes in a Greenland ice core were examined to infer long-term relationships between agricultural activities, soil NO_x emissions, and subsequent regional transport and deposition. Results of this investigation demonstrate that nitrate isotopes in ice cores, coupled with newly constrained isotopic compositions of NO_x emission sources, provide a novel means for estimating contemporary and historic contributions from individual NO_x emission sources to deposition.

TABLE OF CONTENTS

LIST OF TABLES

LIST OF FIGURES

PREFACE

This work was primarily funded by the United States Department of Agriculture's Agriculture and Food Research Initiative (Grant #05-13204-6800-00000-404178). It was also partially funded by the Electric Power Research Institute and the Geological Society of America.

This work would not have been possible without the aid of many generous collaborators and Ammonia monitoring network (AMoN) site operators. This includes Timothy Gish (USDA), Laura McConnell (USDA), John Briggs (KSU),Ronaldo Maghirang (KSU), Gary Lear (US EPA), David Gay (NADP), Stephanie Shaw (EPRI), Jane Clougherty (Pitt) and Leah Cambell (Pitt), AMoN: Matt Nowak, Amy Robinson, Fred Diver, Gary Conley, Kevin Crist, Brent Auvermann, Sarah Dawsey, John Walker, Wayne Robarge, Heather Cravens, and April Hathcoat.

I would like to acknowledge all those at the University of Pittsburgh who helped with laboratory work, field work, and data interpretation. This includes John Cala, Katie Tuitie, Mollie Kish, Marion Divers, Lucy Rose, and Dan Bain. Thanks to Katie Redling for performing isotope analysis and corrections of a majority of my samples.

Thanks to my committee members for all of their comments and guidance. A special thanks to my advisor, Emily Elliott, who shared her knowledge and experience and helped me grow as a scientist. Finally, thanks to my family for supporting me through my time in graduate school.

1.0 INTRODUCTION

Nitrogen is essential for life, but the majority of N in the biosphere is present as N_2 (78% of the air by volume) which is unusable by plants and animals. Natural processes including bacterial metabolism, lightning, and biomass burning, fix N_2 to reactive nitrogen (Nr) (e.g. NO_y, NH_x) forms that can be used by plants and animals. Before the industrial revolution, these natural processes controlled the amount of Nr reaching the environment. The industrial revolution increased fossil fuel combustion (via industry and the internal combustion engine) which produces Nr emissions. The industrial revolution also brought a higher standard of living and increased the rate of population growth. This brought an increased food demand which could only be met by increasing N fertilizer for crops. The amount of Nr produced by natural processes and fossil fuel combustion even when combined with that found in Peruvian guano and Chilean saltpeter reserves could not provide enough N fertilizer to meet the demands of a growing global population. The lack of N fertilizer prompted the invention of the Haber-Bosch process in which N_2 from the air (an effectively unlimited N resource) is reacted with H_2 over a catalyst to form NH_3. This process provided ample amounts of commercially produced N fertilizer to feed a population that grew from 1.6 to 6 billion people in the 20^{th} century [*Townsend et al.,* 2010]. 40% of that population is estimated to be dependent on commercial fertilizer [*Smil,* 2001].

While advances in industry and production of fertilizer have increased the world's population and standard of living, Nr inputs coinciding with these advancements have caused global anthropogenic Nr inputs to double natural inputs with U.S. anthropogenic Nr inputs being 4X that of natural inputs [*Galloway et al.,* 2004; *Davidson et al.,* 2012]. The excess Nr inputs include NO_x and NH_3 emissions that have increased by a factor of five since the industrial revolution [*Galloway et al.,* 2004]. These Nr emissions and subsequent deposition lead to harmful impacts to the environment, such as water and air quality degradation, soil acidity, acid rain, lacustrine and estuarine eutrophication, and decreased biodiversity. Nr emissions are also detrimental to human health. NO_x aids in the formation of tropospheric ozone which causes respiratory problems, and NH_3 reacts with SO_2 and NO_x to form fine particulate matter (PM) which is associated with respiratory and cardiovascular disease [*Pope and Dockery,* 2006]. The EPA estimates $PM_{2.5}$ caused 130,000 premature deaths in 2005. These adverse effects on ecosystem and human health have caused policy-makers to enact air quality regulations.

In many developed countries actions have been taken to reduce NO_x emissions (e.g. low-NO_x burners and selective catalytic reduction in power plants, and three way catalytic converters in vehicles) but NH_3 emissions have less stringent regulations and are generally unregulated in the U.S. [*Davidson et al.,* 2012]. U.S. NO_2 concentrations decreased ~40% from 1980 to 2006, but NH_3 emissions have continued to increase and are expected to constitute 60% of the N in atmospheric deposition [*Davidson et al.,* 2012]. While developed countries are regulating NO_x emissions, developing countries often have unregulated fossil fuel combustion. For example, from 2006 to 2009, NO_2 concentrations in East Asia increased 18.8% [*Lasmal et al.,* 2011]. This rapid increase is of concern given that developing countries will continue to expand thus increasing energy and food demands that are directly proportional to Nr demand and emissions.

Concerns regarding globally increasing Nr emissions and associated negative impacts on ecosystem and human health have prompted air quality scientists, ecologists, policy-makers, and epidemiologists to attempt to quantify Nr emission sources and transport as an initial step for developing Nr mitigation techniques. This is a challenging task as N has numerous valence states, allowing for varying chemical reactions and associated Nr products; this is confounded by long atmospheric lifetimes of some Nr species and subsequent transport over long distances [*Schlesinger et al.,* 2009].

The work presented here aims to apply isotope techniques to aid in the quantification of the sources and transport of Nr emissions, specifically NO_x and NH_3. The nitrogen isotopic ratios ($\delta^{15}N$) of Nr emissions are unique to emission sources but reports of the isotopic ratios of these sources are limited. Advances in the isotopic analysis techniques of Nr have allowed for an order of magnitude decrease in sample mass required for isotopic analysis. For example, results presented here, utilized 10-20 nanomole quantities of nitrate for isotopic analysis. This minute mass requirement allowed use of inexpensive passive samplers to collect low concentration gaseous Nr from individual emission sources and ambient samples across a range of land use settings. Equipped with these sampling techniques and advances in isotope analysis, we then set out to conduct the most comprehensive inventory of the isotopic compositions of NO_x and NH_3 sources to date. NO_x emissions were sampled from vehicles, power plants, fertilized soils, and various livestock waste sources (Chapter 5). NH_3 emissions were sampled from vehicles, power plants, volatilized fertilizer, marine aerosol, and various volatilized livestock waste sources (Chapter 2). Armed with NO_x and NH_3 source isotopic signatures, we then used isotopic ratios of ambient Nr to trace the transport and deposition of emissions across

landscapes including dairy farms, concentrated animal feeding operation, tallgrass prairies, conventionally managed cornfields, barrier island dunes, and urban systems (Chapters 3 and 6).

After assessing the effectiveness of using isotopic ratios to trace Nr emissions across these local scales, we scaled up our investigations to examine Nr transport at regional scales. We collaborated with the National Atmospheric Deposition Program's Ammonia Monitoring Network to sample NH_3 isotopic composition at nine sites across the U.S and the resulting data were used to investigate spatio-temporal trends in NH_3 sources to varying regions of the U.S. (Chapter 4). To further investigate regional transport of Nr emissions, nitrate isotopes in a Greenland ice core were examined to infer long-term relationships between agricultural activities, soil NO_x emissions, and subsequent regional transport and deposition (Chapter 7).

2.0 CONSTRAINING THE ISOTOPIC COMPOSITION OF AMMONIA EMISSIONS USING A NEW METHOD FOR ISOTOPIC ANALYSIS OF LOW CONCENTRATION SAMPLES

2.1 INTRODUCTION

Ammonia (NH_3) emissions in the form of wet and dry atmospheric deposition are a substantial source of nitrogen pollution to sensitive terrestrial, aquatic, and marine ecosystems [*Walker et al.*, 2000; *Chimka et al.*, 1997; *Fowler et al.*, 1998; *Davidson et al.*, 2012]. Excess nitrogen loading to these ecosystems can lead to eutrophication (e.g., algal blooms, hypoxia) of surface waters, decrease biodiversity, and increase soil acidity [*Galloway et al.*, 2004]. NH_3 emissions are directly related to ammonium (NH_4^+) deposition. Precipitation NH_4^+ concentrations have increased at 90% of monitoring sites in the U.S. from 1985 to 2002 (National Trends Network, National Atmospheric Deposition Program (NADP)), while increases exceeded 50% over a large area of the Central U.S. [*Lehmann et al.*, 2005]. Consequently, NH_3 emissions and resulting deposition have become of particular concern to air quality managers, modelers, and epidemiologists.

Pinpointing NH_3 emission sources and quantifying NH_3 contributions from individual sources is important for management strategies designed to reduce adverse impacts from NH_3 emissions. Global NH_3 emissions are dominated by agricultural activities (livestock operations and fertilizer applications). For example, in 2008, it is estimated that agricultural sources contributed 80% of NH_3 emissions in the U.S. In contrast, NH_3 emissions produced as a byproduct of technologies used to reduce NO_x emissions from fossil fuel combustion (i.e., in vehicle engines and in electricity generation in power plants) accounted for less than 10% of the nation's NH_3 emissions [*Davidson et al.,* 2012]. Although the primary source of NH_3 is from agriculture, fossil-fuel combustion can be a major NH_3 emission source in urban areas [*Kirchner et al.,* 2005]. NH_3 is emitted from vehicles equipped with three-way catalytic converters (TWC) during reduction of NO to reduce NO_x emissions [*Matsumoto et al.,* 2006]. NH_3 emissions from road traffic have increased with increased implementation of TWCs in the 1980's. By 2000, ~95% of vehicles in the U.S. were equipped with TWCs [*Cape et al.,* 2004]. NH_3 concentrations along heavily trafficked roadways have been reported to be 3 to 5 times higher than background NH_3 concentrations [*Matsumoto et al.,* 2006; *Kean et al.,* 2000; *Perrino et al.,* 2002] and NH_3 concentrations near roadways decrease by 90% within 10m from the roadway [*Cape et al.,* 2004]. NH_3 is also emitted from electrical generating units equipped with selective catalytic reduction (SCR) and selective non-catalytic (SNCR) NO_x reduction technologies. The SCR process injects ammonia (NH_3) into the power plant flue gas stream where the gas is passed over a catalyst (V_2O_5) in the presence of oxygen. NO_x and NH_3 react to form N_2 and water vapor.

$$4NO + 4NH_3 + O_2 \rightarrow 4N_2 + 6H_2O \qquad (1)$$

If the entire NH_3 reagent doesn't react this can lead to 'NH_3 slip' in the plant emissions. NH_3 in the emissions can also be present as 'fuel NH_3' formed from the combustion of the N in fossil fuel. However, the magnitude of this source is uncertain [*Bouwman et al.,* 1997]. Other non-agricultural sources of NH_3 emissions include oceans, human waste, soils, and vegetation [*Galloway et al.,* 2004]. These NH_3 sources are difficult to quantify due to their broad spatial distribution and general lack of NH_3 emission data [*Roadman et al.,* 2003]. Dependable quantification of NH_3 sources is of growing importance due to the observed increases in NH_4^+ deposition rates.

The stable isotopic composition of NH_3 ($\delta^{15}N$-NH_3) can aid in the quantification of NH_3 sources. NH_3 emitted from the most prevalent source, livestock waste, is reported to yield negative values from livestock barns (-37 ‰ to -9‰) [*Freyer,* 1978*; Heaton,* 1987*; Hristov et al.,* 2009] and laboratory incubations of liquid manure (-43‰ to -37‰) [*Schulz et al.,* 2001]. During NH_3 volatilization, the lighter ^{14}N atom more readily volatilizes causing low $\delta^{15}N$ values in the emitted NH_3. In comparison, reported $\delta^{15}N$-NH_3 values of NH_3 emitted from coal combustion (-7‰ to +2‰) [*Freyer,* 1978] are considerably higher than those from livestock emissions. Together, these studies suggest that the isotopic composition of NH_3 from major emissions sources may be helpful in source apportionment studies. However, to use this approach, a comprehensive characterization of isotopic compositions associated with various NH_3 sources is required; this task is complicated by the challenge of analyzing isotopic compositions of NH_3 sources, particularly those with low concentrations. In the present study, we: 1) develop a method for the isotopic analysis of low concentration NH_4^+ samples, and 2) report a comprehensive $\delta^{15}N$-NH_3 inventory of agricultural and fossil fuel based NH_3 sources.

2.2 METHODS

2.2.1 NH_3 emission collection methods for concentration and isotope analysis

Passive samplers are ideal for the collection of dry nitrogen deposition they are less expensive than active samplers, easy to use, and do not require electricity [*Pulchalski et al.,* 2011; *Elliott et al.,* 2009; *Golden et al.,* 2008]. These advantages allow for multiple deployments at a single site. Passive samplers, either Ogawa or Adapted Low-Cost Passive High Absorption (ALPHA), have been used in previous studies to collect NH_3 emissions and monitor NH_3 concentrations [*Rogers et al.,* 2009; *Sather et al.,* 2008; *Siefert et al.,* 2004; *Tang et al.,* 2001; *Cape et al.,* 2004; *Sutton et al.,* 2004; *Skinner et al., 2004 and 2006*] The Ogawa is a double-sided passive diffuse sampler equipped with a diffusive end cap, followed by a stainless steel screen, and a 14mm quartz filter impregnated with phosphorous acid. The ALPHA is a circular polyethylene vial (26 mm height, 27 mm diameter) with one open end. The vial contains a position for a 25mm phosphorous acid impregnated filter and PTFE membrane for gaseous NH_3 diffusion [*Tang et al.,* 2009].

Here, the Ogawa passive sampler was only used at a small dairy operation field site. The sampling surface was smaller than that of the ALPHA sampler, and thus minimized the amount of NH_3 collected for subsequent isotope analysis. Also, when compared to a reference method (annual denuder active sampling) for measuring NH_3 concentrations, the ALPHA samplers had the lower median percent difference (-2.4) relative to a reference method when compared to Ogawa (-37%) [*Pulchalski et al.,* 2011] while duplicate ALPHA and Ogawa samplers had a precisions of 7 and 6%, respectively [*Pulchalski et al.,* 2011].

During this study, ALPHA blanks in a sealed mason jar traveled with the deployed

ALPHA samplers and were later analyzed for [NH_3] to allow for a "blank correction". ALPHA samplers are used by a national NH_3 monitoring network in the United Kingdom where the monthly sampling detection limit is reported as 0.02 μg/m^3 (UK National Ammonia Monitoring Network). In addition to the use of passive sampling, for collection of NH_3 emissions from a coal-fired power plant, we used a modified EPA Method 7 [*EPA method 7; Felix et al.*, 2012] in which a phosphorous acid absorbing solution was used instead of a H_2SO_4/H_2O_2 solution.

2.2.2 NH_3 concentration analysis method

After collection on the passive sampler filters, NH_3 was eluted with Milli-Q water and analyzed as NH_4^+ using the phenolate method [*Eaton et al.*, 2005] and a Thermo Evolution 60S UV-vis. NH_3 air concentrations were calculated according to Ogawa or ALPHA sampler protocol [*Ogawa* 2006*, Tang et al.*, 2009].

2.2.3 Method development for nitrogen isotopic analysis of low [NH_4^+] samples

One drawback to using passive samplers is that N collected is often insufficient for conventional isotope analysis, generally requiring greater than 3.5μmol N. To resolve this problem, we developed a new method for δ^{15}N-NH_3 isotopic analysis that combines two existing methods (Figure 2.1). An oxidation method [*Zhang et al.*, 2007] employing a hypobromite oxidation solution was used to oxidize the NH_4^+ (diluted to 10μM NH_4^+) in the sample to nitrite (NO_2^-). After oxidation, sample pH is adjusted to between 3 and 9 using 6N HCl. 20 nmoles of sample NO_2^- is then converted to N_2O using the bacterial denitrifier *Pseudomonas aureofaciens* and introduced to an Isotope Ratio Mass Spectrometer (IRMS) [*Sigman et al.*, 2001]. The pH

adjustment is needed because the high pH created by the addition of the bromate oxidizing agent to the sample is toxic to the denitrifying bacteria. Samples were analyzed for $\delta^{15}N$ values using an Isoprime Trace Gas and Gilson GX-271 autosampler coupled with an Isoprime Continuous Flow IRMS at the University of Pittsburgh, *Regional Stable Isotope Laboratory for Earth and Environmental Research*. Values are reported in parts per thousand relative to atmospheric N_2 as follows:

$$\delta^{15}N\ (‰) = \frac{(^{15}N/^{14}N)_{sample} - (^{15}N/^{14}N)_{standard}}{(^{15}N/^{14}N)_{standard}} \times 1000 \qquad (2)$$

International reference standards USGS34, USGS32, USGS25, and USGS26 were used for data correction. All samples were analyzed using this method except the power plant NH_3 sample that also contained nitrate. For this sample, $\delta^{15}N\text{-}NO_3$ was initially analyzed using the denitrifier method. Then, sample NH_4^+ was oxidized to NO_2^- and resulting sample was analyzed for $\delta^{15}N\text{-}NO_3$ and/or $\delta^{15}N\text{-}NO_2$ using the denitrifier method. The $\delta^{15}N\text{-}NH_4$ in the sample was calculated using the mixing equation:

$$\delta^{15}N\text{-}NO_3 \text{ and/or } \delta^{15}N\text{-}NO_2 = f*\delta^{15}N\text{-}NO_3 + (1\text{-}f)*\delta^{15}N\text{-}NH_4 \qquad (3)$$

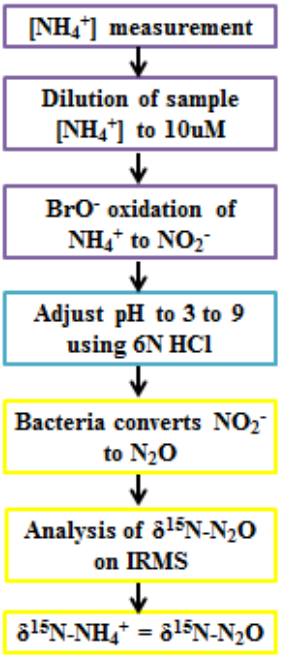

Figure 2.1: Method schematic for the isotopic analysis of NH_4.

2.2.4 NH_3 emission source sampling

Livestock waste volatilization emissions: Ogawa passive samplers were deployed inside a 150-head dairy barn in Western Pennsylvania and directly outside the barn's ventilation fans. The samplers were deployed for one month (6/28/09 to 7/28/09). Additional characterization of livestock waste occurred at the USDA ARS, Beltsville Agricultural Research Center (BARC), Beltsville, MD that manages turkey and dairy operations. ALPHA samplers were deployed in spring/summer 2010 and 2011 (5/21/10 to 6/09/10 and 6/24/11 to 7/22/11) in an open-air, 150 dairy cow barn equipped with ventilation fans. ALPHA samplers were also deployed in spring/summer 2010 and 2011 (5/21/10 to 6/09/10 and 6/24/11 to 7/22/11) in a closed room fitted with ventilation fans containing ~60 Tom turkeys. Lastly, in summer 2010 (8/6/10 to

8/21/10) ALPHA passive samplers were deployed at a concentrated animal feeding operation (CAFO) in central KS that contained 30,000 head of beef cattle in ~59 ha.

Vehicular emissions: ALPHA NH_3 samplers were deployed in the ventilation portion of a moderately trafficked tunnel (Squirrel Hill Tunnel, ~35,000 vehicles a day) in Pittsburgh, Pennsylvania (USA) to collect NH_3 emitted from a large fleet of vehicles. Samplers were deployed monthly from 4/10 to 5/10.

Coal-fired power plant emissions: Power plant emissions were sampled on January 25, 2011 from the stack of a coal-fired power plant equipped with selective-catalytic reduction technology (SCR) as part of a larger sampling effort to characterize $\delta^{15}N$ of power plant NO_x emissions [*Felix et al.,* 2012].

Urea-Ammonia-Nitrate fertilizer volatilization

Industrial fertilizer volatilization was characterized at the USDA ARS facility in Beltsville, Maryland (USA) in a conventionally managed cornfield (Field B) that is part of a larger study Optimizing Production Inputs for Economic and Environmental Enhancement (OPE3) site. Field B at OPE-3 represents traditional farming practices common in Midwestern states, mainly corn row crops with a uniform application of urea-ammonia-nitrate (UAN) commercial fertilizer [*USDA,* 2012]. In summer 2010 and 2011 (6/19/10 to 7/22/10 and 6/23/11 to 7/22/11) ALPHA passive samplers were deployed at 3 sites over Field B after 135 kg N/ha application of UAN.

Marine emissions: The National Atmospheric Deposition Program Ammonia Monitoring Network (AMoN) operates a NH_3 passive sampling site located at a coastal site in the Cape Romain National Wildlife Refuge, SC (USA). ALPHA passive samplers were deployed monthly at this site for a year (7/09 to 6/10) to collect a primarily marine NH_3 source.

2.3 RESULTS AND DISCUSSION

2.3.1 Method development for isotopic analysis of low [NH_4^+] samples

The bromate oxidation-denitrifier method developed herein is for $\delta^{15}N\text{-}NH_3$ analysis of low concentration NH_3 samples. Conversion of NH_4^+ to NO_2^- is quantitative [*Zhang et al.,* 2007] and only 20 nmol N are required for analysis. No blank is created (N_2O) from the addition of the bromate oxidizing agent or 6N HCl. For the method standard deviations of USGS standards USGS25 and USGS 26 are $\pm$0.7‰ (n= 45) (Figure 2.2). This method is less time-intensive and eliminates the use of toxic chemicals used in a prior method [*Zhang et al.,* 2007] for analysis of low concentration samples. Results presented hereafter use this method for analysis of $\delta^{15}N\text{-}NH_3$, with the exception of the power plant stack NH_3 sample.

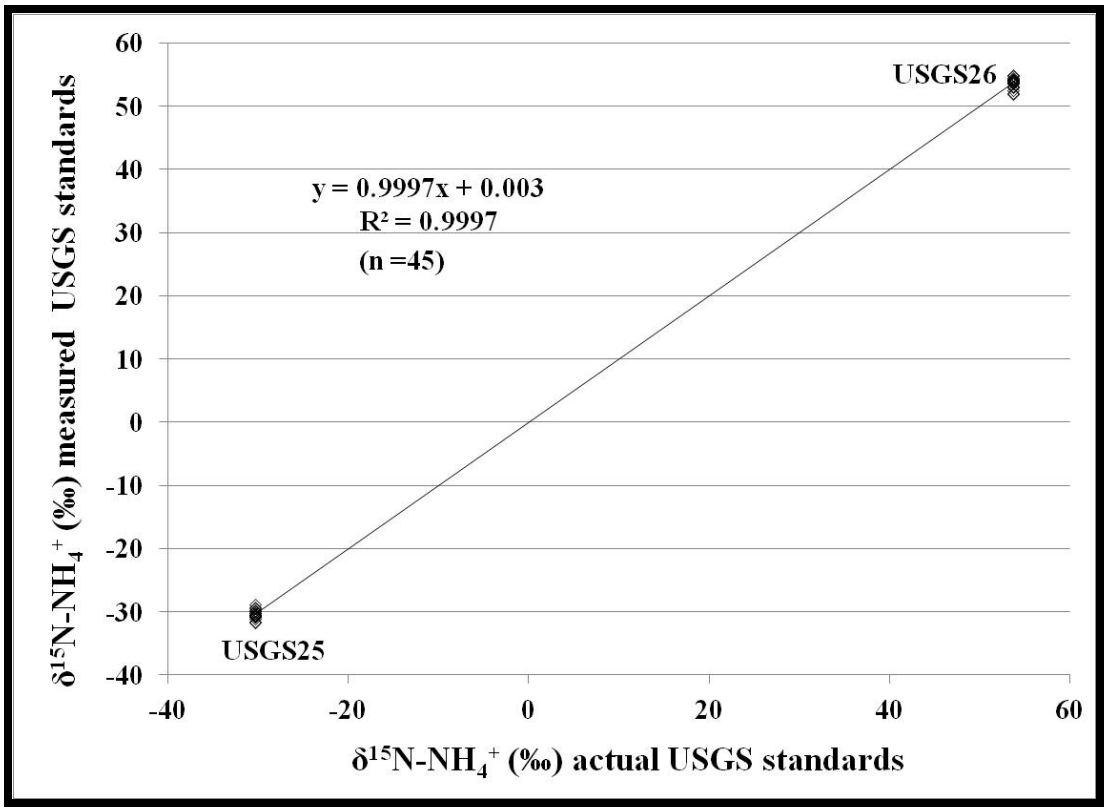

Figure 2.2: Actual vs. measured δ^{15}N-NH_4^+ values for USGS25 and 26 international standards

2.3.2 NH_3 collection for isotope analysis

Ogawa passive samplers were only used during a pilot study at the small dairy operation because the sampling surface was smaller than that of the ALPHA, and thus limited the amount of NH_3 collected for isotopic analysis. The δ^{15}N-NH_3 standard deviation among Ogawa samplers is not reported because one filter in the sampler was used for isotopic analysis and the other was used for NH_3 concentrations. ALPHA samplers were used throughout the remaining study sites wherein the average standard deviation for triplicate ALPHA samplers was ±2.9‰ and ranged from 1.5 to 4.5‰. Triplicate samplers were deployed on a single post and thus collected NH_3 at slightly varying heights and from varying directions. Thus, it is likely that

physical differences in deployment among the triplicate samplers are partially responsible for the observed ranges in triplicate samplers.

Isotope fractionation during NH_3 collection by the ALPHA sampler is expected to be minimal based on an earlier study that examined controls on ambient $\delta^{15}N\text{-}NH_3$ [*Skinner et al.,* 2004]. Fractionation during NH_3 diffusion through the ALPHA PTFE membrane is minimal as similar $\delta^{15}N\text{-}NH_3$ values are reported among diffusion tube samplers, moss bag, and shuttle samplers [*Skinner et al.,* 2006]. Further, it was determined that passive samplers do not differentially fractionate isotope ratios due to wind speed or NH_3 concentrations [*Skinner et al.,* 2006]. In a separate fumigation study, ALPHA samplers were exposed off and on for a four week period to a NH_3 fumigation source (+2.8 $\pm$ 0.5‰) [*Skinner et al., 2004*]. The $\delta^{15}N$ value of the NH_3 collected by an ALPHA sampler 1m from the source was -0.7‰. This offset of 3.5‰ was explained by the fact that the ALPHA sampler was 1m from the source and was sampling ambient NH_3 (-8 + 1.4 ‰; measured 50m upwind of NH_3 fumigation source) during the periods when the NH_3 fumigation source was turned off [*Skinner et al.,* 2004].

2.3.3 $\delta^{15}N\text{-}NH_3$ of NH_3 sources

$\delta^{15}N\text{-}NH_3$ values of livestock waste emissions collected in this study (-56 to -23‰) are similar to the range of literature $\delta^{15}N\text{-}NH_3$ values collected at livestock operations and during laboratory incubations (-43 to -9‰) [*Freyer,* 1978; *Heaton,* 1987; *Hristov et al.,* 2009; *Schulz et al.,* 2001]. This range in $\delta^{15}N$ values is a function of the initial $\delta^{15}N$ values of livestock waste, variations in the bacteria population that hydrolyze the urea in the waste releasing NH_3, as well as factors that influence kinetic fractionation rates associated with NH_3 volatilization including temperature, wind, pH, cation exchange capacity of the substrate, and moisture availability (e.g.

mitigation techniques) [*Hristov et al.,* 2011]. For instance, increasing ambient temperature in a livestock operation increases the dissociation of ammonium to ammonia [*Hristov et al.,* 2011] increasing NH_3 volatilization rates while decreasing fractionation factors. Li et al. [2012] report higher temperatures lead to less fractionation between ammonium and aqueous ammonia (e.g. 45.4‰ at 23 ^oC and 33.5‰ at 70 ^oC).

The isotopic compositions of NH_3 from volatilized fertilizer ranged from -48 to -36‰ for samples collected over the cornfield after the two 135 kg N/ha fertilizer applications. The ambient NH_3 concentrations ($[NH_3]$) increased 3 to 14 times after 135 kg N/ha fertilizer applications, and it is assumed the majority of the NH_3 being sampled was from volatilized fertilizer. During the volatilization process, fractionation occurs during air-surface (soil and vegetation) exchange of NH_3. Vegetation (via stomatal or cuticular processes) is a source or sink of NH_3 depending on atmospheric $[NH_3]$ concentration, meteorology and surface characteristics [*Walker et al.,* 2006, 2009]. This suggests that $\delta^{15}N\text{-}NH_3$ values collected over the cornfield may also be partially representing the $\delta^{15}N\text{-}NH_3$ values produced from NH_3 air-surface exchange processes. The range in $\delta^{15}N\text{-}NH_3$ values of volatilized fertilizer NH_3 overlaps the range of livestock waste values, therefore isotopic techniques do not differentiate between these two agricultural sources. This result was expected since the kinetic fractionation affecting both isotopic signatures is volatilization. Both livestock waste and fertilizer are reported to have similar starting material isotope values. Hristov et al. 2009 report cattle urine, feces and diet as having $\delta^{15}N$ values of +0.5 to +1.9‰, +2.3 to +3.0‰ and +1.1 to +4.2‰, respectively. Similarly, fertilizer has average $\delta^{15}N$ values of 0 $\pm$ 2‰ [*Bateman et al.,* 2007]; thus similar fractionation factors (30 to 60‰) [*Frank et al.,* 2004] would result in an overlapping $\delta^{15}N\text{-}NH_3$ range.

In comparison, $\delta^{15}N\text{-}NH_3$ values in vehicle exhaust (-4.6 to -2.2‰) and coal combustion (-7 to +2‰ [*Freyer,* 1978] and -11.3, -14.6‰), are higher than $\delta^{15}N\text{-}NH_3$ values observed from livestock waste or fertilizer volatilization. This difference most likely arises from different high temperature fractionation pathways. Vehicles equipped with three way catalytic converters form NH_3 as a secondary pollutant of the NO_x reduction process. Catalyst temperatures and air-to-fuel ratios are reported to be primary factors in the formation of NH_3 in vehicle exhaust [*Heeb et al.,* 2008]. NH_3 from coal combustion is due to 'fuel NH_3' or 'NH_3 slip' from NO_x reduction technology. The $\delta^{15}N\text{-}NH_3$ from coal combustion reported by Freyer 1978 (-7 to +2‰) most likely represents 'fuel NH_3' rather than 'NH_3 slip' because NH_3 was sampled from coal furnaces and factories by Freyer [1978] took place prior to the advent of SCR NO_x reduction technology. The $\delta^{15}N\text{-}NH_3$ from coal combustion reported in this study (-11.3, -14.6‰) is most likely from 'NH_3 slip' attributed to unreacted anhydrous NH_3 from the SCR unit. Anhydrous NH_3 is reported to have a $\delta^{15}N\text{-}NH_3$ value of -1 to -2‰ [*Gormly et al.,* 2009] but undergoes reaction with NO_x in the SCR unit and any 'NH_3 slip' can react with SO_3 or H_2SO_4 [*Wilburn et al., 2004*] causing further fractionation. In summary, the results of this $\delta^{15}N\text{-}NH_3$ source inventory reveal that NH_3 emitted from volatilized livestock waste and fertilizer have relatively low $\delta^{15}N$ values, allowing it to be differentiated from other sources such as vehicle exhaust emissions and coal combustion (Table 2.1, Figure 2.3).

While the marine NH_3 source is expected to be insignificant relative to major NH_3 sources, in a coastal or open ocean environment it could be significant. $\delta^{15}N\text{-}NH_3$ values from the Cape Romain coastal site ranged from -10.2 to -2.2‰ with a mean of -4.7 $\pm$ 2.7‰. This range is similar to the $\delta^{15}N\text{-}NH_4^+$ range (-8 to -5‰) of aerosols collected over the Atlantic Ocean assumed to be of marine-biogenic NH_3 origin [*Jickells et al.,* 2005]. The range in marine source

$\delta^{15}N\text{-}NH_3$ values may be due to fractionation occurring during air-sea NH_3 flux that is dependent on temperature and pH [*Jickells et al.*, 2005]. It is also important to note that the Cape Romain site $\delta^{15}N\text{-}NH_3$ values may represent a mix of terrestrial NH_3 sources and therefore may not represent solely a marine NH_3 source.

Table 2.1: $\delta^{15}N\text{-}NH_3$ of ammonia sources, source location, and sampling method

Location	Source	$\delta^{15}N\text{-}NH_3$ (‰)	N = # samples	Sample method
Poultry facility, BARC	Turkey waste	-56 , -36	2	ALPHA
Dairy barn, BARC	Cow waste	-27 , -23	2	ALPHA
Cornfield, BARC	Volatilized fertilizer	-48 to -36	6	ALPHA
Dairy barn, Western PA	Cow waste	-28, -23	2	Ogawa
Cattle CAFO, KS	Cow waste	-38	1	ALPHA
Squirrel Hill Tunnel, Pittsburgh, PA (inside tunnel)	Vehicle exhaust	-4.6, -2.2	2	ALPHA
SCR equipped coal-fired power plant, US	Power plant emissions (NH_3 slip)	-11.3, -14.6	2	EPA method 7
Cape Romain National Wildlife Refuge	Marine source	-10.2 to -2.2	7	ALPHA

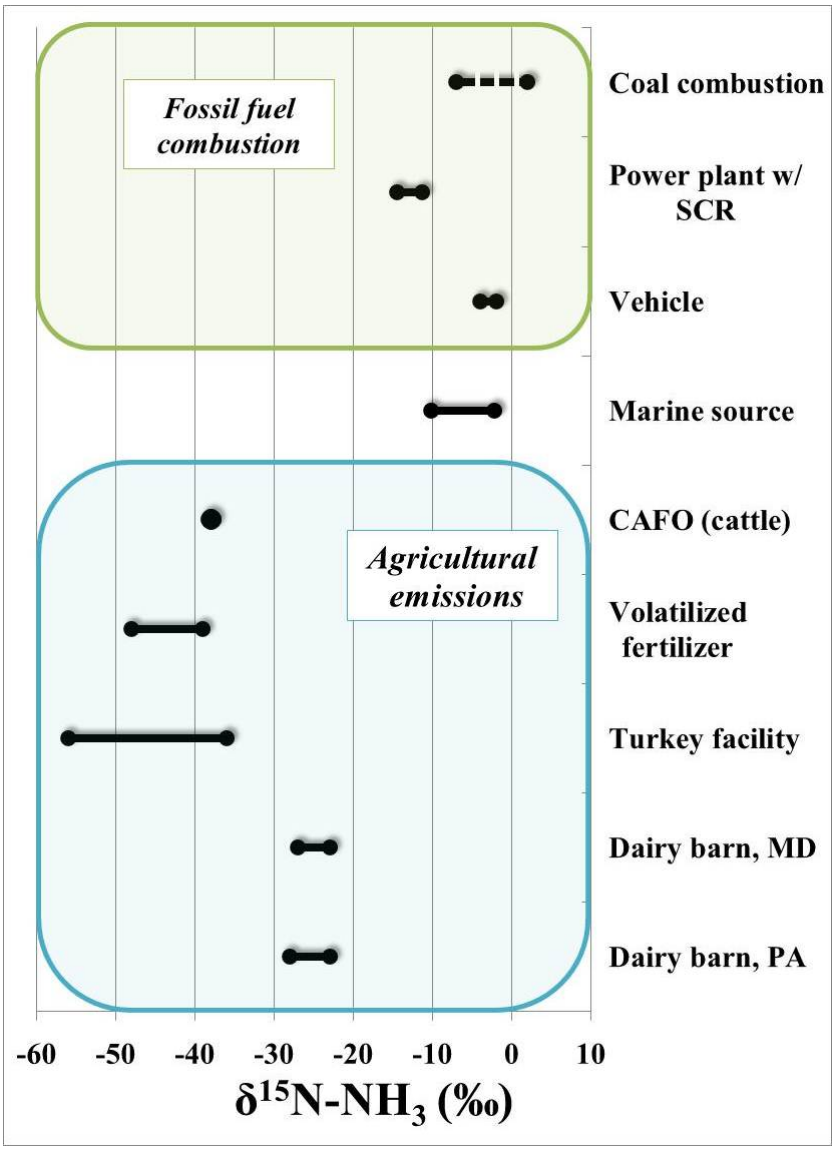

Figure 2.3: $\delta^{15}N\text{-}NH_3$ values of emissions sources from this study are solid lines and $\delta^{15}N\text{-}NH_3$ values from coal combustion from Freyer [1978] is a dotted line.

2.4 CONCLUSION

Dependable quantification of NH_3 sources is of growing importance due to recent increases in ammonium deposition (NH_4^+) rates that are directly proportional to NH_3 emissions. This work provides a new method for isotopic analysis of low concentration NH_4^+ samples that will allow for further investigation of NH_3 emissions. Using this method to analyze NH_3 emissions, a more comprehensive $\delta^{15}N$-NH_3 inventory of agricultural, fossil fuel and marine NH_3 sources has been created. The results of this $\delta^{15}N$-NH_3 source inventory reveal that NH_3 emitted from volatilized livestock waste and fertilizer have relatively low $\delta^{15}N$ values, allowing it to be differentiated from other sources such as vehicle exhaust emissions and coal combustion. The isotopic source signatures presented in this emission inventory can be used as an additional tool in sourcing NH_3 emissions and tracing their transport across localized landscapes and regions. This quantification and insight to the transport of NH_3 emissions is an important step in devising strategies to reduce future NH_3 emissions.

3.0 EXAMINING THE TRANSPORT OF AMMONIA EMISSIONS ACROSS LANDSCAPES USING NITROGEN ISOTOPE RATIOS

3.1 INTRODUCTION

Ammonia (NH_3) emissions are directly related to wet and dry atmospheric deposition of NH_3 and ammonium (NH_4^+); together these reactive N sources constitute a substantial source of nitrogen pollution to sensitive terrestrial, aquatic, and marine ecosystems [*Walker et al.,* 2000; *Chimka et. al.,* 1997; *Fowler et al.,* 1998; *Davidson et al.,* 2012]. Ammonium concentrations in wet deposition increased at 90% of National Atmospheric Deposition Program National Trends Network (NADP/NTN) sites from 1985 to 2002 [*Lehmann et al.,* 2005]. Additionally, given that NO_x (NO_x =NO + NO_2) emissions have decreased 36% since the implementation of the Clean Air Act and Amendments, and NH_3 is generally unregulated in the U.S., NH_3 is predicted to constitute 60% of total nitrogen deposition by 2020 [*Davidson et al.,* 2012]. Consequently, NH_3 emissions, transport, and depositional processes have become of increasing concern to air quality managers, modelers, and epidemiologists.

Global NH_3 emissions are dominated by agricultural activities (livestock operations and fertilizer applications). For example, in a review of NH_3 inventories reported for China, European Union, and U.S, livestock waste and fertilizer contribute between 80 and 93% of total NH_3 emissions [*Reis et al.,* 2009]. In contrast to NO_x emissions that are predominately fossil fuel based, agricultural NH_3 emissions occur in rural settings and may be deposited in more nitrogen (N) sensitive ecosystems. Excess N loading to sensitive ecosystems can lead to eutrophication (i.e., algal blooms, hypoxia) of surface waters, decrease biodiversity, and increase soil acidity [*Galloway et al.,* 2004].

Although the primary sources of NH_3 are agricultural, fossil-fuel combustion can be a major NH_3 emission source in urban areas [*Kirchner et al.,* 2005]. NH_3 is emitted from vehicles equipped with three-way catalytic converters (TWC) during reduction of NO to reduce NO_x emissions [*Matsumoto et al.,* 2006] and ~95% of vehicles in the U.S. are equipped with TWCs [*Kean et al.,* 2000]. NH_3 is also emitted as 'fuel NH_3' from electrical generating units (EGUs) and as 'NH_3 slip' from EGUs equipped with selective catalytic reduction and selective non-catalytic NO_x reduction technologies. These fossil fuel based NH_3 emissions are significant in urban areas where NO_x and SO_2 can react with NH_3 to form fine particulate matter. Increases in particulate matter lead to decreased visibility and significant potential human health effects (e.g., respiratory and cardiovascular disease) that are exacerbated in densely populated urban areas [*Pope and Dockery,* 2006].

Agricultural and fossil fuel emissions are usually associated with rural and urban areas, respectively. However, NH_3 has an atmospheric lifetime of a few hours to 5 days and can also react with acidic gases to form NH_4^+ aerosols with longer lifetimes (1 to 15 days) and thus be transported over regional scale distances [*Aneja et al.,* 2001]. Consequently, investigating

emission transport from individual NH_3 sources is important for understanding the impact of agricultural and fossil fuel emissions to urban and rural areas, respectively.

NH_3 emissions associated with agricultural and fossil fuel activities have distinctly different nitrogen isotopic compositions ($\delta^{15}N\text{-}NH_3$) [*Chapter 2*]; these isotopic "fingerprints" can then hypothetically be used to characterize the transport of the varying NH_3 source emissions. For example, volatilized livestock waste NH_3 emitted from dairy operations, poultry operations, and concentrated animal feeding operations have low $\delta^{15}N\text{-}NH_3$ values (-56‰ to -23‰) [*Chapter 2*]. Similarly, volatilized fertilizer NH_3 emitted from cropland soils also have low values (-48 ‰ to -36‰) [*Chapter 2*]. In comparison, reported $\delta^{15}N\text{-}NH_3$ values of NH_3 emitted from coal combustion (-7 to +2‰) [*Freyer,* 1978], 'NH_3 slip' from EGU's (-14.6 to -11.3‰) [*Chapter 2*], and vehicles (-4.6 to -2.2‰) [*Chapter 2*] are considerably higher than those from livestock and fertilizer emissions. Building on this knowledge of varying isotopic signatures among NH_3 sources, we: 1) document the utility of $\delta^{15}N$ in ambient NH_3 to examine transport of NH_3 across various land-use types (dairy operation, conventionally managed cornfield, concentrated animal feeding operation (CAFO), and tallgrass prairie); 2) use an isotope mixing model to predict first approximations of NH_3 source contributions to ambient NH_3 concentrations; 3) relate modeled NH_3 deposition flux to measured $\delta^{15}N\text{-}NH_3$ values and; 4) use $\delta^{15}N$ to investigate NH_3 sources in an urban region.

3.2 METHODS

3.2.1 NH_3 emission collection methods for concentration and isotope analysis

Passive samplers, either Ogawa or Adapted Low-Cost Passive High Absorption (ALPHA), have been used in previous studies to collect NH_3 emissions and monitor NH_3 concentrations [*Rogers et al.,* 2009; *Sather et al.,* 2008; *Siefert et al.,* 2004; *Tang et al.,* 2001; *Cape et al.,* 2004; *Sutton et al.,* 2004; *Skinner et al.,* 2004; 2006; *Chapter 2*]. The Ogawa is a double-sided passive diffuse sampler equipped with a diffusive end cap, followed by a stainless steel screen, and a 14mm quartz filter impregnated with phosphorous acid. The ALPHA is a circular polyethylene vial (26 mm height, 27 mm diameter) with one open end. The vial contains a position for a 25mm phosphorous acid impregnated filter and PTFE membrane for gaseous NH_3 diffusion [*Tang et al.,* 2009]. In this study, Ogawa samplers were only used at the small dairy operation field site because the sampling surface was smaller than that of the ALPHA sampler, thus minimizing the amount of NH_3 collected for subsequent isotope analysis. During this study, ALPHA blanks in a sealed mason jar traveled with the deployed ALPHA samplers and were later analyzed for [NH_3] so the 'blank concentration' could be subtracted from concentration of deployed samplers.

3.2.2 NH_3 concentration analysis method

After collection on the passive sampler filters, NH_3 was eluted with Milli-Q water and analyzed as NH_4^+ using the phenolate method [Eaton et al., 2005] and a Thermo Evolution 60S UV-vis. NH_3 air concentrations were calculated according to Ogawa or ALPHA sampler protocol [*Ogawa* 2006*; Tang et al.,* 2009].

3.2.3 Nitrogen isotopic analysis of NH_3 samples

Briefly, this method employs hypobromite oxidation to quantitatively convert NH_4^+ in a sample to nitrite (NO_2^-). After oxidation, sample pH is adjusted whereupon sample NO_2^- is converted to N_2O using the bacterial denitrifier *Pseudomonas aureofaciens* and introduced to an Isotope Ratio Mass Spectrometer (IRMS) [*Sigman et al.,* 2001]. For this study, samples were analyzed for $\delta^{15}N$ values using an Isoprime Trace Gas and Gilson GX-271 autosampler coupled with an Isoprime Continuous Flow IRMS at the University of Pittsburgh, *Regional Stable Isotope Laboratory for Earth and Environmental Research*. Values are reported in parts per thousand relative to atmospheric N_2 as follows:

$$\delta^{15}N\ (‰) = \frac{(^{15}N/^{14}N)_{sample} - (^{15}N/^{14}N)_{standard}}{(^{15}N/^{14}N)_{standard}} \times 1000 \qquad (1).$$

International reference standards USGS34, USGS32, USGS25, and USGS26 were used for data correction. Standard deviations of USGS standards USGS34 and USGS32 are $\pm$ 0.2‰ and USGS25 and USGS26 are $\pm$ 0.7‰.

3.2.4 Calculating NH_3 deposition flux from concentrations

To estimate NH_3 fluxes deposited to a landscape surrounding a concentrated animal feeding operation (CAFO), deposition flux was modeled using a simplified approach according to European Environment Agency "Guidance on modeling the concentration and deposition of ammonia emitted from intensive farming" (2010). Deposition flux is calculated as:

$$F = V_d * C \qquad (2)$$

where C is [NH_3] at each transect sampling site, V_d is ammonia dry deposition velocity (m/s), and F is deposition flux (μg NH_3 m^{-2} s^{-1}). Given a large range in potential NH_3 deposition velocities, we calculate NH3 flux using two different approaches. The first approach uses reported deposition velocity associated with grassland (0.002 m/s) [*European Environment Agency,* 2010]. The second approach uses concentration dependent deposition velocities where higher NH_3 concentrations result in lower deposition velocity [*Cape et al.,* 2008]. For this approach, NH_3 concentrations ranging from 20 -30, 30-80, and > 80 μg/m^3 result in NH_3 deposition velocities of 0.01, 0.005, and 0.003 m/s, respectively.

3.2.5 Description of sites for NH_3 source sampling and transects

Small dairy barn transect

In Summer 2009, a pilot study was conducted to assess the effectiveness of passive samplers for collection of NH_3 for subsequent isotopic analysis. A transect was established extending from a small, 150-head dairy barn in Western Pennsylvania downwind to the edge of a forest. Ogawa passive samplers were placed at the upwind opening of the dairy barn, 10m outside the barn directly near ventilation fans, 50m, and 200m downwind from the dairy barn. The passive samplers were deployed for one month (6/28/09 to 7/28/09).

Conventionally managed cornfield transect

At the USDA ARS facility in Beltsville Maryland (USA), the Optimizing Production Inputs for Economic and Environmental Enhancement (OPE3) site consists of four adjacent watersheds that are managed with different crop management systems. Field B at OPE-3 was chosen as a sampling transect site because it represents traditional farming practices common in

Midwestern states, mainly corn row crops with a uniform application of urea-ammonia-nitrate industrial fertilizer applied with planting (35 lbs N /ac) and later as side-dressing (120 lbs/ ac). [*USDA,* 2012]. Urea Ammonia Nitrate (UAN) was the fertilizer applied. The fertilizer is "side-dressed" meaning that the nitrogen is applied to the soil subsurface within the root zone. The sampling transect began at the midpoint of Field B and ended in a downwind riparian area (Figure 3.1). A site upwind of the transect was also sampled directly adjacent to the cornfield and near a commuter road. The transect at Field B was sampled a total of four times over a two-year period (Table 3.1). Although this transect was established to sample NH_3 volatilization from fertilizers, it was adjacent to a commuter road and within 500m of the Baltimore-Washington parkway (a heavily trafficked road with ~51,000 vehicles/day) [*MD Department of Transportation*, 2011].

Table 3.1: Description of conventionally managed cornfield sampling sessions.

Sampling Session	Date	Fertilizer Application
1	5/22/10 to 6/3/10	35 lbs N/ac
2	6/19/10 to 7/22/10	120 lbs N/ac
3	6/2/11 to 6/19/11	35 lbs N/ac
4	6/23/11 to 7/22/11	120 lbs N/ac

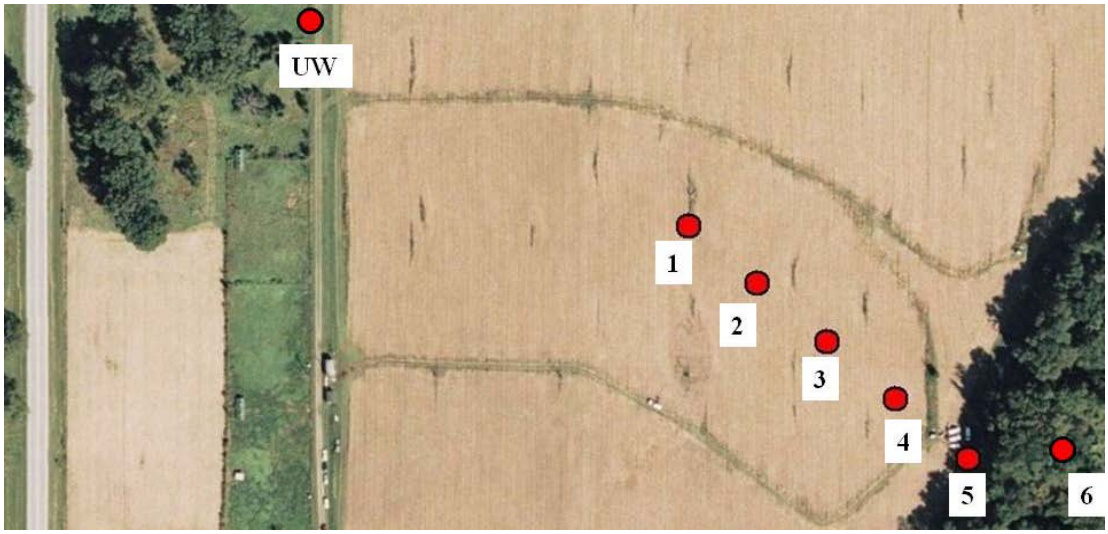

Figure 3.1: Conventionally managed cornfield. Red circles represent NH_3 passive sampling sites.

Confined animal feeding operation transect and livestock waste

A concentrated animal feeding operation (CAFO) containing 30,000 head of beef cattle over 59 ha [*Bonifacio, 2009*] was sampled in central Kansas (Figure 3.2). A transect was established extending from the CAFO edge (0 m) to 5 downwind sites (30, 130, 230, 330 m, and 1.6 km from the CAFO edge). The average wind direction during the summer in at the CAFO site is from the south and southeast [*Bonifacio, 2009*]. The CAFO passive sampling was conducted from 8/6/10 to 8/21/10.

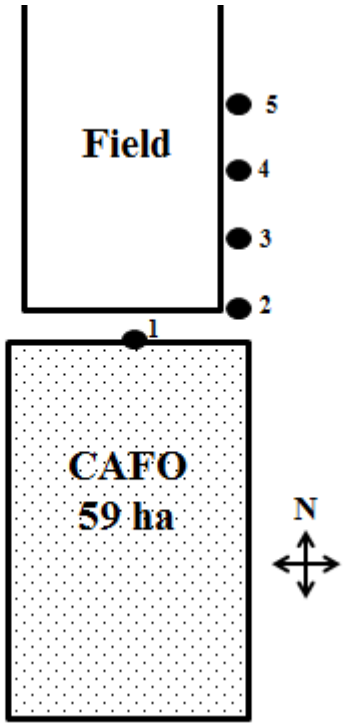

Figure 3.2: Diagram of concentrated animal feeding operation. Not to scale.

Native tallgrass prairie

Konza Prairie Biological Station (KPBS) is a 3,487 ha native tallgrass prairie preserve located in the Flint Hills of Kansas [*Konza LTER*, 201]) and home of the Konza Long-term Ecological Research (LTER). Konza is divided into sections subjected to management treatments including grazing, nongrazing, burning, and nonburning. To characterize ambient NH_3 backgrounds, we established a transect (5 sites ~ 50 m apart) in Section K2A, an ungrazed plot subject to a two year burn cycle. Konza passive sampling was conducted from 8/5/10 to 8/21/10.

Pittsburgh, PA urban region sampling

In summer 2012, (7/5/12 to 7/19/12) ALPHA passive samplers were deployed on ten telephone poles at a height of 10 ft. throughout the city of Pittsburgh, PA (population 307,000) (Figure 3.3).

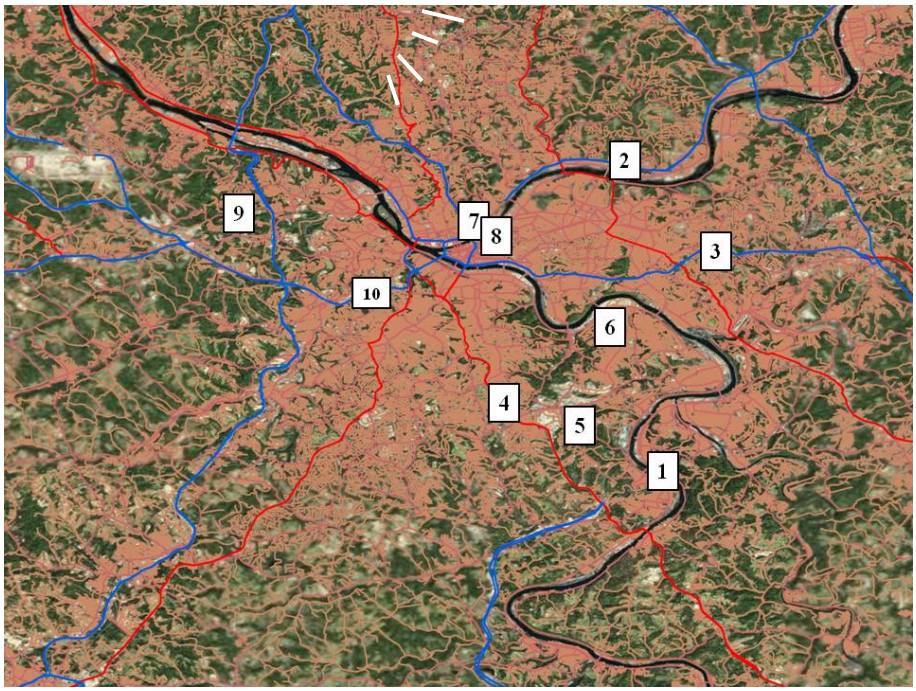

Figure 3.3: Pittsburgh sampling sites are shown by site number.

3.3 RESULTS AND DISCUSSION

3.3.1 NH_3 collection for isotope analysis

Ogawa passive samplers were only used during a pilot study at the small dairy operation because the sampling surface was smaller than that of the ALPHA, and thus limited the amount of NH_3 collected for isotopic analysis. The $\delta^{15}N\text{-}NH_3$ standard deviation among Ogawa samplers is not reported because one filter in the sampler was used for isotopic analysis and the other was used for NH_3 concentrations. ALPHA samplers were used throughout the remaining study sites and the average standard deviation for triplicate ALPHA samplers is ±2.9‰ and ranged from 1.5 to 4.5‰. Triplicate samplers were deployed on a single post and thus collected NH_3 at slightly varying heights and from varying directions. Thus, physical differences in deployment among the triplicate samplers may be partially responsible for the large range in standard deviations observed herein. Results from collection using ALPHA samplers for NH_3 collection and subsequent isotopic analysis are described further in Chapter 2.

3.3.2 Dairy Barn transect

Results from the pilot study at the small dairy barn operation demonstrate that passive samplers collect sufficient NH_3 for isotope analysis, and further that the $\delta^{15}N\text{-}NH_3$ values follow a systematic pattern with distance from the facility (Figure 3.4). As less livestock waste emissions are present downwind, the $\delta^{15}N\text{-}NH_3$ value increases toward the ambient, background value. These pilot study results across a relatively small landscape transect provided important proof-of-concept and demonstrate that more intensive sampling at larger transect locations would be possible.

Site	[NH_3] ($\mu g/m^3$)	$\delta^{15}NH_3$ (‰)
1	165.6	-22.8
2	128.2	-28.5
3	46.8	-21.7
4	19.1	-17.7

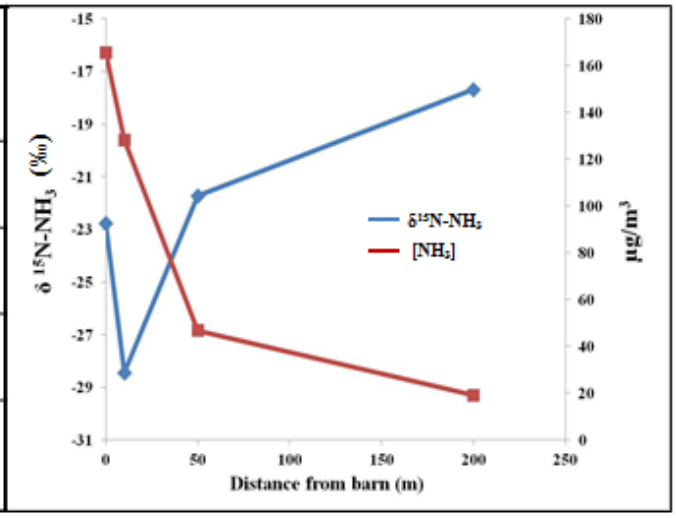

Figure 3.4: [NH_3] and $\delta^{15}N$-NH_3 at the small dairy barn transect. Standard deviation is not reported because one filter was used for concentration and the duplicate was used for isotope analysis.

3.3.3 Konza tallgrass prairie transect

Mean $\delta^{15}N$-NH_3 values from samples spanning the Konza tallgrass prairie transect span a small range (-4.9 to -8.8‰) and are within the standard deviation of the $\delta^{15}N$-NH_3 the ALPHA samplers (Figure 3.5). This is expected as there is no immediate NH_3 point source near the transect. Thus these samples represent ambient NH_3 over the prairie and demonstrate the absence of a gradient in a setting not influenced by a single dominant NH_3 source. The mean $\delta^{15}N$-NH_3 value (-7.0 $\pm$ 1.6‰) observed at Konza may represents mixing of NH_3 emitted from prairie soils with volatilized waste from a grazing bison herd (~300) in a separate section of the Konza reserve.

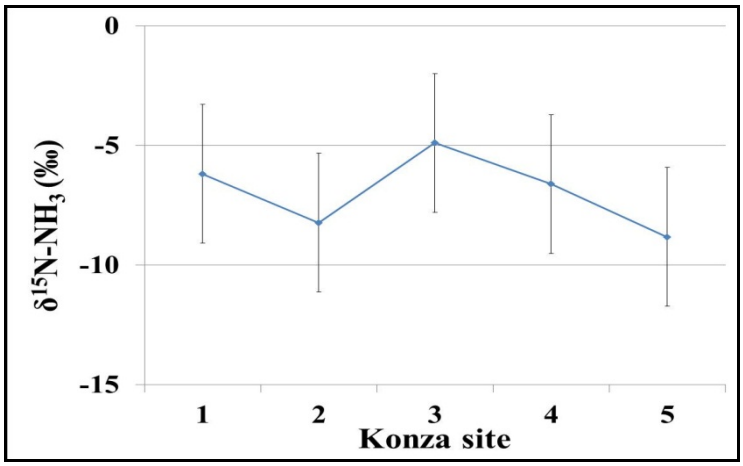

Figure 3.5: δ^{15}N-NH_3 values at Konza tallgrass prairie transect.

3.3.4 Conventionally managed cornfield transect

NH_3 concentration, δ^{15}N-NH_3

Table 3.2 summarizes [NH_3] and δ^{15}N-NH_3 data from the conventionally managed cornfield. Concentrations of NH_3 are higher at sampling sites over the cornfield and decrease significantly away from the field into the riparian area (Figure 3.6). Higher [NH_3] at sites over the cornfield result from volatilization of the applied fertilizer. Lower [NH_3] at sites in the riparian area suggest decreasing fertilizer source with distance from the edge of field and possible 'scrubbing out' or uptake of NH_3 by the riparian vegetation. While plants can grow exclusively on atmospheric NH_3, bi-directional exchange between air and plant is more common where, exchange rate is a function of environmental conditions [*Erisman et al.;* 2007, *Walker et al.;* 2006]. [NH_3] over the cornfield after the 120 lbs N/acre fertilizer application increased 3 to 14 times over the field relative to the initial 35 lbs N/acre fertilizer application (Figure 3.6).

δ^{15}N-NH_3 values are higher at the upwind site due to vehicle exhaust NH_3 contribution (Figure 3.7). At the sites over the cornfield (1 to 4) lower δ^{15}N-NH_3 values indicate contribution of volatilized fertilizer. At the sites over the cornfield after the 35 lb N/ac and 120 lb N/ac fertilizer application, average δ^{15}N-NH_3 values were -14.2‰ and -40.7‰, respectively. Lower δ^{15}N-NH_3 values following the 120 lb N/ac application indicate a larger contribution from fertilizer to ambient NH_3.

Given that fertilizer δ^{15}N values range from 0 $\pm$ 2‰ [*Bateman et al.,* 2007], this suggests an average fractionation factor between NH_4^+ $_{(fertilizer)}$ and NH_3 (g) of 40.7‰. This fractionation factor falls within the previously reported range (30 to 60‰) for NH_3 volatilization [*Frank et al.,* 2004]. Additionally, fractionation over the cornfield can also occur during air-surface (soil and vegetation) exchange of NH_3. Vegetation (via stomatal or cuticular processes) is a source or sink of NH_3 depending on atmospheric [NH_3] concentration, meteorology and surface characteristics [*Walker et al.,* 2006; 2008]. This suggests that δ^{15}N-NH_3 values collected over the cornfield may also partially represent δ^{15}N-NH_3 values produced from NH_3 air-surface exchange processes.

Table 3.2: NH_3 concentration and $\delta^{15}N$-NH_3 at the BARC cornfield transect

	Session 1 35 lbs N/ac		Session 2 120 lbs N/ac		Session 3 35 lbs N/ac		Session 4 120 lbs N/ac	
Site	$[NH_3]$ ($\mu g/m^3$)	$\delta^{15}N$-NH_3 (‰)	$[NH_3]$ ($\mu g/m^3$)	$\delta^{15}N$-NH_3 (‰)	$[NH_3]$ ($\mu g/m^3$)	$\delta^{15}N$-NH_3 (‰)	$[NH_3]$ ($\mu g/m^3$)	$\delta^{15}N$-NH_3 (‰)
1	2.5	-17.4	21.3	-38.5	4.8	-7.0	17.6	-31.7
2	3.9	-13.1	20.7	-39.4	1.3	-28.6	17.7	-45.3
3	3.0	-7.8	19.8	-41.4	3.9	-16.9	15.1	-44.9
4	1.9	-9.1	21.6	-36.3	4.6	-14.0	13.0	-48.0
5	1.4	-8.5	12.6	-33.3	1.5	-9.5	12.4	-41.1
6	1.4	-5.1	12.5	-27.9	9.1	-2.1	6.8	-25.6
UW	3.6	-1.3	9.2	-30.4	5.0	-12.3	9.3	-19.6

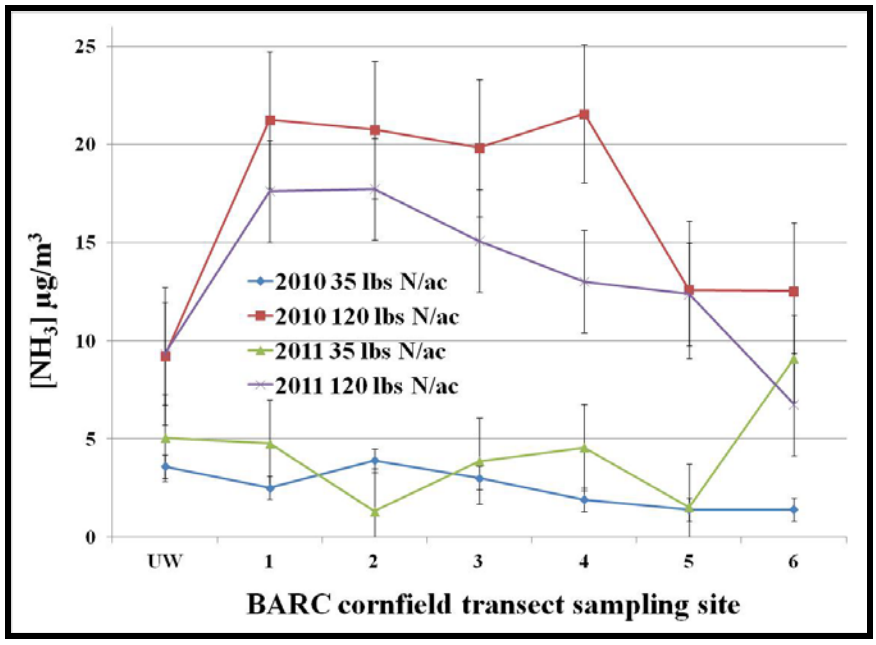

Figure 3.6: $[NH_3]$ for each BARC cornfield sampling session

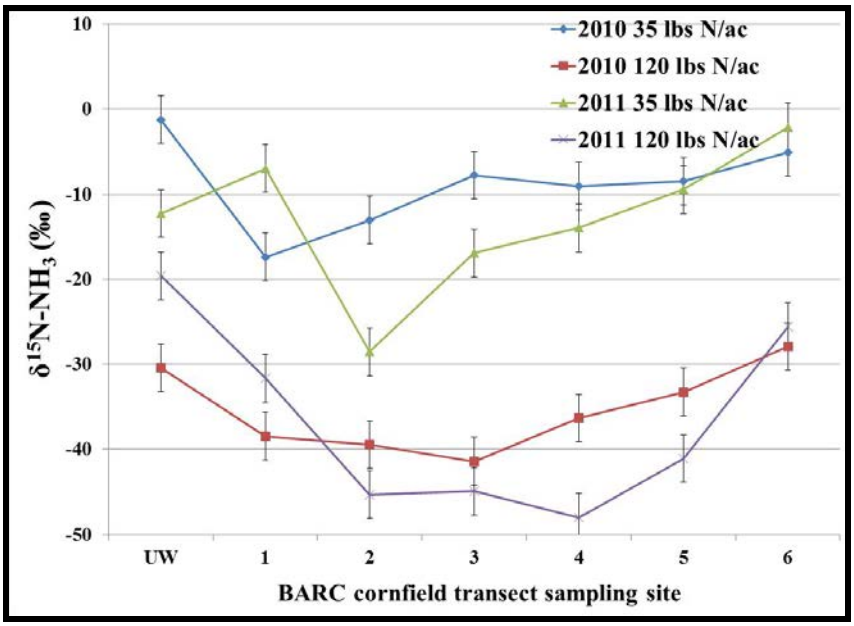

Figure 3.7: δ^{15}N-NH_3 values for each BARC cornfield sampling session.

Predicting % NH_3 source contribution at a conventionally managed cornfield

To predict % NH_3 source contribution to the air [NH_3] at a conventionally managed cornfield, an isotope mixing model was developed.

$$\delta^{15}\text{N-NH}_{3obs} = f_{vehicle}*(\delta^{15}\text{N-NH}_{3vehicle}) + (1-f_{vehicle})*(\delta^{15}\text{N-NH}_{3fertilizer}) \quad (5)$$

It is assumed that the two main contributors to [NH_3] at the field site are vehicle exhaust and volatilized fertilizer. For this model, δ^{15}N-NH_3 values for vehicle NH_3 (-4.6 to -2.2‰) are from a moderately trafficked Pittsburgh, Pennsylvania (USA) tunnel [*Chapter 2*]. The range of δ^{15}N-NH_3 values for volatilized fertilizer NH_3 (-48.0 to -36.3‰) are from Sites 2, 3, and 4 of the cornfield transect after both 120 lb N/ac fertilizer applications. The relative percent contributions from vehicle and volatilized fertilizer emissions to ambient [NH_3] are shown (Figure 3.8) where the percent contribution is the maximum likelihood estimate (MLE) derived from Monte Carlo simulation (n =1000) for each data point at each site. The average

contribution of vehicle NH_3 emissions to NH_3 over the cornfield (Sites 1-4) after the 35 lb N/ac fertilization and 120 lb N/ac fertilization was 72% and 3%, respectively. These results suggest that ambient air over a crop field adjacent to commuter or highly trafficked roadway receives a majority of its NH_3 emissions from vehicles during periods of low or no fertilization. However during larger fertilizer application, volatilized fertilizer NH_3 emissions over the field exceed that of vehicles. In some cases, the modeled source contributions are infeasible (e.g., > 100% or < 0%). This may result from an unknown NH_3 source not considered here or variability in $\delta^{15}N$-NH_3 source signatures.

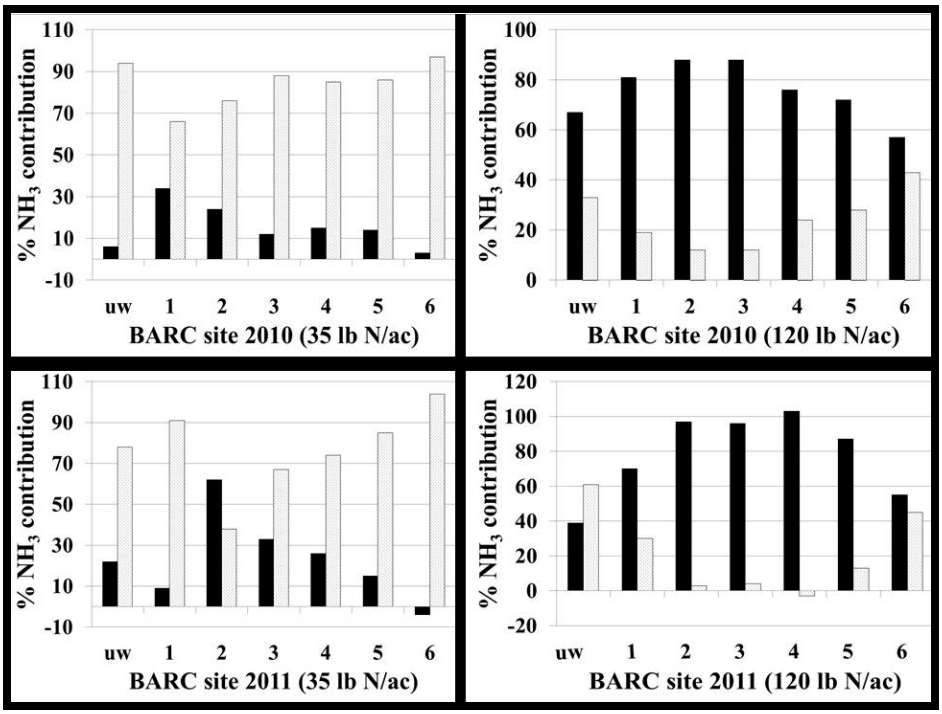

Figure 3.8: Percent NH_3 contribution from vehicle exhaust and volatilized fertilizer after each fertilizer application. Contribution maximum likelihood estimations were obtained using Monte Carlo simulations. Black bars are fertilizer contribution and gray bars are vehicle contribution.

3.3.5 CAFO

CAFO [NH_3] and $\delta^{15}N$-NH_3

NH_3 concentrations decrease significantly within the first 100 m of the CAFO (109.3 µg/m^3), are elevated and consistent over the next ~350m (~50 µg/m^3) (Figure 3.9), and then decline significantly at 1600m downwind of the CAFO (26.9 µg/m^3). This range in observed [NH_3] at the CAFO is much higher compared to [NH_3] measured at the closest AMoN site (Konza prairie, KS, 1.5 µg/m^3) during the same period [*AMoN*, 2012]. $\delta^{15}N$-NH_3 values increase and [NH_3] decrease with increasing distance from the CAFO indicating decreasing contributions from livestock waste.

Site	[NH_3] (µg/m^3)	$\delta^{15}NH_3$ (‰)
1	109.3	-38.3
2	60.1	-19.9
3	60.4	-20.4
4	49.5	-14.3
5	51.0	-16.7
DW	26.9	-14.1

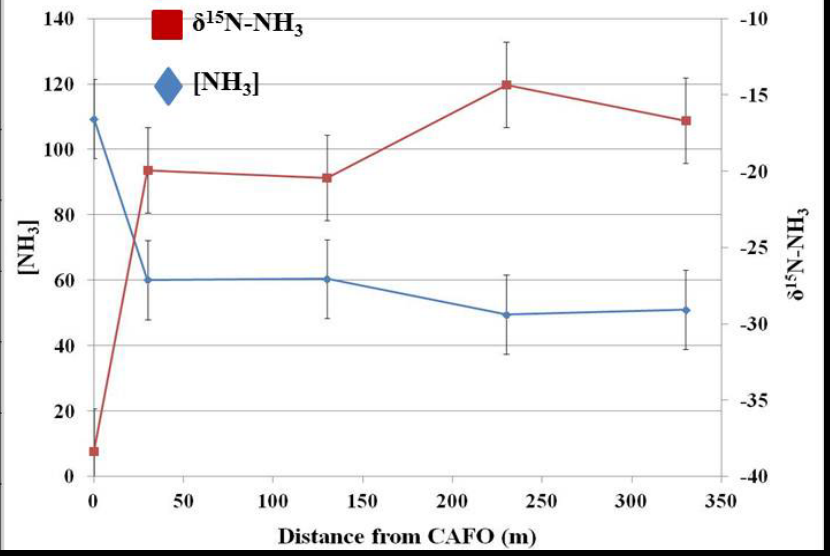

Figure 3.9: $\delta^{15}N$-NH_3 values and [NH_3] at the CAFO.

CAFO NH_3 deposition flux

NH_3 deposition flux at sites downwind of the CAFO were calculated to investigate the amount of NH_3 being deposited onto the landscape from livestock waste emissions. Depending

on the deposition velocity value chosen (i.e. deposition velocity associated with grassland or velocity associated with varying [NH_3]), the flux varies by an order of magnitude. The highest deposition flux (grassland deposition velocity) indicates that landscapes downwind from the CAFO receive from 9.9 to 41.5 lbs N/ac during August. Lower NH_3 deposition fluxes are predicted for this same landscape during August using concentration-dependent NH_3 deposition velocities (from 4.9 to 6.2 lbs N/ac). For comparison, the conventionally managed cornfield field site discussed earlier receives two fertilizer applications during the growing season totaling 155 lbs/N acre/yr. Thus, although these modeled estimates of NH_3 soil deposition flux span a large range, they suggest that CAFO emissions provide substantial additional loads of reactive N available to crops. The implication of these results is that crops downwind of CAFOs likely require less fertilizer due to this subsidy. Further, modeled soil deposition flux is strongly correlated with δ^{15}N-NH_3 values across the CAFO transect (R^2 = 0.99, p = 0.0002 and R^2 =.71, p = 0.07) (Figure 3.10). This suggests that NH_3 emitted from the CAFO is being deposited on the soil, and that isotope ratios may be a valuable tool for predicting contributions of livestock emissions to NH_3 deposition flux.

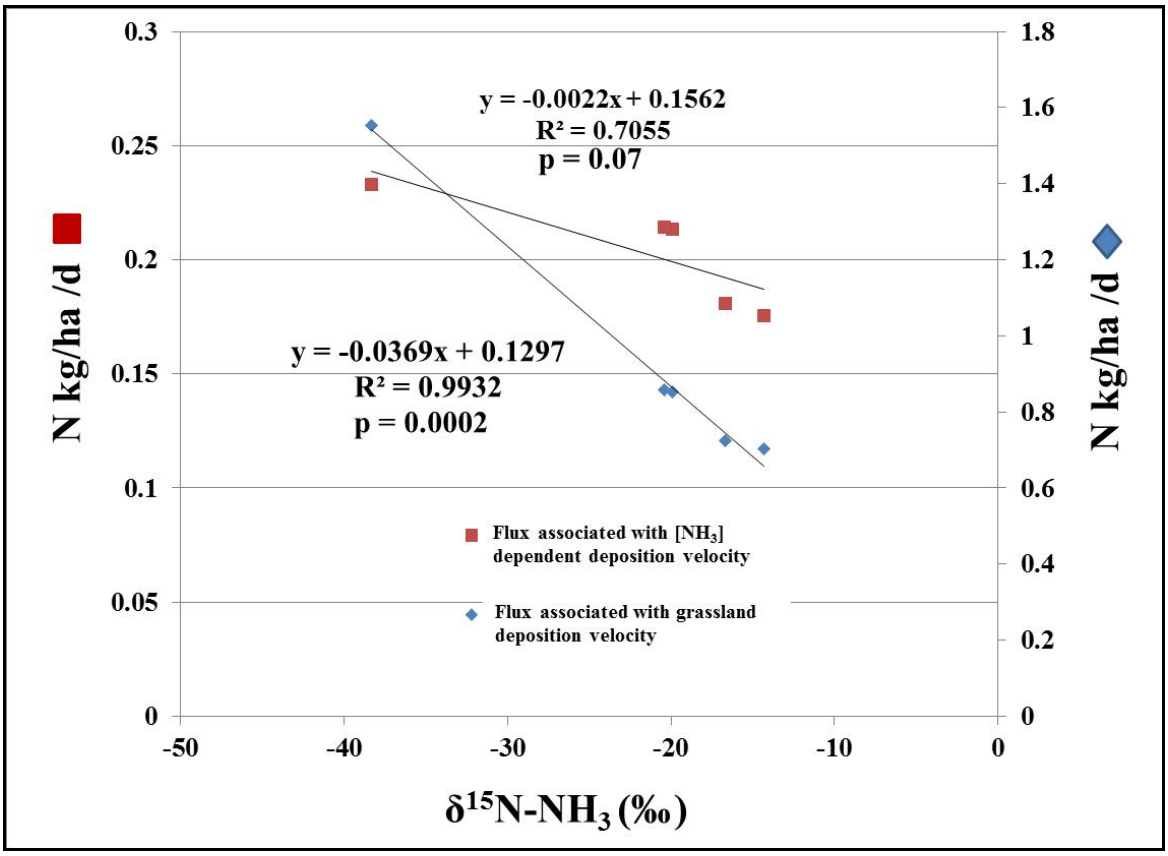

Figure 3.10: δ^{15}N-NH_3 values vs. modeled NH_3 deposition flux 330m across the CAFO transect.

3.3.6 Pittsburgh, PA urban region sampling

NH_3 concentrations in the Pittsburgh region range from 1.1 to 12.4 µg/m^3 with a mean of 4.7 $\pm$ 3.7 µg/m^3 (Figure 3.11). This range of urban [NH_3] indicates that across a relatively small region, NH_3 concentrations, and thus presumably emissions, vary over a large range. δ^{15}N-NH_3 values range from -22.9 to +0.7‰ with a mean value of -8.5 $\pm$ 7.2‰ (Figure 3.12). δ^{15}N-NH_3 values from eight of the ten sites fall within the vehicle and power plant emission δ^{15}N-NH_3 source signatures (Figure 3.13). This suggests that although NH_3 emission inventories suggest that agricultural NH_3 emissions are responsible for 80 to 93% of the global NH_3 emissions, in

urban areas NH_3 emitted from fossil fuel combustion is more significant. The sites with the highest [NH_3] and δ^{15}N-NH_3 values are upwind of the largest industrial NH_3 point source in the Pittsburgh, PA region [*EPA TRI*, 2012] (Figure 3.12). In comparison, at two sites, δ^{15}N-NH_3 values fell between vehicle/power plant and livestock/fertilizer δ^{15}N-NH_3 source signatures. This could result from mixing of fossil fuel NH_3 with NH_3 transported from agricultural activity in surrounding rural areas, or the contributions of another isotopically light NH_3 source. The site with the lowest δ^{15}N-NH_3 value (-22.9‰) is situated on a road between two golf courses that likely received fertilizer application during the summer sampling period. Volatilized fertilizer NH_3 emissions would contribute a low δ^{15}N-NH_3 value at this site. Together, these results indicate that while NH_3 emissions, concentrations, and isotopic composition vary widely in an urban area over short distances, we demonstrate that coupling passive sampling of ambient ammonia and δ^{15}N-NH_3 may be an effective and relatively inexpensive approach for discerning complex source attribution in these settings.

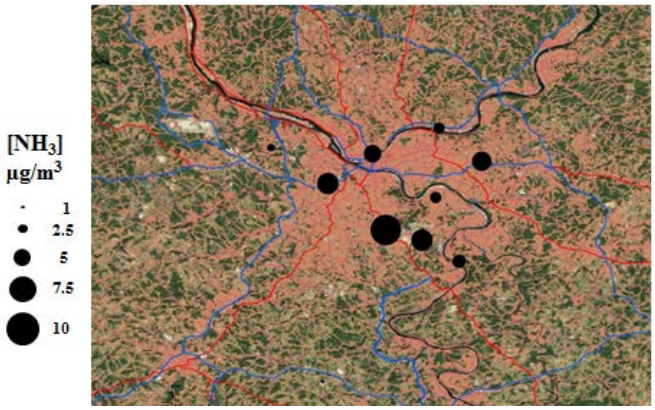

Figure 3.11: [NH_3] at the Pittsburgh sampling sites are represented by proportional black circles.

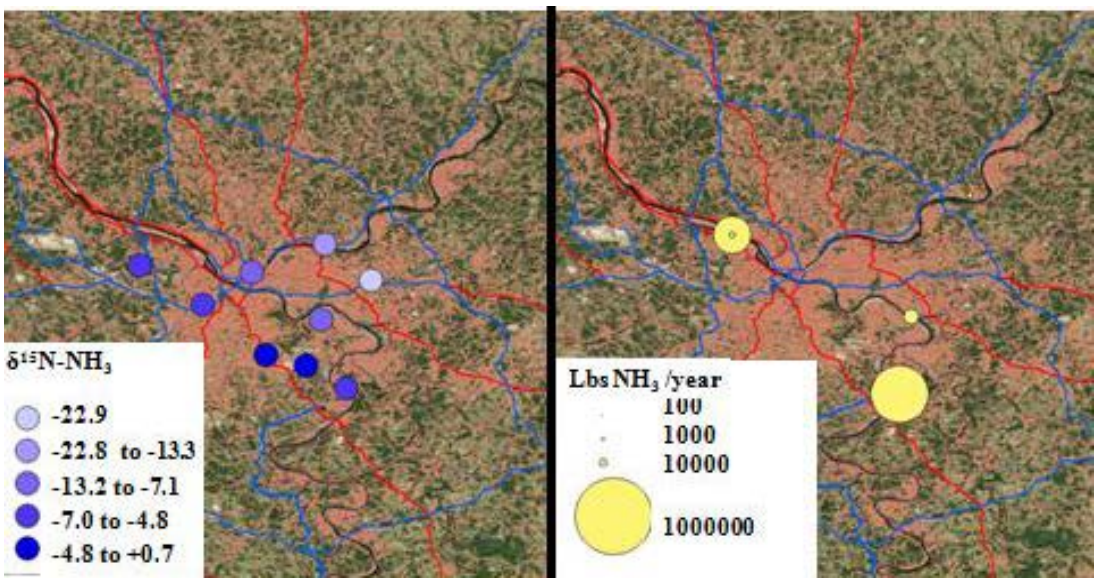

Figure 3.12: δ^{15}N-NH_3 at the Pittsburgh sampling sites are represented colored circles. Proportional yellow circles represent industrial point source emissions (lbs NH_3/ year) (US EPA TRI).

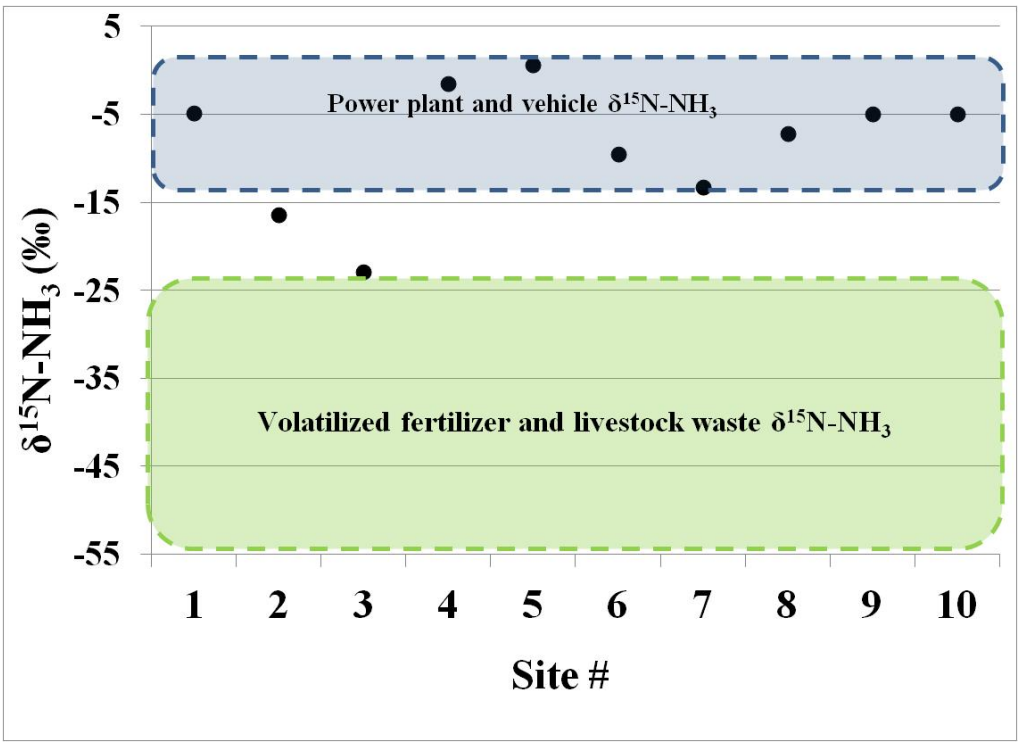

Figure 3.13: δ^{15}N-NH_3 values at Pittsburgh plotted with the vehicle/power plant [*Chapter 2, Freyer,* 1978] and livestock/fertilizer [*Chapter 2*] δ^{15}N-NH_3 source signature.

3.4 CONCLUSION

NH_4^+ deposition in the U.S. has been on the rise over the last two decades (with increases exceeding over 50% in a large area of the central U.S. [*Lehmann et al.*, 2005] and its subsequent adverse impacts on the environment have led to mounting concern by air quality managers and epidemiologists. Quantifying NH_3 contributions from individual sources and understanding NH_3 emission transport are important for reducing adverse impacts from NH_3 emissions. We sampled ambient NH_3 across various land-use types to demonstrate how the stable isotopic composition of NH_3 can be used to characterize the transport of NH_3 emissions across

landscapes. At a sampling transect where we assume two major NH_3 sources, we use ambient $\delta^{15}N\text{-}NH_3$ values to predict source contributions to a landscape. These source contribution estimates can aid in determining NH_3 emission abatement techniques at a local scales. Ambient $\delta^{15}N\text{-}NH_3$ values are significantly correlated with modeled deposition flux suggesting that isotopic composition can indicate sources of NH_3 deposition flux to landscapes. Lastly, while ambient [NH_3] across an urban region can vary greatly, variable $\delta^{15}N\text{-}NH_3$ values suggest more insight into local NH_3 sources can be gained using this approach.

4.0 NITROGEN ISOTOPIC COMPOSITION OF AMMONIA AT AMMONIA MONITORING NETWORK SITES: IMPLICATIONS FOR REGIONAL AMMONIA TRANSPORT

4.1 INTRODUCTION

Ammonium (NH_4^+) in wet deposition has been shown to be increasing at 90% of National Atmospheric Deposition Program National Trends Network (NADP/NTN) sites across the U.S. with increases exceeding 50% in a large area of the central U.S. [*Lehman et al.*, 2005]. Given that NH_3 emissions are generally unregulated in the U.S., NH_x (NH_3 + NH_4^+) is predicted to constitute 60% of nitrogen deposition by 2020 [*Davidson et al.,* 2012]. This NH_x deposition can contribute to eutrophication (i.e., algal blooms, hypoxia) of surface waters, decrease biodiversity and increase soil acidity. Prior to deposition at the Earth surface, NH_3 emissions can react with acidic species to form particulate aerosols that decrease visibility and that are linked to human health impacts (respiratory and cardiovascular disease) [*Pope and Dockery,* 2006]. These adverse effects have led to growing concern regarding the increasing NH_x deposition rates in both wet and dry deposition across the U.S. As a consequence, there is now heightened interest

in improving our understanding of NH_3 emission sources, the processes controlling the formation of NH_4^+ aerosols subject to long-range transport, and ultimately the deposition of NH_3 products in wet and dry deposition. As a result of this growing concern, U.S. monitoring networks for wet and dry deposition chemistry, the National Atmospheric Deposition Program (NADP) and the Clean Air Status and Trends Network (CASTNET), respectively, have established a new monitoring program, the "Ammonia Monitoring Network (AMoN)." The program began in fall 2007, became an official NADP network in October 2010, and has rapidly expanded to include more than 50 sites [*AMoN*, 2012]. The network aims to provide long term ambient NH_3 concentration data that aids air quality modelers, ecologists and policy-makers in validating atmospheric models, estimating N deposition, and assessing $PM_{2.5}$ compliance [*AMoN*, 2012].

To supplement the AMoN network data, we sampled NH_3 at a subset of nine monitoring sites and analyzed the samples for the isotopic composition of NH_3. The isotopic composition of ambient NH_3 ($\delta^{15}N\text{-}NH_3$) provides insight into the emission sources contributing to the ambient NH_3 concentrations. For instance the primary sources of NH_3, volatilized livestock waste and fertilizer, generally are reported to have low $\delta^{15}N\text{-}NH_3$ values, -56‰ to -23‰ and -48‰ to -36‰, respectively [*Chapter 2*]. In contrast, $\delta^{15}N\text{-}NH_3$ values of NH_3 emitted from coal combustion (-7 to +2‰) [*Freyer,* 1978], 'NH_3 slip' from coal-fired power plants (-14.6 to -11.3‰) [*Chapter 2*] and vehicles (-4.6 to -2.2‰) [*Chapter 2*] are considerably higher than those from livestock and fertilizer emissions (Figure 4.1). This distinction between the $\delta^{15}N\text{-}NH_3$ values associated with fossil fuel combustion and agricultural emissions sources allows for inference into the transport of NH_3 emissions from these sources to the individual AMoN sites. This work couples recent NH_3 source $\delta^{15}N$ measurements with observed $\delta^{15}N\text{-}NH_3$ values at AMoN sites and aims to: 1) investigate the spatial and temporal trends of $\delta^{15}N\text{-}NH_3$ across the

U.S.; 2) infer NH_3 source contributions; 3) produce an isotope mixing model to predict δ^{15}N-NH_3values at the U.S. county level; 4) and use the mixing model to compare predicted and observed δ^{15}N-NH_3values, allowing insight into NH_3 emission transport.

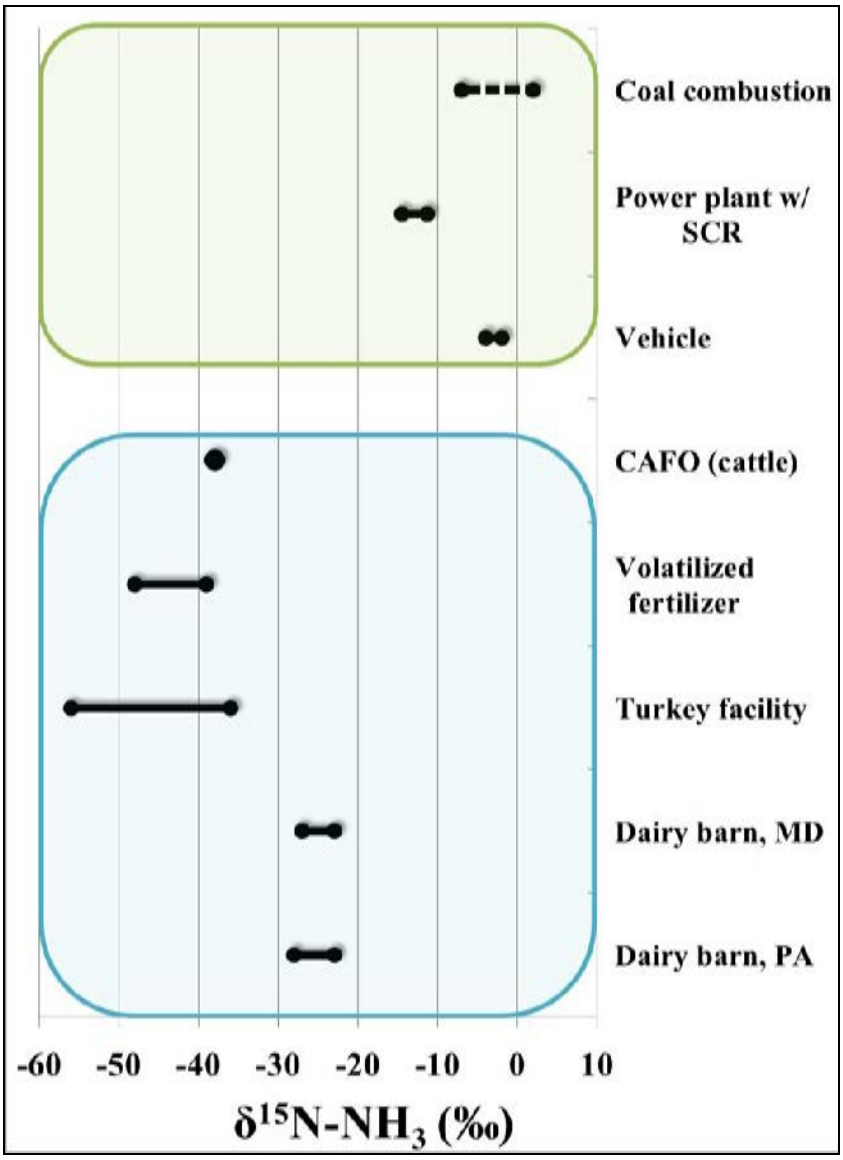

Figure 4.1: δ^{15}N-NH_3 values of significant NH_3 sources. [*Chapter 2, Freyer,* 1978]

4.2 METHODS

4.2.1 NH_3 collection and Ammonia monitoring network sites

NH_3 was collected at nine Ammonia Monitoring Network sites (Figure 4.2, Table 4.1) monthly for a year from 7/2009 to 6/2010. At the beginning of each month, five ALPHA samplers (four field samplers and one travel blank) were shipped in coolers containing ice packs. ALPHA passive samplers were placed in sealed mason jars containing ammonia absorbing packets (API Ammo-Chips) before placement in the cooler to reduce potential blanks during transport and storage. The ALPHA sampler is a circular polyethylene vial (26 mm height, 27 mm diameter) with one open end. The vial contains a position for a 25mm phosphorous acid-impregnated filter and PTFE membrane for gaseous NH_3 diffusion (Tang et al. 2009). In a comparative study of passive NH_3 samplers, concentrations obtained using ALPHA samplers were most similar to the reference NH_3 collection method (phosphorous acid coated glass annular denuders) (-2.4% lower), with a reported precision of 7% among duplicate sampler [*Pulchalski et al., 2011*]. Detection limits for the ALPHA samplers are reported by the United Kingdom National Ammonia Monitoring Network (NAMN) as 0.02 $\mu g/m^3$ for monthly deployments.

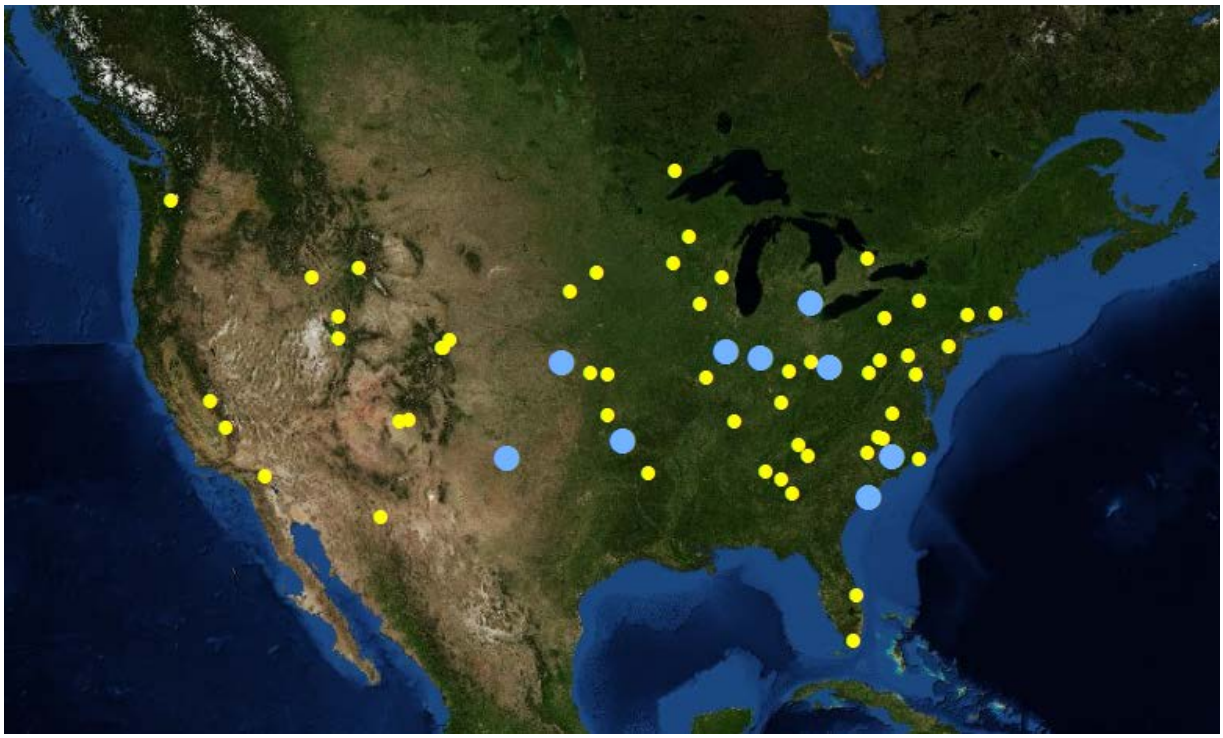

Figure 4.2: Ammonia monitoring network sites (blue and yellow circles). Sites used in this study (blue circles).

Table 4.1: AMoN sites used in this study and potential NH_3 emission sources in the general vicinity of sites.

AMoN Site	Site Description and possible NH_3 Sources
TX43	Dry land cropland also used for winter cattle grazing. Cattle > 0.5 mile away.
OK99	Rural, grazing cattle surrounding
OH02	Rural, 11 coal-fired power plants within a 60-mile radius
IN99	Urban, downtown Indianapolis
SC05	Barrier Islands - maritime forest, beaches, salt marsh, and open water
IL11	Agriculture peak spring/fall, power plants, SCRs
KS24	Oil Refinery, fertilizer manufacturing, soybean crop 1mile, concentrated animal feeding operations in region
MI96	Urban, Detroit
NC35	Rural, concentrated animal feeding operations in region

4.2.2 NH_3 concentration method

After collection on the passive sampler filters, NH_3 was eluted with Milli-Q water and analyzed as NH_4^+ using the phenolate method [*Eaton et al., 2005*] and a Thermo Evolution 60S UV-vis. NH_3 air concentrations were calculated according to the ALPHA sampler protocol [*Tang et al., 2009*]. An NH_3 travel blank was also analyzed and the blank concentration was subtracted from sample concentrations for each set of monthly samples collected at individual sites.

4.2.3 NH_3 isotopic analysis

Isotopic analysis of the samples followed Felix et al. [*Chapter 2*]. Briefly, an oxidation method [*Zhang et al., 2007*] using a hypobromite oxidation solution was used to oxidize the NH_4^+ (diluted to 10µM NH_4^+) in the sample to nitrite (NO_2^-). After oxidation, the sample pH is adjusted to between 3 and 9 using 6N HCl. 20 nmoles of sample NO_2^- is then converted to N_2O using the bacterial denitrifier *Pseudomonas aureofaciens* and introduced to an IRMS [*Sigman et al., 2001*]. The pH adjustment is needed because the high pH created by the addition of the bromate oxidizing agent to the sample is toxic to the denitrifying bacteria. Samples were analyzed for $\delta^{15}N$ values using an Isoprime Trace Gas and Gilson GX-271 autosampler coupled with an Isoprime Continuous Flow Isotope Ratio Mass Spectrometer (CF-IRMS) at the University of Pittsburgh. Values are reported in parts per thousand relative to atmospheric N_2 as follows:

$$\delta^{15}N\ (‰) = \frac{(^{15}N/^{14}N)_{sample} - (^{15}N/^{14}N)_{standard}}{(^{15}N/^{14}N)_{standard}} \times 1000 \qquad (1).$$

International reference standards USGS34, USGS32, USGS25, and USGS26 were used for data correction.

4.2.4 Predicting U.S. $\delta^{15}N$-NH_3 for U.S. Counties

An isotope mixing model (Equation 2) was used to predict $\delta^{15}N$-NH_3 values for all counties in the U.S., by coupling average $\delta^{15}N$-NH_3 values for major NH_3 sources (Table 6.2) and a county level NH_3 emission inventory for 2002 [*Davidson C. et al., 2002*].

$$\delta^{15}NH_{3(predicted)} = f_{livestock\ waste} * \delta^{15}NH_{3(livestock\ waste)} + f_{fertilizer} * \delta^{15}NH_{3(fertilizer)} + f_{vehicle} * \delta^{15}NH_{3(vehicle)} + f_{industry} * \delta^{15}NH_{3(industry)} \quad (2)$$

Four major NH_3 sources included in the inventory including livestock waste, fertilizer, vehicle, and industry in which 56 specific sources constitute these categories (Table A4). This inventory was the only U.S. county level NH_3 emission inventory known to us at the time. Representative $\delta^{15}N\text{-}NH_3$ values of volatized NH_3 from livestock waste and fertilizer are used (Table 4.2), in addition to measured $\delta^{15}N\text{-}NH_3$ values from vehicle sources representative of combined 'fuel NH_3' and emissions resulting from the three way catalytic converter reaction. For the industrial NH_3 emissions, only coal combustion is considered, as $\delta^{15}N\text{-}NH_3$ for other industrial NH_3 sources are poorly characterized. Also other sources such as marine aerosols, biomass burning, and soil emissions are not well constrained and therefore not considered in this mixing model. However, these sources are expected to be minor compared to agricultural and industrial emissions.

Table 4.2: Major NH_3 sources, $\delta^{15}N\text{-}NH_3$ range, and representative $\delta^{15}N\text{-}NH_3$ used in the isotope mixing model.

Source	$\delta^{15}N\text{-}NH_3$ range (‰)	Representative $\delta^{15}N\text{-}NH_3$ (‰)	Reference:
Livestock waste	-56 to -23	-33.0	*Chapter 2*
Volatilized Fertilizer	-48 to -36	-42.6	*Chapter 2*
Vehicle	-4.6 to 2.2	-3.4	*Chapter 2*
Industry	-7 to +2	-2.5	*Freyer 1978*

4.3 RESULTS AND DISCUSSION

4.2.5 NH_3 concentration and $\delta^{15}N$-NH_3

Mean NH_3 concentrations [NH_3] for all sites were 1.8 µg/m^3 with a range of 0.0 to 13.0 µg/m^3 (n = 94) (Figure 4.3). Mean $\delta^{15}N$-NH_3 values for all sites were -15.6‰ with a range of -42.4 to +7.1‰ (n = 86) (Figure 4.3). Ten percent of the samples were investigated for standard deviation of concentration and isotopic composition among co-located samplers by analyzing samplers deployed in quadruplicate. [NH_3] standard deviation among samplers was 0.4 ug/m^3. $\delta^{15}N$-NH_3 standard deviation among samplers ranged from 2.1 to 6.6 ‰ with an average of 4.3 ‰. This high standard deviation generally resulted from single outliers for some quadruplicate deployments. When these outliers are excluded, standard deviation ranges from 0.0 to 2.5‰ with an average of 1.7‰.

To investigate temporal $\delta^{15}N$-NH_3 trends, combined mean $\delta^{15}N$-NH_3 values of all sites were calculated for each season (Winter = Dec, Jan, Feb; Spring = Mar, Apr, May; Summer = Jun, Jul, Aug; Fall = Sep, Oct, Nov). Mean $\delta^{15}N$-NH_3 values are lowest during the spring months (mean = -21.1‰) (Figure 4.4). These low values in spring likely results from an increase in agricultural activity (fertilizer application) during spring and warming temperatures that cause livestock waste to more readily volatilize, as both volatilized fertilizer and livestock waste have relatively low $\delta^{15}N$-NH_3 values compared to other NH_3 sources. Fertilizer application rates peak in March for the south-central U.S., and east and west coasts while April is the peak application period in the northern mid-west states [*Goebes et al., 2003*]. These fertilizer peak periods correspond to the lowest mean monthly $\delta^{15}N$-NH_3 averaged across all sites during the study year (Figure 6.4). Additionally, the mean $\delta^{15}N$-NH_3 values are relatively lower during fall months, (-

13.9‰) as Fall is the second highest period of fertilizer application [*Goebes et al., 2003*]. These average trends suggest that local/regional differences in the timing of fertilizer application rates may play a role in temporal trends in $\delta^{15}N\text{-}NH_3$ values observed at individual sites.

Mean $\delta^{15}N\text{-}NH_3$ values are highest during summer and winter months, -11.3 and -12.4‰, respectively (Figure 6.4). Less fertilizer is applied during summer months due to the likelihood of increased volatilization and in winter months due to frozen soils not allowing for fertilizer injection and infiltration [*Bouwman et al.,* 1997; *Goebes et al.,* 2003]. Power plant energy consumption peaks during the summer and winter months [*EIA,* 2012]. Fossil fuel combustion and 'NH_3 slip' have higher $\delta^{15}N\text{-}NH_3$ values than agricultural sources. Higher $\delta^{15}N\text{-}NH_3$ values during the summer may also be attributed to more NH_3 from increased biomass burning due to wild fires. Biomass burning NH_3 is expected to have higher $\delta^{15}N\text{-}NH_3$ values similar to coal combustion NH_3 as it is produced through a similar process. While rising temperatures in the summer would lead to increased livestock waste volatilization, higher temperatures also result in smaller fractionations between ammonium and aqueous ammonia (e.g. 45.4‰ at 23 ^{o}C and 33.5‰ at 70 ^{o}C) [*Li et al.,* 2012]. Thus, although temperature variations can influence fractionation factors, ambient temperature is not significantly correlated with $\delta^{15}N\text{-}NH_3$ values at individual sites. This suggests that changing NH_3 sources, not temperature fluctuations, are contributing to spatio-temporal variability in $\delta^{15}N\text{-}NH_3$ values. Together, these results generally indicate that $\delta^{15}N\text{-}NH_3$ values are lowest in the spring due to peak agricultural emissions, particularly from volatilization of fertilizer, whereas higher $\delta^{15}N\text{-}NH_3$ values in winter are attributable to lower emissions from the agricultural sector and higher power plant emissions.

In addition to seasonality, the $\delta^{15}N\text{-}NH_3$ values were also examined at each site for associations with potential NH_3 emission sources. Relative to established ranges for NH_3

emission sources [*Chapter 2*], observed $\delta^{15}N\text{-}NH_3$ values clearly indicate mixing of sources across this entire range for each month at individual sites (Figure 4.5). Sites with the highest mean $\delta^{15}N\text{-}NH_3$ values are OH02 (-8.9‰) and SC05 (-4.7‰). The OH02 site is located in the Ohio River Valley region characterized by a high density of emissions from coal-fired power plants [*Elliott et al.*, 2007]. While the SC05 site is on a relatively remote, pristine barrier island where the higher mean $\delta^{15}N\text{-}NH_3$ value likely indicates an ocean NH_3 source. For example, Jickells et al. 2005 report a $\delta^{15}N\text{-}NH_4^+$ value of -8 to -5‰ from ocean aerosols. SC05 also has the least variable $\delta^{15}N\text{-}NH_3$ values during the study period, as it is influenced by a single, consistent marine NH_3 source. In contrast, TX43 has the lowest mean $\delta^{15}N\text{-}NH_3$ values (-22.5‰) relative to other sites. Potential sources in the vicinity include fertilized cropland and waste from grazing cattle, both of which have low $\delta^{15}N\text{-}NH_3$ values. Together, observations of trends and relative differences in $\delta^{15}N\text{-}NH_3$ values at individual AMoN sites illustrate how prominent local/regional NH_3 sources influence observed $\delta^{15}N\text{-}NH_3$ values.

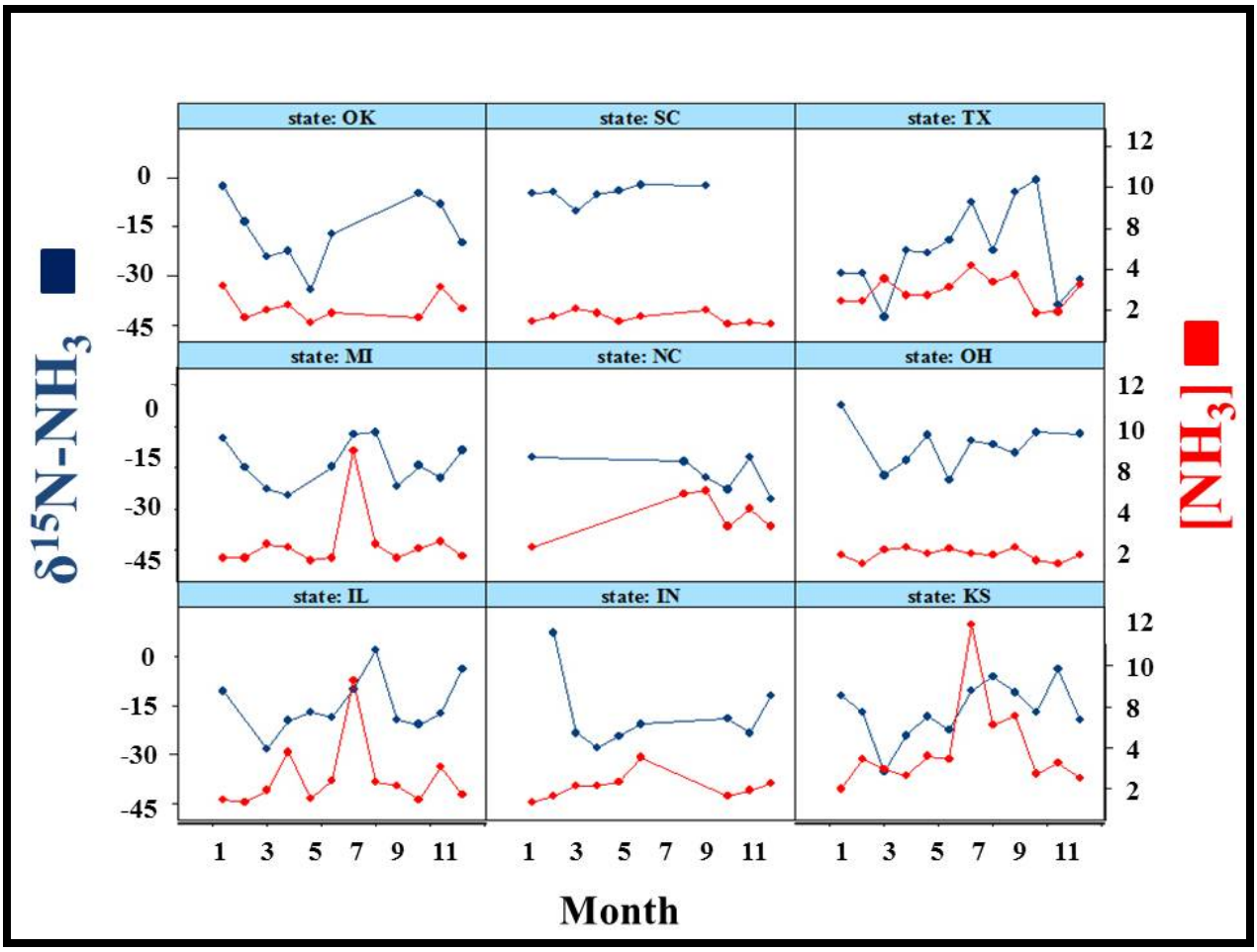

Figure 4.3: [NH_3] (red squares) and δ^{15}N-NH_3 (blue squares) values at the 9 AMoN sites July 2009 through June 2010. Months during this period are represented by a number (January (1)…).

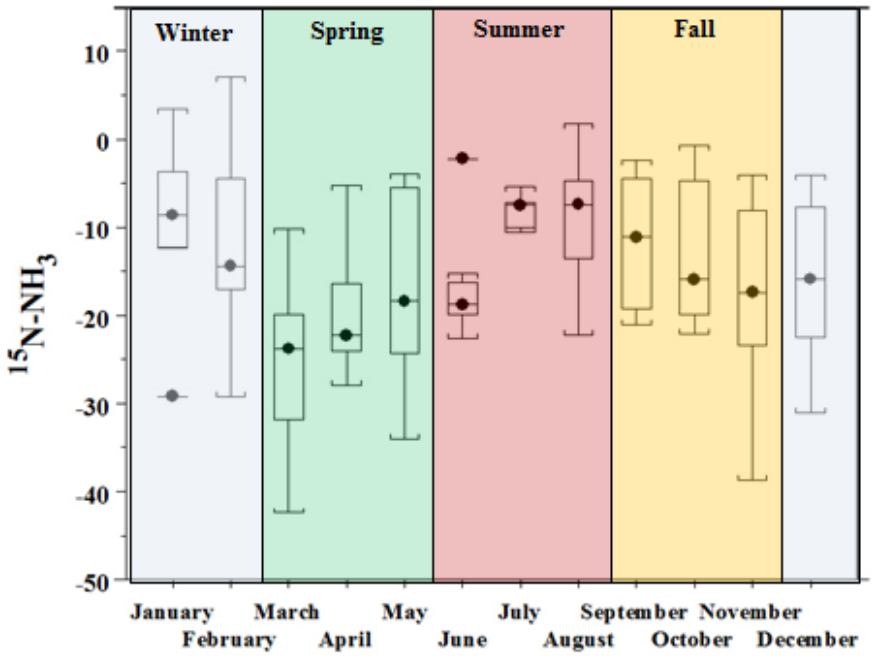

Figure 4.4: Box and whisker plot summarizing range and mean δ^{15}N-NH$_3$ values month observed at 9 AMoN sites.

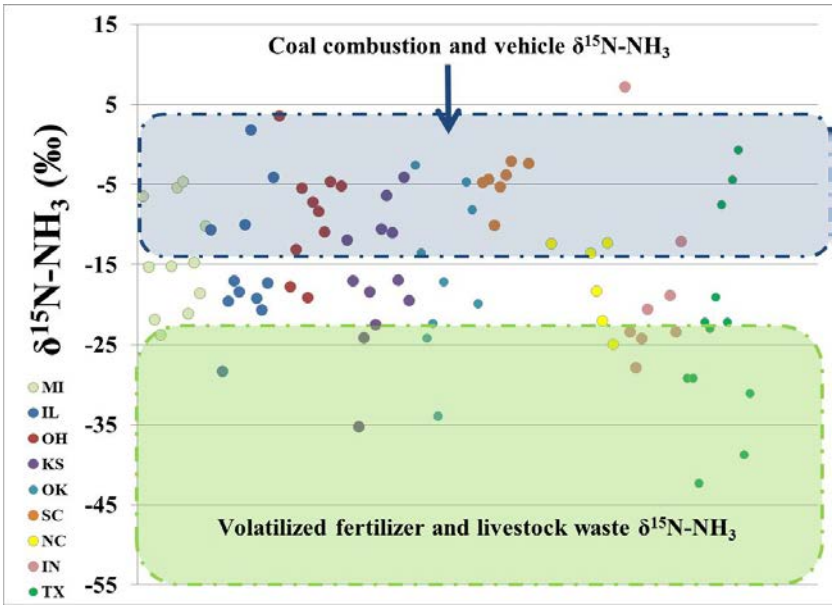

Figure 4.5: δ^{15}N-NH$_3$ at AMoN sites plotted with the range of δ^{15}N-NH$_3$ values for NH$_3$ sources [*Chapter 2, Freyer,* 1978].

4.2.6 $\delta^{15}N\text{-}NH_3$ prediction results

$\delta^{15}N\text{-}NH_3$ predictions for all U.S. counties

Monthly $\delta^{15}N\text{-}NH_3$ values were predicted for each county in the contiguous U.S using a 2002 county level NH_3 source inventory [*Davidson et al.,* 2002] and an isotope mixing model (Figure 4.6). Predicted $\delta^{15}N\text{-}NH_3$ values for all U.S. counties ranged from -42.6‰ (100% fertilizer source contribution) to -2.5‰ (100% industry source contribution) with an annual mean of -32.0‰.

The temporal trends in the predicted $\delta^{15}N\text{-}NH_3$ values are similar to those observed at the 9 AMoN sites reported here. Specifically, mean predicted $\delta^{15}N\text{-}NH_3$ values for U.S. counties are lowest in the spring (-33.1‰) due higher contributions from volatilized fertilizer, whereas predicted $\delta^{15}N\text{-}NH_3$ values are highest during the winter (-30.2‰) (Figure 4.7).

Compared to average observed $\delta^{15}N\text{-}NH_3$ values (Figure 4.4), mean seasonal predicted $\delta^{15}N\text{-}NH_3$ values span a smaller range (-33.1 to -30.2‰ and -21.1 to -12.4‰ for observed and predicted values, respectively) and exhibit less seasonal variation (8.7 and 2.9‰ difference between mean winter and spring for observed and predicted values, respectively). This likely results from the dominance of agricultural emissions in the national inventory in which between 86 to 99% of the U.S. monthly emissions are from fertilizer and livestock waste. Further, this emission inventory assumes constant monthly industrial and vehicle emissions. Thus, our predicted $\delta^{15}N$ values in this model are driven by changes in fertilizer application and livestock waste volatilization. While constant vehicle emissions may be a viable assumption, industrial

NH_3 emissions, especially from electric generation, change throughout the year with varying demands [*EIA*, 2012] and SCR usage.

Industrial NH_3 emissions are further suspect as the inventory (2002) was developed during a time when selective catalytic reduction was not used widely in industry. SCR technology use is now growing in a number of industries (i.e. coal-fired power plants, waste incineration, gas turbines, nitric acid plants, nitrogen fixation process, refinery heaters, cement kilns) [*Foerter et al.*, 2006]. For example, SCR technology usage in coal-fired power plants has risen from ~1% in 2000 to 35.4% in 2008. The SCR process injects ammonia (NH_3) into the power plant flue gas stream after which the gas is passed over a catalyst (V_2O_5) in the presence of oxygen. NO_x and NH_3 react to form N_2 and water vapor.

$$4NO + 4NH_3 + O_2 \rightarrow 4N_2 + 6H_2O \qquad (1)$$

If the entire NH_3 reagent doesn't react this can lead to 'NH_3 slip' in the plant emissions. Thus, increased use of SCR technology may be leading to higher rates of industrial NH_3 emissions relative to when the inventory was created. This NH_3 slip has been documented as having a higher $\delta^{15}N$ value (-15 to -11‰) [*Chapter 2*] than that of volatilized livestock waste or fertilizer. Thus, the potential influence of industrial NH_3 sources, characterized by relatively high $\delta^{15}N\text{-}NH_3$ values and underestimated in the existing emissions inventory, likely contributes to differences between the ranges of observed and predicted $\delta^{15}N\text{-}NH_3$ values, as well as smaller seasonal differences. Despite these differences, predicted U.S. county level $\delta^{15}N\text{-}NH_3$ values have a similar temporal trend relative to these observed values in this study.

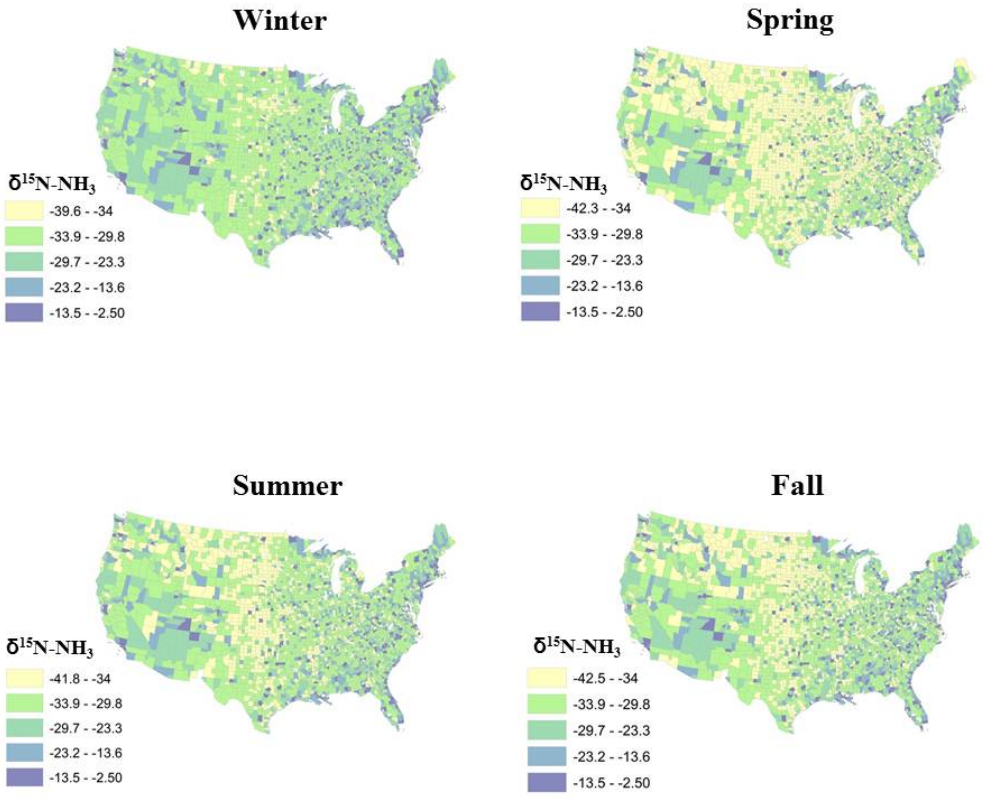

Figure 4.6: Predicted $\delta^{15}N\text{-}NH_3$ values by season for U.S. counties.

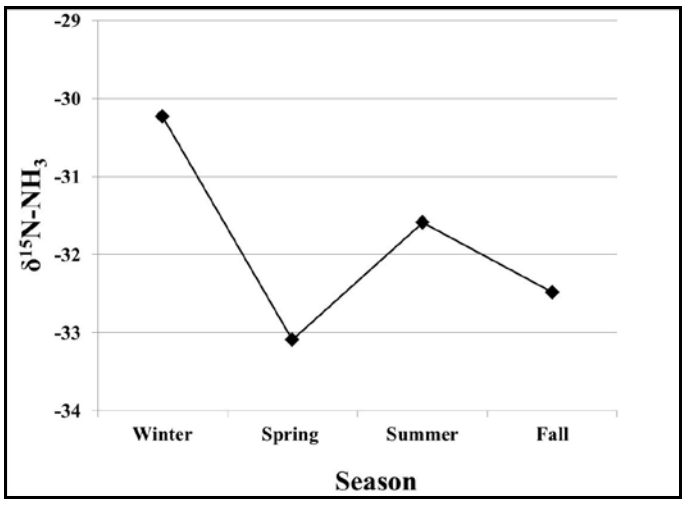

Figure 4.7: Average, seasonal predicted $\delta^{15}N\text{-}NH_3$ values for conterminous U.S. counties.

$\delta^{15}N\text{-}NH_3$ predictions for Ammonia Monitoring Network sites

Predicted $\delta^{15}N\text{-}NH_3$ values for each county were compared to observed AMoN site $\delta^{15}N\text{-}NH_3$ values and a weak correlation was noted (R^2 = 0.04, p=0.05) (Figure 4.8A). This weak correlation was heavily influenced by differences between predicted and observed values at urban AMoN sites in Indianapolis (IN99) and Detroit (MI96). The NH_3 emission inventory accounts for little to no livestock waste or fertilizer NH_3 emissions at the urban sites. Urban counties may not have agricultural NH_3 emissions originating in the county, but NH_3 has an atmospheric lifetime of up to 5 days, which allows for agricultural emissions from neighboring counties to be transported to an urban county. The lack of correlation between predicted and observed values at urban sites indicates that the observed $\delta^{15}N\text{-}NH_3$ values reflect transport of NH_3 emissions from one region to another (i.e. urban to rural or rural to urban).

Another reason for the offset between observed and predicted values seen at the urban AMoN sites is one urban sampling site may not be representative of the whole urban region. For example, Felix et al. [*Chapter 3*] sampled 10 sites in an urban region in Pittsburgh, PA, USA and report a $\delta^{15}N\text{-}NH_3$ range of -22.9 to +0.7‰. This suggests that heterogeneous local urban sources a single representative 'urban region' $\delta^{15}N\text{-}NH_3$ value is not realistic. When the urban AMoN sites' $\delta^{15}N\text{-}NH_3$ data are removed from the regression analysis, a significant correlation is achieved (R^2 = 0.23, p=0.00004) (Figure 8B). The majority of remaining residuals result from due to a under prediction (Figure 8B, data points falling above the 1:1 line). These discrepancies are less apparent when the observed and predicted values are averaged over a year and urban sites are excluded (R^2 = 0.85, p=0.009) (Figure 4.8D). The discrepancies between observed and predicted $\delta^{15}N\text{-}NH_3$ values could be due to the following: 1) transport of NH_3 emissions from

one county to another, 2) undetected NH_3 sources (i.e. ocean, biomass burning, soils) 3) wider ranges in δ^{15}N-NH_3 source signatures than documented to date, 4) source inventory inaccuracies, and/or 5) the gap between source inventory data (2002) and samples data (2009/10).

Although discrepancies do exist between the predicted and observed values, the correlation is significant at the more rural sites and the fact that the model breaks down at urban sites provides insight into possible transport of rural NH_3 emissions into urban area.

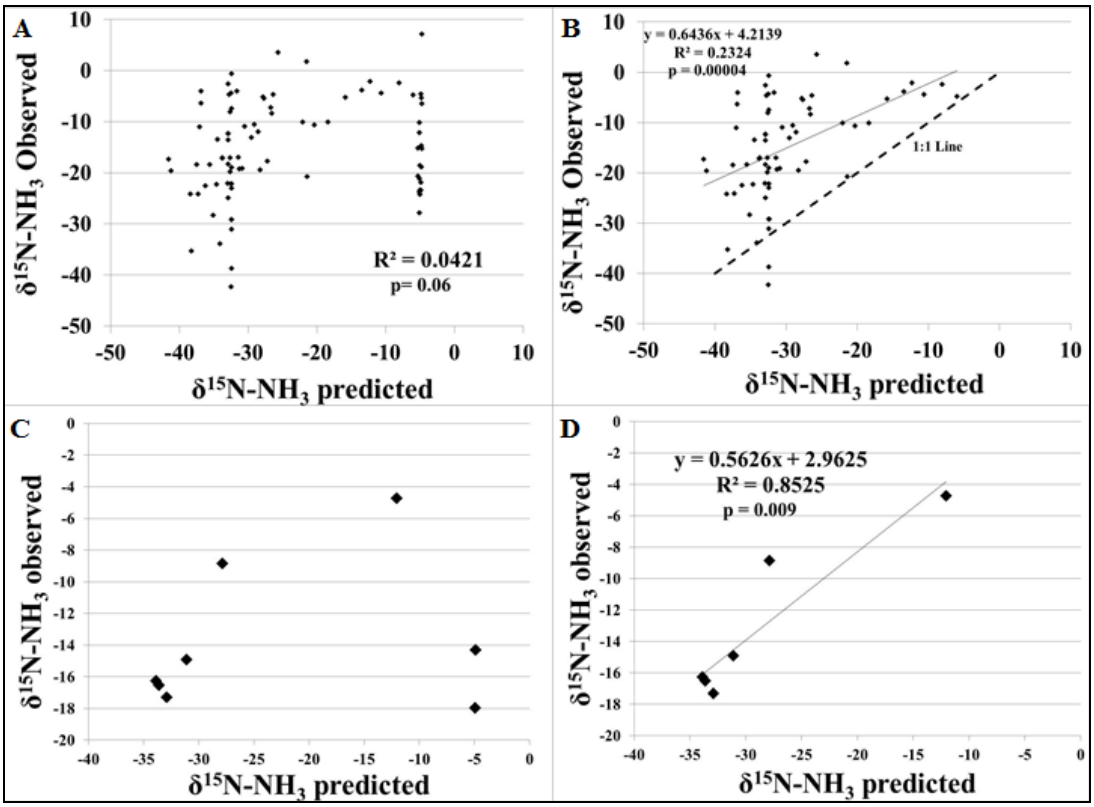

Figure 4.8: A) Observed monthly δ^{15}N-NH_3 at AMoN sites compared to predicted county δ^{15}N-NH_3. B) Observed monthly δ^{15}N-NH_3 at AMoN sites (excluding urban sites) compared to predicted county δ^{15}N-NH_3. C) Observed monthly δ^{15}N-NH_3 at AMoN sites compared to predicted county δ^{15}N-NH_3. D) Observed monthly δ^{15}N-NH_3 at AMoN sites (excluding urban sites) compared to predicted county δ^{15}N-NH_3.

4.3 CONCLUSION

In working with the newly established Ammonia Monitoring Network, we report ambient $\delta^{15}N\text{-}NH_3$ values at 9 locations across the U.S. These $\delta^{15}N\text{-}NH_3$ values provide insight into the temporal trends of the NH_3 sources contributing to monitoring sites in the U.S. The peak in U.S. spring agricultural activity (e.g. fertilizer application, livestock waste volatilization) drives a decreasing trend in $\delta^{15}N\text{-}NH_3$ values at a majority of the sites while higher $\delta^{15}N\text{-}NH_3$ values are observed in winter periods corresponding to less agricultural activity and greater power plant fossil fuel consumption. An isotope mixing model was created to predict county level $\delta^{15}N\text{-}NH_3$ values. When predicted values are compared to observed $\delta^{15}N\text{-}NH_3$ values at AMoN sites, the differences indicate that the emission inventory, and thus our model, does not account for the transport of agricultural emissions to urban areas or urban emissions to agricultural regions. This work provides important proof-of-concept that the isotopic composition of NH_3 is a valuable tool for distinguishing potential emission source contributions to varying regions in the U.S. Moreover, these results demonstrate that $\delta^{15}N\text{-}NH_3$ can be a valuable tool for air quality modelers and policy-makers when improving emission inventories or assessing reduction techniques for various NH_3 sources.

5.0 CONSTRAINING THE ISOTOPIC COMPOSITION OF NO_X EMISSION SOURCES

5.1 INTRODUCTION

Reducing NO_x (NO_x = NO + NO_2) emissions is of global interest due to adverse effects on the environment and human health. NO_x emissions can combine with VOCs to form ground level ozone, particulate matter, and ultimately be oxidized to form nitrate (NO_3^-). Excess NO_3^- is a key factor in the degradation of drinking water, acidic deposition, and estuarine eutrophication [*Galloway et al.,* 2004]. Although natural NO_x sources, including lightning, wildfires, and biogenic soil emissions, account for a portion of global NO_x emissions, the magnitude of these contributions is uncertain [*Reis et al.,* 2009]. Since the Industrial Revolution, anthropogenic NO_x emissions have surpassed natural NO_x emissions; primarily from fossil fuel combustion via electricity generating units (EGUs) and vehicles [*Galloway et al.,* 2004].

Recent and ongoing efforts are aimed at further reducing ambient NO_x concentrations in the U.S and globally [*EPA* 2010a; 2010b; *Bradley et al., 2002*]. Several technologies are available for use in reducing NO_x emissions generated from fossil fuel combustion. NO_x is

produced in Electric Generating Unit (EGU) boilers either by reaction of nitrogen with oxygen in combustion air ("thermal NO_x") or by reaction of fuel nitrogen (e.g. coal) with combustion oxygen ("fuel NO_x") [*Bradley et al.,* 2002]. Low NO_x burners limit the availability of oxygen to combine with nitrogen in the fuel and have been employed in many electric generating unit (EGU) boilers. However, low NO_x burners do not necessarily reduce NO_x emissions sufficiently to meet emissions standards. To further reduce stack NO_x emissions, post-combustion NO_x reduction must also be employed. Selective catalytic reduction (SCR) is one such post-combustion technology which can reduce NO_x emissions by 80 to 90% [*Srivastava et al.,* 2005]. SCRs have been utilized by coal fired EGUs for decades and are globally recognized as the most efficient NO_x emission control technology [*Srivastava et al.,* 2005]. The SCR process injects ammonia (NH_3) into the EGU flue gas stream where the gas is passed over a catalyst (V_2O_5) in the presence of oxygen. NO_x and NH_3 react to form N_2 and water vapor (Equation 1).

$$4NO + 4NH_3 + O_2 \rightarrow 4N_2 + 6H_2O \qquad (1)$$

Selective non-catalytic reduction (SNCR) is a similar post-combustion NO_x reduction technology that employs NH_3 or urea as a reagent and does not use a catalyst because it operates at higher temperatures. The SNCR process is 15 to 66% less efficient than the SCR process [*Srivastava et al.,* 2005]. Vehicles also emit thermal and fuel NO_x. Important in the reduction of vehicle NO_x emissions is the three way catalytic converter (TWC) which dissociates NO_x to O and N atoms which then form N_2 and O_2 molecules. By 2000, ~95% of vehicles in the U.S. were equipped with TWCs [*Cape et al.,* 2004].

While the primary sources of NO_x, fossil fuel combustion via vehicles and EGU's, have been reduced since the Clean Air Act and Amendments, other unregulated sources can be locally significant (i.e. fertilized soils, biomass burning, lightning, livestock waste). Microbial

denitrification and nitrification in soils can produce NO_x emissions and it is reported that soil nutrient enrichment via fertilizer application can contribute to large pulses of biogenic soil NO_x [*Veldkamp et al.,* 1997]. For example, Hudman et al. [2010] report a 50% increase in soil NO_x over the agricultural Great Plain in June 2006 due to rainwater induced pulsing. Jaeglé et al [2005] suggest that during the summer in the northern mid-latitudes, soil NO_x emissions can reach half that of fossil fuel combustion sources.

This microbial denitrification and nitrification also occurs in livestock and human waste and thus can be another NO_x emission source [*McElroy et al.,* 2005]. NO_x produced from lightning can also be a significant NO_x source to remote areas and is estimated to contribute up to 70% of the NO_x concentration below 500 mbar over the North Atlantic in July [*Levy et al.,* 1996). While air quality modelers are aware of these non-fossil fuel-based NO_x emission sources, their diffuse nature makes them difficult to quantify. For instance, Holland et al. [1999] report a global soil NO_x emission range of 4–21 Tg N yr^{-1} while recent studies have reported a lightning-produced NO_x range of 1 to 20 Tg yr^{-1} (*Schumann et al.,* 2007).

The isotopic composition of NO_x and its oxidation products (NO_y) can illuminate sources contributing to ambient NO_x concentrations and subsequent wet and dry NOy deposition. For example, significant correlations were observed between $\delta^{15}NO_3$ in precipitation, dry deposition and EGU NO_x emissions within a 400 km source region [*Elliott et al.,* 2007, 2009]. As another example, $\delta^{15}N\text{-}NO_2$ values adjacent to a road way are significantly higher due to vehicle emissions than those values 400 m away [*Redling et al.,* 2012].

Despite these indications that $\delta^{15}N$ may be a robust tracer of NO_x source contributions, documentation of $\delta^{15}N$ in NO_x emission sources is limited. Heaton [1990] measured NO_x emitted from four South African coal-fired EGUs and $\delta^{15}N$ values ranged from +6 to +13‰; a

δ^{15}N-NO_x range more positive than the values reported for other NO_x sources. For example, NO_x resulting from vehicle fossil fuel combustion δ^{15}N values range from -13 to -2‰ [*Heaton*, 1990), while other studies of vehicle emissions, roadside denuders, roadside vegetation, and roadside gaseous NO_2 have reported δ^{15}N values of +3.7, +5.7, +3.8, and +4‰, respectively [*Amman et al., 1999; Moore, 1977; Pearson et al., 2000; Redling et al., in review*]. In contrast, δ^{15}N values of natural sources, including lightning and biogenic NO_x from soils, have lower δ^{15}N values from 0 to 2‰ and from -49 to -19‰, respectively [*Hoering 1957; Li et al., 2008*] (Figure 5.1). While these initial measurements of source δ^{15}N-NO_x values allow approximation of relative source contributions, further characterization of δ^{15}N-NO_x is required to reduce uncertainty, enable quantification of source contributions, and further understand post-emission transformations of NO_x on isotopic values.

While emission source is a key factor in δ^{15}N-NO_y values, δ^{18}O-NO_y generally reflect oxidation pathways [*Michalski et al.,* 2003]. If there is an "initial" δ^{18}O-NO_2 source signature, it is generally believed to be subsequently masked during oxidation reactions. NO is rapidly oxidized to NO_2 by ozone (O_3) and NO and O_3 rapidly exchange O throughout the daytime. The high δ^{18}O value of O_3 (+90‰ to +122‰) [*Hastings et al., 2003; Michalski et al., 2003*] alters the original δ^{18}O value of the NO_x source. NO_2 then undergoes further oxidation through O_3, OH radical, or halogen bromides to HNO_3 and NO_3 deposition products.

To understand the sources and processes leading to isotopic composition of these deposition products, we investigate the isotopic composition of the primary NO_x emissions and subsequent NO_y products. Through this work we: 1) provide evidence for the use of inexpensive passive samplers to collect NO_2 emissions for subsequent nitrogen and oxygen isotopic analysis;

and 2) present a comprehensive inventory of $\delta^{15}N\text{-}NO_2$, $\delta^{18}O\text{-}NO_2$ values to aid in constraining the isotopic signatures of NO_x emission sources and ambient $\delta^{15}N$ and $\delta^{18}O$ of NOy .

5.2 METHODS

5.2.1 NO_2 and HNO_3 emission collection methods for concentration and isotope analysis

Passive samplers are ideal for the collection of dry nitrogen deposition as they are less expensive, easy to use, and do not require electricity relative to active samplers (*Pulchalski et al.,* 2011; *Elliott et al.,* 2009; *Golden et al.,* 2008). These advantages enable multiple deployments at a single site. Ogawa NO_2 passive samplers and HNO_3 samplers have been used in previous studies to collect NO_2 and HNO_3 emissions for NO_2 and HNO_3 concentrations and isotopic analysis [*Redling et al., in review, Bytnerowicz et al.,* 2005, *Elliott et al.,* 2009]. The Ogawa is a double-sided passive diffuse sampler equipped with a diffusive end cap, followed by a stainless steel screen, and a 14 mm quartz filter impregnated with phosphorous acid. The HNO_3 sampler is a sampler designed by Bytnerowicz, et al. 2005 in which the HNO_3 is collected in the sampler using a 47mm nylon filter. In this study, HNO_3 samplers were used to collect all HNO_3 emissions and the Ogawa passive samplers were used collect NO_2 emissions from NO_2 sources except power plants. Emissions from power plants were sampled at four power plants (A, B, C, D) as follows [*Felix et al.,* 2012, Table 1 contains a key to the acronyms for each power plant's reduction technology]:

SCR/OFA/LNB NO_x collection (Plant A): The sampling method used in this study was modified from U.S. EPA Method 7, "Determination of Nitrogen Oxide Emissions from Stationary Sources". Briefly, a 25 mL aliquot of absorbing solution (6 mL hydrogen peroxide (H_2O_2) in 1 L of ~0.05 M sulfuric acid (H_2SO_4)) was transferred to a flask, which was attached to a sampling train, evacuated, and purged before the grab sample was collected [*EPA method 7*]. The probe of the sampling train was placed into the stack during sampling and the stack emissions collected into the evacuated flask containing the absorbing solution. After a sampling period of approximately 15 seconds, the flask was removed from the train and sealed. The contents of the flask were shaken for 2 minutes and allowed to sit for at least 16 hours, allowing all NO_x gas to oxidize to nitrate. The contents were then transferred to a 100 mL Teflon bottle and frozen for shipping. Samples were stored frozen until further analysis.

OFA/LNB NO_x collection and comparison of absorbing solutions (Plant B): Sample collections at the LNB stack included the comparison of multiple NO_x absorbing solutions, including dilute H_2SO_4/ H_2O_2, dilute sodium hydroxide/hydrogen peroxide ($NaOH$-H_2O_2), and 1.68M triethanolamine (TEA). The dilute H_2SO_4-H_2O_2 was prepared as described above. The dilute $NaOH$-H_2O_2 solution was made by adding 6 mL of 3% hydrogen peroxide to 1 liter ~0.1M NaOH. TEA absorbing solution was shown by Nonomura et al. 1996 to absorb NO_2 with both NO_2^- and NO_3^- being present in the resulting solution.

SCR/OFA/LNB, SNCR/OFA/LNB, OFA/LNB NO_x collection (Plant C): Sample collections at Plant C used a dilute H_2SO_4-H_2O_2, NO_x absorbing solution.

SCR and SCR off NO_x collection (Plant D): Sample collections at Plant D used a dilute H_2SO_4/ H_2O_2, NO_x absorbing solution.

Table 5.1: Summary of EGU emission technologies employed in this study.

Acronym	Technology	Purpose
FGD	Flue-gas desulfurization	Reduces SO_2 emissions from the flue gas
LNB	Low NO_x burner	Reduces NO_x emissions by limiting the availability of oxygen in the fuel
OFA	Over fire air	Reduces NO_x emissions by introducing air to produce more complete fuel combustion
SCR	Selective catalytic reduction	Reduces NO_x emissions by reacting NO_x with NH_3 over a catalyst to form N_2
SNCR	Selective non-catalytic reduction	Reduces NO_x emissions by reaction NO_x with urea or ammonia to form N_2

5.2.2 NO_2 concentration analysis method

Nitrate and nitrite concentrations of power plant stack samples were analyzed using a Dionex ICS 2000 Ion Chromatograph. All other nitrite samples were analyzed using a Thermo Evolution 60S UV-vis. During this study, NO_2 and HNO_3 sampler blanks in a sealed mason jar traveled with the deployed field samplers and were later analyzed for [NO_2] and [HNO_3] to allow for a blank correction.

5.2.3 NO_2 or HNO_3 isotopic analysis method

For isotopic analysis, a denitrifying bacteria, *Pseudomonas aureofaciens*, was used to convert 20 nmoles of NO_2^- or NO_3^- into gaseous N_2O prior to isotope analysis [*Sigman et al.*, 2001]. Samples were analyzed for $\delta^{15}N$ in duplicate using an Isoprime Trace Gas and Gilson GX-271 autosampler coupled with an Isoprime Continuous Flow Isotope Ratio Mass

Spectrometer (CF-IRMS) at the University of Pittsburgh *Regional Stable Isotope Laboratory for Earth and Environmental Science Research*. Nitrogen and oxygen isotopic ratios are reported in parts per thousand relative to atmospheric N_2 and VSMOW as follows:

$$\delta\ (‰) = \frac{(R)_{sample} - (R)_{standard}}{(R)_{standard}} \times 1000 \qquad (2).$$

where R denotes the ratio of the heavy to light isotope (e.g., $^{15}N/^{14}N$ or $^{18}O/^{16}O$).

International reference standards USGS34, USGS32, USGS35 and IAEA N3 were used for data correction. Replicates had an average standard deviation (σ) of 0.2 ‰ for $\delta^{15}N$ and of 0.5 ‰ for $\delta^{18}O$. For HNO_3 samples containing more than 2% NO_2, the NO_2 was removed prior to isotopic analysis using sulfamic acid [*Granger et al.*, 2009].

5.2.4 NO_x emission source sampling

Power plant emissions (Felix et al. 2012)

Sample collection was conducted at four separate coal-fired power plants located in the Northeast and Midwest U.S. (hereafter referred to as Plants A-D as described below). All four plants burned regional bituminous coal and were equipped with limestone-based flue gas desulfurization systems. Table 1 describes emission control technologies used at each of the plants. Plant A, a 550 MW gross annual power production facility that employs overfire air (OFA) systems, selective catalytic reduction emission control technology (SCR), and low NO_x burners (LNB) for NO_x emissions reduction was sampled on May 6, 2009. After initial sample collection and isotopic analysis, additional experiments were conducted using various absorbing solutions at a second facility (Plant B) on December 8, 2009. Plant B, also a 550 MW gross

annual power production facility, employs LNB and OFA systems (i.e., no SCR). A third plant, Plant C, was sampled on January 25 to 27, 2011. Two separate EGUs at Plant C were tested, each producing about 650 MW. One EGU employed LNB, OFA, and SCR, and the other EGU employed LNB, OFA, and SNCR. The latter unit was also tested with the SNCR turned off (e.g. only LNB and OFA were operating). Plant D, sampled April 5 and April 6, 2011, burned low sulfur Powder River Basin coal, produced 660 MW, and also had a limestone FGD system and SCR system. Plant D does not have LNB or OFA. The SCR system at Plant D was also shut off for an additional NO_x reduction treatment scenario.

Vehicular emissions

Ogawa NO_2 samplers were deployed in the ventilation portion and directly outside a moderately trafficked tunnel (Squirrel Hill Tunnel, ~35,000 vehicles a day) in Pittsburgh, Pennsylvania (USA) to collect NO_2 emitted from a large fleet of vehicles. Samplers were deployed monthly in the ventilation portion from 5/10 to 5/11 and outside the tunnel from 1/11 to 5/11. Monthly deployment saturated the collection capacity of the Ogawa filters so additional studies were conducted with shorter deployment times (9, 4, and 3 days) to determine whether saturation is associated with an isotopic fractionation. The effect of sampler deployment height on $\delta^{15}N\text{-}NO_2$ values was also tested by deploying samplers simultaneously at 1 m, 2 m, and 3 m, once for 3 days and once for 4 days. HNO_3 was also collected with passive samplers monthly from in the ventilation potion of the tunnel from 5/10 to 5/11 and outside the tunnel from 1/11 to 5/11.

Emissions from fertilized soils

$NO\text{-}NO_2$ emitted as a by-product of nitrification and denitrification reactions in fertilized soils were sampled at the USDA ARS facility in Beltsville, Maryland (USA). The sampling

location was a conventionally managed cornfield (Field B) that is part of a larger study, Optimizing Production Inputs for Economic and Environmental Enhancement (OPE3). Field B at OPE-3 represents traditional farming practices common in Midwestern states, mainly corn row crops with a uniform application of urea-ammonia-nitrate (UAN) commercial fertilizer [*USDA*, 2012]. To sample soil emissions, Ogawa samplers were placed in a Teflon flux chamber installed over the fertilized soils. Samplers were installed directly following 120 lb N/ac fertilizer application (6/19/10 to 7/22/10) and 35 lb N/ac fertilizer application (6/2/11 to 6/19/11).

Emissions from livestock waste

NO_x emissions from livestock waste were characterization at turkey and dairy operations at the USDA ARS, Beltsville Agricultural Research Center (BARC), Beltsville, MD. Ogawa samplers were deployed from 6/24/11 to 7/22/11 in an open-air, 150 dairy cow barn equipped with ventilation fans. Ogawa samplers were also deployed from 6/24/11 to 7/22/11 in a closed room fitted with ventilation fans containing ~60 Tom turkeys. Lastly, in summer 2010 (8/6/10 to 8/21/10) Ogawa passive samplers were deployed at a concentrated animal feeding operation (CAFO) in central KS that contained 30,000 head of beef cattle in ~59 ha.

5.3 RESULTS AND DISCUSSION

5.3.1 NO_2 collection for isotope analysis

Ogawa samplers were deployed in duplicate (4 sample filters, 2 per sampler) at seven sampling sites to obtain standard deviation among sample filters. The standard deviation for $\delta^{15}N$ and $\delta^{18}O$ was 0.7‰ and 1.5‰, respectively. HNO_3 samplers were not tested for deviation

in this study due to a lack of available samplers during field sampling. Elliott et al. [2009] report the standard deviation among HNO_3 samplers as a range from 0 to 0.3‰ and 0.3 to 1.0‰ for $\delta^{15}N$ and $\delta^{18}O$, respectively.

5.3.2 $\delta^{15}N$ and $\delta^{18}O$ of emission sources

$\delta^{15}N$ values of NO_2 and HNO_3 emissions sampled from representative sources are summarized in Table 5.2 and Figure 5.1. The following sections discuss isotopic variability among emissions sources.

Table 5.2: $\delta^{15}N$ and $\delta^{18}O$ of NO_2 /HNO_3 sources, source location, and sampling method

Location	Source	Analyte	$\delta^{15}N$ (‰)	$\delta^{18}O$ (‰)	N = # samples	Sample method
Poultry facility, BARC	Turkey waste	NO_2	-8.5	31.9	1	Ogawa
Dairy barn, BARC	Cow waste	NO_2	-20.4	37.8	1	Ogawa
Cornfield, BARC	Fertilized soil	NO_2	-26.5, -30.8	-21.5, -20.2	2	Ogawa
Cattle CAFO, KS	Cow waste	NO_2	-29.0	13.3	1	Ogawa
Squirrel Hill Tunnel, Pittsburgh, PA	Vehicle exhaust	NO_2	15.0 $\pm$ 1.6	-7.8 $\pm$ 6.7	22	Ogawa
Squirrel Hill Tunnel, Pittsburgh, PA	Vehicle exhaust	HNO_3	6.2 $\pm$ 2.9	37.1 $\pm$ 12.7	15	HNO_3 sampler
SCR equipped coal-fired power plant, US	Power plant emissions	NO_x	19.4 $\pm$ 2.3	NA	16	EPA method 7
SNCR equipped coal-fired power plant, US	Power plant emissions	NO_x	14.2 $\pm$ 0.8	NA	3	EPA method 7
SNCR equipped coal-fired power plant, US	Power plant emissions	NO_x	10.6 $\pm$ 1.0	NA	23	EPA method 7

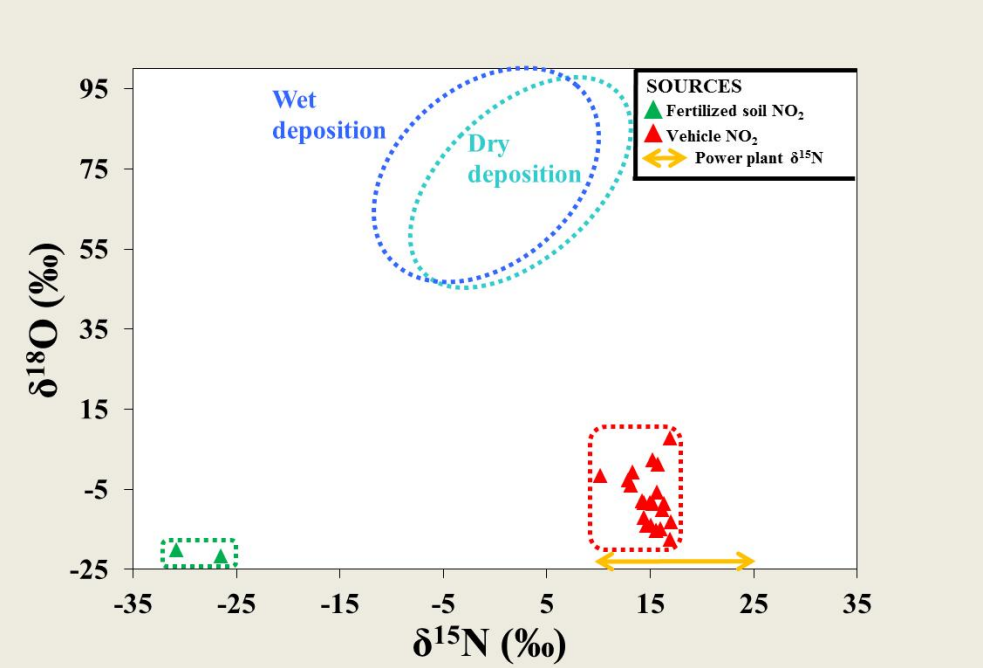

Figure 5.1: δ^{15}N-NO_2 and δ^{18}O-NO_2 values of emissions sources from this study relative to the range of observed values in wet and dry deposition in the continental U.S. [*Kendall et al.*, 2007].

5.3.3 δ^{15}N of power plant NO_x emissions [*Felix et al.*, 2012]

Plant A: Coal-fired EGU with SCR/LNB

NO_x concentrations in the SCR stack ranged from 29.2 to 37 ppm (average = 32 ppm, st dev. ±1 ppm), as measured by the continuous emission monitoring (CEM) system installed at the power plant. Nitrate concentrations of the grab samples collected at the SCR-equipped EGU using the absorbing solution (H_2SO_4/H_2O_2) ranged from 4.2 ppm to 16.7 ppm (average = 7 $\pm$ 5 ppm). Samples collected using the grab sample method had a mean δ^{15}N-NO_3 value of +20‰ $\pm$ 2‰ (n = 5). The relatively large standard deviation is due to one low δ^{15}N measurement of +15.5‰. If this sample is discarded, the standard deviation among remaining samples is 0.8‰

and the mean $\delta^{15}N\text{-}NO_3$ value is +19.5‰. Based on these results, we determined that the grab sample method and associated modifications were adequately precise for future stack sampling sessions.

Plant B: Coal fired EGU with LNB

NO_x concentrations during sampling at the LNB-equipped EGU ranged from 100.5 to 170.8 ppm (average = 132 ppm, st. dev. = ±16 ppm) as measured by the Continuous Emission Monitoring (CEM) system installed at the power plant. Nitrate concentrations in the H_2SO_4 grab samples ranged from 25.7 ppm to 35.2 ppm (average = 27 $\pm$ 6 ppm) and the samples did not contain nitrite (i.e., the HNO_2 and NO_2 absorbed was oxidized). The H_2SO_4 grab samples had a mean $\delta^{15}N\text{-}NO_3$ value of +9.8 $\pm$ 0.8‰ (n = 4). The NaOH grab sample nitrate concentrations ranged from 14.6 ppm to 22.3 ppm (average = 19 $\pm$ 3 ppm); these samples contained nitrite (i.e., not all NO_2 and HNO_2 oxidized) however quantification of nitrite concentrations on the IC was problematic due to overlapping sulfate peaks. The NaOH samples had a mean $\delta^{15}N\text{-}NO_3/\ NO_2$ value of +11.0 $\pm$ 0.9‰ (n = 4). The TEA grab sample nitrate concentrations ranged between 8.3 ppm and 19.0 ppm (average = 12 $\pm$ 5ppm); these samples also contained nitrite, so determination of nitrite concentrations in these samples using the IC was again problematic due to an unidentified overlapping peak. The TEA samples had a mean $\delta^{15}N\text{-}NO_3/\ NO_2$ value of +10.1 $\pm$ 0.5‰ (n = 4). The mean $\delta^{15}N$ value for grab samples in all three solutions was +10.1 $\pm$ 0.5‰ (n = 12). $\delta^{15}N$ values were not significantly different among absorbing solution treatments ($\alpha = 0.05$, $p = 0.14$) (ANOVA: Single factor) indicating consistent results.

Plant C: Coal fired EGU with SCR/OFA/LNB, and Coal fired EGU with SNCR/OFA/LNB ("SNCR on") and OFA/LNB ("SNCR off")

NO_x concentrations during sampling at the SNCR/OFA/LNB equipped EGU ranged from 7.8 to 16.7 ppm (average = 15.2 ppm, st. dev. = ±1.0 ppm). The SNCR/OFA/LNB sample nitrate concentrations ranged from 18.3 ppm to 29.7 ppm (average = 24.8 $\pm$ 5.8 ppm). The SNCR/OFA/LNB grab samples had a mean δ^{15}N-NO_3 value of + 14.2‰ $\pm$ 0.8‰ (n = 3).

NO_x concentrations during sample at the OFA and LNB-equipped EGU ranged from 15.4 to 16.6 ppm (average = 16.0 ppm, st. dev. = ±0.3 ppm). The OFA/LNB sample nitrate concentrations ranged from 30.3 ppm to 31.8 ppm (average = 31.0 $\pm$ 0.8 ppm). The OFA/LNB grab samples had a mean δ^{15}N-NO_3 value of + 12.2‰ $\pm$ 0.4‰ (n = 3).

NO_x concentrations during sample collection at the SCR/OFA/LNB-equipped EGU ranged from 8.9 to 18.6 ppm (average = 15.8 ppm ±0.8 ppm). Nitrate concentrations in the SCR/OFA/LNB H_2SO_4 grab samples ranged from 3.4 ppm to 5.0 ppm (average = 4.1 $\pm$ 0.8 ppm). The SCR/OFA/LNB H_2SO_4 grab samples had a mean δ^{15}N-NO_3 value of +20‰ $\pm$ 5‰ (n = 3).

Plant D: Coal fired EGU with SCR system on ("SCR on") and *Coal fired EGU with SCR system off ("SCR off")*

NO_x concentrations during sampling at *"SCR on"* EGU ranged from 26 to 31.6 ppm (average = 29 ppm, st. dev. = ± 2 ppm). The *"SCR on"* sample nitrate concentrations ranged from 12.8 ppm to 13.7 ppm (average = 12.9 ppm, st. dev. = $\pm$ 0.4 ppm). The *"SCR on"* grab samples had a mean δ^{15}N-NO_3 value of + 19.3‰ $\pm$ 0.5‰ (n = 8).

NO_x concentrations during sample at the "SCR off" EGU ranged from 134.7 ppm to 155 ppm (average = 149 ppm, st. dev. = $\pm$ 5 ppm). The '"SCR off" sample nitrate concentrations ranged from 23.2 ppm to 38.1 ppm (average = 32 ppm, st. dev. = $\pm$6 ppm). The "SCR off" grab samples had a mean δ^{15}N-NO_3 value of + 10.5‰ $\pm$ 0.8‰ (n = 8).

Comparison of absorbing solutions.

Similar δ^{15}N-NO_x values observed using all three absorbing solutions suggest absorbing solution reactions do not affect measured δ^{15}N-NO_x values. All sampling techniques and post-sampling treatment among the absorbing solutions were essentially identical. In comparing absorbing solutions during the NO_x collection at Plant B, the grab sample method using the H_2SO_4 absorbing solution showed the greatest precision of δ^{15}N values within replicate samples (st. dev. = $\pm$ 0.2‰) and a standard deviation of $\pm$ 0.8‰ from sample to sample. As a result, subsequent NO_x emission sampling at Plant C and D employed the H_2SO_4 absorbing solution.

The influence of emission controls on δ^{15}N-NO_x values:

Figure 5.2 summarizes the ranges of $\delta^{15}NO_x$ values relative to power plant technology at each plant. The large difference in values observed between samples from the various SCR-equipped (+19.5, +19.8, and +19.3‰ at Plant A, Plant C, and Plant D, respectively) and non-SCR-equipped EGU samples (+9.8, +12.2, and 10.5‰ at Plant B, Plant C, and Plant D, respectively) likely results from the SCR reaction. When NO_x reacts with injected NH_3 over a catalyst, the resulting N_2 forms from the nitrogen atoms in each reactant. The higher δ^{15}N value associated with the SCR NO_x emissions suggests that the isotope with less mass, ^{14}N, preferentially reacts with NH_3, whereas the isotope with more mass, ^{15}N, is subsequently released to the atmosphere. This suggests that N_2 product is subject to kinetic fractionation during the reaction between NO_x and NH_3 at the high temperatures in the power plant stacks. Kinetic fractionation would favor the ^{14}N reacting to form the N_2 product. Note that a similar

magnitude effect was noted whether the SCR and non-SCR comparison was made across plants or at different units within the same plant. The fact that the SNCR/OFA/LNB δ^{15}N-NO_x value (Plant C 14.2‰) falls between the OFA/LNB and SCR/OFA/LNB values indicates that while the SNCR/OFA/LNB may be more efficient than the OFA/LNB technology alone, it is not more efficient than the SCR/OFA/LNB technology. The difference between SNCR/OFA/LNB and SCR/OFA/LNB values could also result from the competing SNCR reaction wherein the SNCR reagent (NH_3 or urea) reacts to form NO_x [*Srivastava et al., 2005*]. The higher standard deviation among samples from SCR operations (2, 5, and 0.5‰ at Plants A, C, and D, respectively) may be due to varying efficiency in the SCR technology or varying NO_x concentrations in the stack gas; both of which would lead to varying NH_3 to NO_x reaction ratios and thus variable nitrogen isotope fractionation. For instance, if the NO_x to NH_3 reaction ratio is greater than 1, then NO_x does not fully react. This will lead to the less massive ^{14}N atom in NO_x reacting first thus resulting in kinetic fractionation. The degree of kinetic fractionation may vary with the varying NO_x to NH_3 reaction ratio. These various reactions and reaction efficiencies in different NO_x reduction technologies are allowing for varying isotope signatures associated with different NO_x reduction technologies.

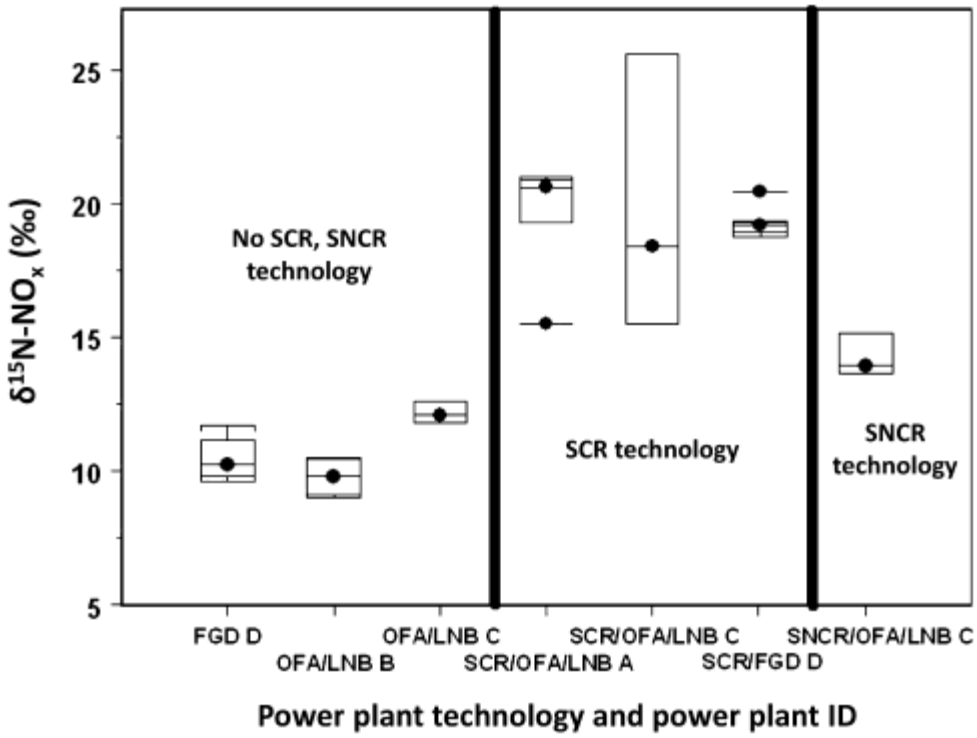

Figure 5.2: δ^{15}N-NO_x from power plants by emission control type [from *Felix et al.*, 2012].

5.3.4 δ^{15}N and of vehicular emissions

The δ^{15}N-NO_2 values of vehicular emissions ranged from to +10.2 to +17.0 ‰ with a mean of +15.0 + 1.6‰. Filters in the Ogawa samplers were saturated by the end of the month deployment time. To test for fractionation due to saturation, filters were also deployed for a periods of 9 (n =2) days, 4 days (n=3) and 3 (n=3) days in which time the filters did not saturate. Saturated filters and unsaturated filters had mean δ^{15}N-NO_2 values of +15.4$\pm$ 0.9‰ and +14.2 $\pm$ 2.6‰, respectively. This negligible difference indicates that saturation of the filters does not cause isotopic fractionation.

The effect of sampler deployment height on $\delta^{15}N\text{-}NO_2$ values was also tested by deploying samplers simultaneously at 1m, 2m, and 3m, once for 3 days and once for 4 days (Figure 5.3). NO_2 concentrations decreased linearly with deployment height suggesting NO_2 may be deposited readily with only a portion being transported into upper levels of the atmosphere (Figure 5.3). Additionally NO_2 concentrations were higher during the work week (Monday through Friday afternoon) relative to the weekend (Friday afternoon through Sunday), presumably due to weekly variations in traffic density. $\delta^{15}N\text{-}NO_2$ values for the 4 day deployment spanned a small range compared to the 3 day deployment. Standard deviation among samplers deployed at various heights during the 3 and 4 day deployments were $\pm$ 0.8 and $\pm$ 0.2‰, respectively (Figure 5.3) so deployment height was not as significant factor in value $\delta^{15}N\text{-}NO_2$ observed. This suggests that the while NO_2 from vehicles is more concentrated at lower heights, vehicle NO_2 at the tunnel is still the major source at the higher deployment heights.

HNO_3, an oxidation product of NO_2, was also collected at the tunnel and the $\delta^{15}N\text{-}HNO_3$ values ranged from to +0.9 to +11.1‰ with a mean of +6.2 + 2.9‰ (Figure 5.4). $\delta^{15}N\text{-}HNO_3$ values are on average 8.8 ‰ lower than the $\delta^{15}N\text{-}NO_2$ values at the tunnel indicating a portion of this difference is likely due to fractionation during oxidation to the HNO_3. The5. offset could also result from mixing with a source characterized by a lower $\delta^{15}N$ value (Figure 5). $\delta^{15}N$ of NO_2 and HNO_3 is significantly correlated with $\delta^{18}O$ of NO_2 and HNO_3 (R^2=0.87, $p<0.00001$) indicating that both $\delta^{15}N$ and $\delta^{18}O$ values are affected during oxidation reactions to HNO_3 (Figure 5.4).

$\delta^{15}N\text{-}NO_2$ values from vehicle emissions reported in this study (+10 to +17‰) are higher than previous studies. For example, NO_2 collected by Amman et al., [1999] and Redling et al.,

[2012] had δ^{15}N-NO_2 values ranging from +2 to +10‰. These collections occurred at distances up to 10m from the road, and thus were potentially influenced by mixing with other NO_2 sources, altered δ^{15}N-NO_2 in the mixture. Moore [1977] collected vehicle NO_x that had δ^{15}N values ranging from +3.4 to +3.9‰, while another study collected vehicle NO_x from idling vehicles yielding δ^{15}N-NO_x values ranged from -13 to -2‰ [*Heaton*, 1987]. During idling, engines require a higher air to fuel ratio. Since vehicle NO_x is comprised of both 'fuel' and 'thermal' NO_x, changing this ratio should alter the resulting δ^{15}N by changing the proportion of N originating from the fuel or air, and also the resulting combustion efficiency [*EPA*, 1999]. As a consequence, it is expected that idling NO_x reported previously is not necessarily representative of vehicle NO_x emitted from vehicles. Moore [1977] collected vehicle NO_x that had δ^{15}N values ranging from 3.4 to 3.9. These δ^{15}N values were obtained before the production of vehicles equipped with three way catalytic converters to reduce NO_x emissions. The TWC dissociates NO_x in vehicle emissions to N and O atoms that then recombine to form N_2 and O_2. If this process is not quantitative, it will likely alter the δ^{15}N of the remaining NO_x passing over the catalyst relative to the original emissions. The NO_x that dissociates more readily will contain the lighter ^{14}N atom leaving the NO_x more enriched in ^{15}N. This suggests that as NO_x reduction technologies have changed through the years and become more efficient, the δ^{15}N-NO_x values of vehicle emissions have increased. This phenomenon is also observed as efficiency of SCR technology in power plants increased [*Felix et al.*, 2012].

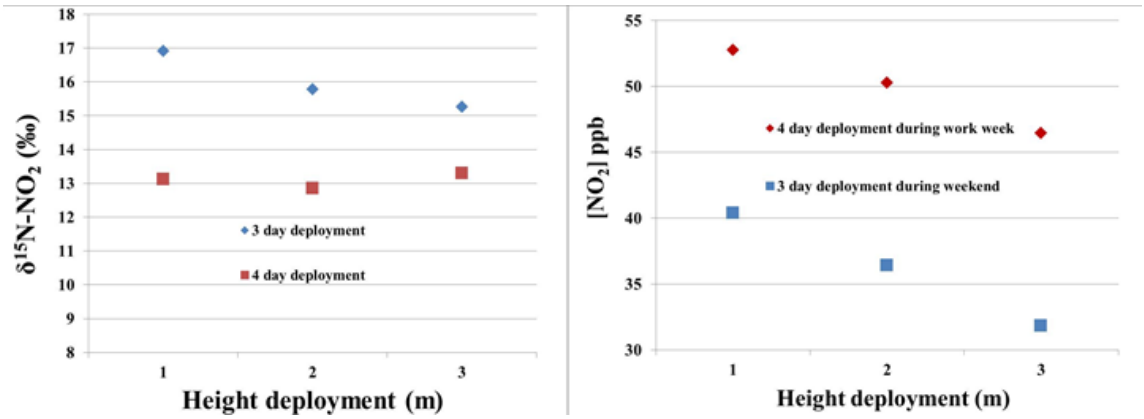

Figure 5.3: The effect of Ogawa sampler deployment height on δ^{15}N-NO_2 values and NO_2 concentrations.

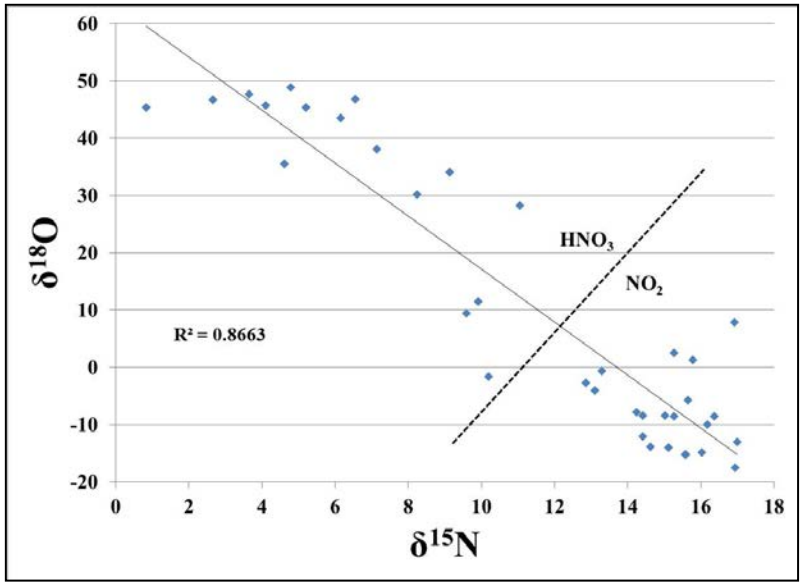

Figure 5.4: δ^{15}N vs. δ^{18}O of vehicle NO_2 and HNO_3 emissions. The dotted line separates NO_2 and HNO_3 emissions.

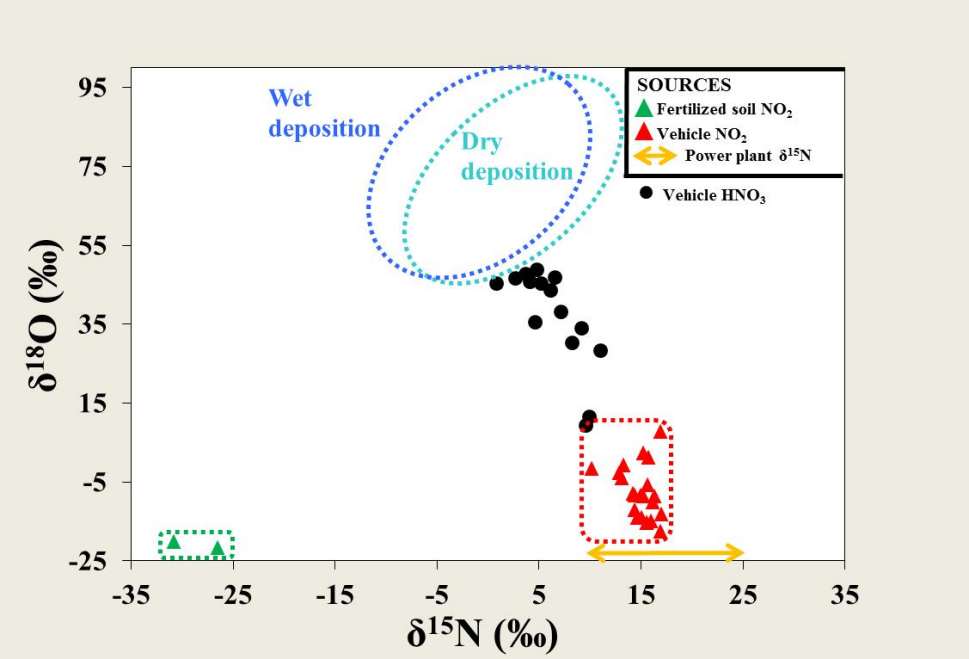

Figure 5.5: $\delta^{15}N$ and $\delta^{18}O$ of HNO_3 vehicle emissions plotted with $\delta^{15}N$-NO_2 and $\delta^{18}O$-NO_2 values of emissions sources from this study.

5.3.5 NO_2 concentration, $\delta^{15}N$ and of $\delta^{18}O$ of fertilized soils emissions

NO_2 concentrations sampled in flux chambers at a fertilized cornfield were 19.8 and 40.0 ppb following 120 lb N/ac (6/19/10 to 7/22/10, 33 days) and 35 lb N/ac (6/2/11 to 6/19/11, 15 days) fertilizer applications, respectively. This difference in NO_2 concentration is likely due to the difference in sampling period. The longer sampling period has a lower concentration because it is sampling a longer period of time after the initial NO_x pulse due to fertilization. The relatively high observed NO_2 concentrations in the chambers reflect the accumulation of NO_2 in the flux chamber from soils and are much high than ambient NO_2 concentration measurements at nearby (~4 ppb).

Two $\delta^{15}N\text{-}NO_2$ (-26.5, -30.8‰) and $\delta^{18}O\text{-}NO_2$ (-21.5, -20.2‰) values were obtained from the emission of NO_2 from fertilized soils. The resulting $\delta^{15}N\text{-}NO_2$ range is within the range of soil $\delta^{15}N\text{-}NO$ collected in laboratory experiments reported by Li and Wang [2008] (-50 to -20‰). In comparison to Li and Wang [2008], the results reported here represent an integrated $\delta^{15}N$ value of biogenic NO_2 emissions over 33 day and 17 day deployment periods in an actual field setting. The average values (-35.5 and -29.1‰) of the two lab experiments performed by Li and Wang [2008] are much closer to our values that represent an integrated emission $\delta^{15}N$ value.

Observed low $\delta^{15}N$ values of soil-derived NO_2 are expected as N_2O produced by the same denitrification and nitrification reactions has $\delta^{15}N$ values as low as -46.6‰ within a few days of irrigation of fertilized fields [*Perez et al.*, 2001]. Denitrification and nitrification are biological processes that kinetically favor the ^{14}N in the product gases [*Shearer*, 1988, *Baggs*, 2008]. Moreover, nitrification generally shows greater depletion of ^{15}N (and thus lower $\delta^{15}N$ values) in the NO and N_2O products than denitrification [*Li and Wang*, 2008; *Baggs*, 2008]

N_2O produced during denitrification and nitrification is also depleted in ^{18}O. Similarly, in this study, $\delta^{18}O$ values of soil NO_2 are low (-21.5, -20.2‰) relative to other NO_x sources. These low $\delta^{18}O\text{-}NO_2$ values may reflect the incorporation of isotopically depleted groundwater (~-10‰) during NO producing reactions. Although subsequent oxidation reactions in the atmosphere alter $\delta^{18}O$ values, it is possible that this uniquely low $\delta^{18}O$ value from soils is not entirely masked in ambient samples [*Elliott et al., in revision*].

5.3.6 NO_2 concentrations, $\delta^{15}N$ and of $\delta^{18}O$ of livestock waste emissions

The NO_2 concentrations obtained from the turkey facility, dairy barn, and CAFO were 7.1, 5.5, 4.0 ppb, respectively. The $\delta^{15}N\text{-}NO_2$ and $\delta^{18}O\text{-}NO_2$ values obtained from the turkey

facility, dairy barn, and CAFO were -8.5, +31.9; -20.4, +37.8; and -29.0, +13.3‰, respectively. It is assumed that these values reflect NO_2 emissions from microbial denitrification and nitrification in the livestock waste. This is reflected in the low $\delta^{15}N$ values similar to those observed from fertilized soils. The turkey facility has a $\delta^{15}N\text{-}NO_2$ value 20‰ higher than the mean fertilized soils; this suggests that the constant flow of fresh air into the turkey pens via ventilation fans may be introduce mixing with another NH_3 source with higher $\delta^{15}N$ into the facility. The $\delta^{18}O\text{-}NO_2$ values of the livestock waste emissions were significantly higher than that from fertilized soil NO_x. This is most likely due to the soil emissions being sampled in a chamber directly over the soils while the samplers in the livestock facilities were sampled above the animals allowing emissions from waste to experience oxidation via O_3 that would increase the $\delta^{18}O$ value.

5.4 CONCLUSION

Due to the adverse effects of excess N deposition, air quality regulations have been implemented that brought about improvements in NO_x reduction technology for fossil fuel based NO_x emission sources. Differences among $\delta^{15}N\text{-}NO_x$ values from power plants with varying emission reduction technologies reported in this work suggest that monitoring changes in $\delta^{15}N\text{-}NO_x$ and its oxidation products can be a valuable tool for assessing the effectiveness of SCR or SNCR technology for reducing power plant NO_x contributions to reactive nitrogen deposition. Varying $\delta^{15}N\text{-}NO_x$ values reported from vehicle emissions suggest that this concept may also be applied to changing NO_x reduction technologies and efficiencies in vehicles.

The $\delta^{15}N\text{-}NO_x$ values reported from power plant and vehicle emissions are higher than those of biogenic NO_x emissions originating form fertilized soils and livestock waste. This difference between $\delta^{15}N$ values of fossil fuel based sources and biogenic sources allows for identification and possible quantification of source contributions to ambient NO_x concentrations.

6.0 EXAMINING THE TRANSPORT OF NO_2 AND HNO_3 ACROSS LANDSCAPES USING STABLE ISOTOPE RATIOS

6.1 INTRODUCTION

NO_x (NO and NO_2) emissions are directly proportional to wet and dry atmospheric deposition of NO_2 and its oxidation products (NO_y). Deposition of oxidized nitrogen compounds are a substantial source of nitrogen pollution to sensitive terrestrial, aquatic, and marine ecosystems [*Walker et al.,* 2000; *Chimka et. al.,* 1997; *Fowler et al.,* 1998; *Davidson et al.,* 2012]. NO_x (NO_x =NO + NO_2) emissions are regulated in the U.S. and have decreased 36% since the implementation of the Clean Air Act and Amendments [*Davidson et al.,* 2012]. While these reductions are promising, NO_x emissions are largely unregulated in developing South American and East Asian countries where NO_x emissions to expected to rise globally [*Townsend,* 2010]. For example, from 2006 to 2009, NO_2 concentrations in East Asia increased 18.8% [*Lasmal et al.,* 2011]. Consequently, NO_x emissions and resulting transport and deposition have become of increasing international concern to air quality managers, modelers, and epidemiologists.

Global NO_x emissions are dominated by fossil fuel combustion (e.g. coal-fired power plants and vehicles). For example, in a review of NO_x inventories reported for China and the U.S., vehicles and power generation together contribute 59% and 89% of the total NO_x emissions, respectively [*Reis et al.,* 2009]. While these fossil fuel emissions are emitted from urban settings, they are subject to transport in the atmosphere and can thus be deposited in more nitrogen (N) sensitive ecosystems. Excess N loading to these N sensitive ecosystems can lead to eutrophication (i.e., algal blooms, hypoxia) of surface waters, decrease biodiversity, and increase soil acidity [*Galloway et al,* 2004]. Although NO_x emissions are predominately fossil fuel based, other natural sources can be locally significant (e.g. lightning, soil microbes, biomass burning). These natural emission sources are difficult to quantify due to their diffuse spatial distribution and lack of direct emission measurements. For instance, Holland et al. [1999] report a global soil NO_x emission range of 4–21 Tg N yr^{-1} and recent studies have reported a lightning-produced NO_x range of 1 to 20 Tg yr^{-1} [*Schumann et al.,* 2007].

Stable isotope techniques are an emerging tool used in the source quantification of nitrogen emissions. NO_x emissions associated with fossil fuel activity and natural processes have distinctly different nitrogen isotopic compositions ($\delta^{15}N\text{-}NO_x$) (Figure 6.1) [*Chapter 5*] that can be used characterize source and transport of NO_x emissions. Coal-fired power plants and vehicles have high $\delta^{15}N\text{-}NO_x$ values, +6 to +20‰ and +3 to +17‰, respectively [*Heaton,* 1987; *Felix et al.,* 2012; *Redling et al., in review; Amman et al.,* 1999; Pearson et al., 2000; Moore 1977]. In comparison, reported $\delta^{15}N\text{-}NO_x$ values of NO_x emitted from fertilized soils (-50 to -20‰) [*Li et al.,* 2008; *Chapter 5*], livestock waste (-29.0 to -8.5‰) and lightning (-0.5 to +1.4‰) [*Hoering,* 1957] are considerably lower than those emissions from fossil fuel combustion. In contrast to the nitrogen isotopic ratio of NO_x, the oxygen isotopic ratio ($\delta^{18}O$) is

generally believed to result from variable oxidation pathways [*Michalski et al.,* 2003, *Hastings et al.,* 2003]. However, a new inventory of $\delta^{15}N\text{-}NO_2$ emissions [*Chapter 5*] reports unusually low $\delta^{18}O\text{-}NO_2$ values of NO_x emitted from soil (-21.5 to -20.2‰) and vehicles (-7.8 $\pm$ 6.7‰). In this study, we build on this knowledge of varying isotopic signatures among NO_x sources and: 1) document the utility of $\delta^{15}N$ and $\delta^{18}O$ in ambient NO_x (and NO_x oxidation product, HNO_3) to examine transport of NO_x across various land-use types (conventionally managed cornfield, concentrated animal feeding operation (CAFO), and dunes on a barrier island); 2) use an isotope mixing model to predict first approximations of NO_x source contributions to ambient NO_x concentrations; 3) reassess whether $\delta^{18}O$ values may retain a source signature in subsequent oxidation reactions.

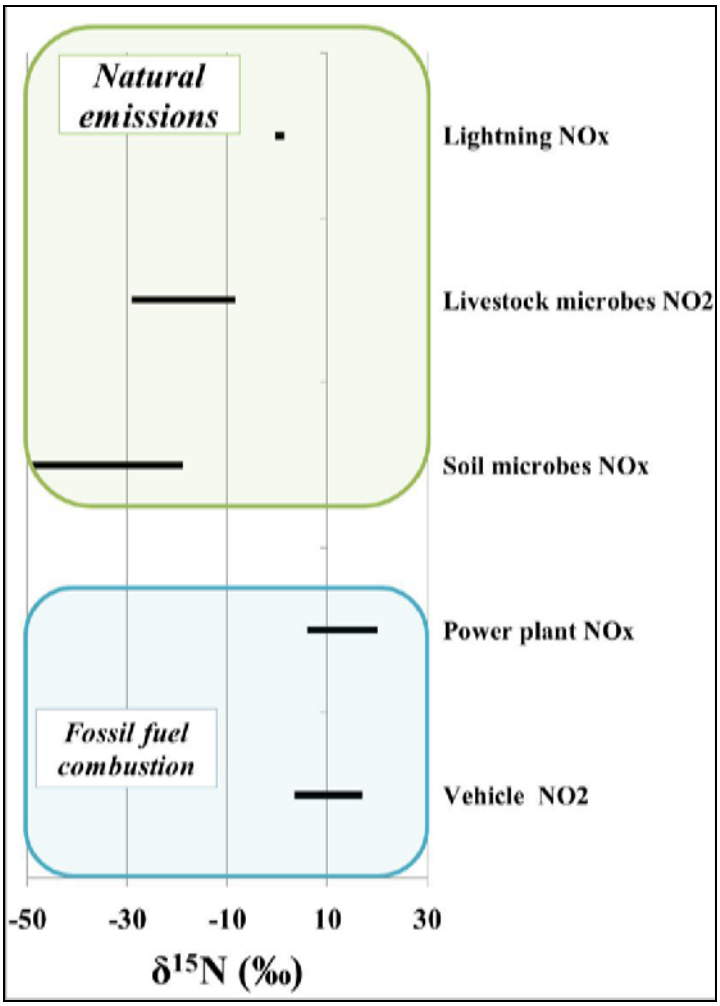

Figure 6.1: $\delta^{15}N$ of NO_x sources.

6.2 METHODS

6.2.1 NO_2 and HNO_3 emission collection methods for concentration and isotope analysis

Passive samplers are ideal for the collection of dry nitrogen deposition as they are less expensive, easy to use, and do not require electricity [*Pulchalski et al.,* 2011; *Elliott et al.,* 2009; *Golden et al.,* 2008]. These advantages allow for multiple deployments at a single site. Ogawa

NO_2 passive samplers and HNO_3 samplers have been used in previous studies to collect NO_2 and HNO_3 emissions for NO_2 and HNO_3 concentrations and isotopic analysis. (*Redling et al., in review; Bytnerowicz et al.,* 2005; *Elliott et al.,* 2009) The Ogawa is a double-sided passive diffuse sampler equipped with a diffusive end cap, followed by a stainless steel screen, and a 14mm quartz filter impregnated with phosphorous acid. The HNO_3 sampler is a sampler designed by Bytnerowicz, et al. [2005] in which the HNO_3 is collected in the sampler using a 47mm nylon filter. In this study, HNO_3 samplers were used to collect HNO_3 emissions and the Ogawa passive samplers were used to collect NO_2 emissions.

6.2.2 NO_2 and NO_3concentration analysis method

Nitrate and nitrite concentrations of power plant stack samples were analyzed using a Dionex ICS 2000 Ion Chromatograph. All other nitrite samples were analyzed using a Thermo Evolution 60S UV-vis. During this study, NO_2 and HNO_3 sampler blanks in a sealed mason jar traveled with the deployed field samplers and were later analyzed for [NO_2] and [HNO_3] to allow for a "blank correction".

6.2.3 NO_2 and HNO_3 isotopic analysis method

For isotopic analysis, a denitrifying bacteria, *Pseudomonas aureofaciens,* was used to convert 20 nmoles of NO_2^- or NO_3^- into gaseous N_2O prior to isotope analysis [*Sigman et al.,* 2001]. Samples were analyzed for $\delta^{15}N$ in duplicate using an Isoprime Trace Gas and Gilson GX-271 autosampler coupled with an Isoprime Continuous Flow Isotope Ratio Mass Spectrometer (CF-IRMS) at the University of Pittsburgh *Regional Stable Isotope Laboratory for*

Earth and Environmental Science Research. Nitrogen and oxygen isotopic ratios are reported in parts per thousand relative to atmospheric N_2 and VSMOW as follows:

$$\delta\ (‰) = \frac{(R)_{sample} - (R)_{standard}}{(R)_{standard}} \times 1000 \qquad (1).$$

where R denotes the ratio of the heavy to light isotope (e.g., $^{15}N/^{14}N$ or $^{18}O/^{16}O$). International reference standards USGS34, USGS32, USGS35 and IAEA N3 were used for data correction. Replicates had an average standard deviation (σ) of 0.2‰ for $\delta^{15}N$ and of 0.5‰ for $\delta^{18}O$.

6.2.4 Description of sites for sampling transects

Conventionally managed cornfield transect

At the USDA ARS facility in Beltsville Maryland (USA), the Optimizing Production Inputs for Economic and Environmental Enhancement (OPE3) site consists of four adjacent watersheds that are managed with different crop management systems. Field B at OPE-3 was chosen as a sampling transect site because it represents traditional farming practices common in Midwestern states, mainly corn row crops with a uniform application of urea-ammonia-nitrate industrial fertilizer applied with planting (35 lbs N/ac) and later as side-dressing (120 lbs N/ac). [*USDA*, 2012]. Urea Ammonia Nitrate (UAN) was the fertilizer applied. The fertilizer is "side-dressed" meaning that the nitrogen is applied to the soil subsurface within the root zone. The sampling transect began at the midpoint of Field B and ended in a downwind riparian area (Figure 6.1). A site upwind of the transect was also sampled directly adjacent to the cornfield and near a commuter road. The transect at Field B was sampled a total of four times over a two-year period

(Table 6.1). Although this transect was established to sample NO_2 emitted from fertilized soils, it was adjacent to a commuter road and within 500m of the Baltimore-Washington parkway (a heavily trafficked road with ~51,000 vehicles/day) [*MD Department of Transportation*, 2011].

Table 6.1: Description of conventionally managed cornfield sampling sessions.

Sampling Session	Date	Fertilizer Application
1	5/22/10 to 6/3/10	35 lbs N/ac
2	6/19/10 to 7/22/10	120 lbs N/ac
3	6/2/11 to 6/19/11	35 lbs N/ac
4	6/23/11 to 7/22/11	120 lbs N/ac

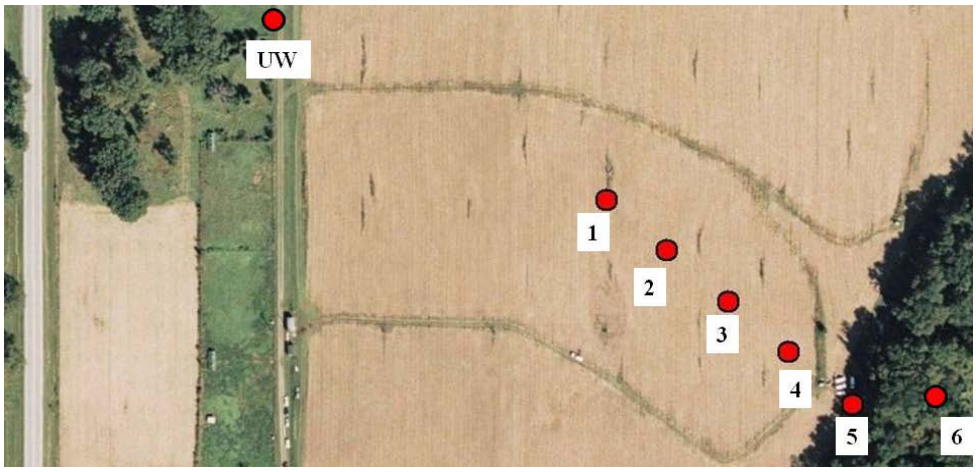

Figure 6.2: Conventionally managed cornfield. Red circles represent NH_3 passive sampling sites.

Confined animal feeding operation transect

A concentrated animal feeding operation (CAFO) containing 30,000 head of beef cattle over 59 ha [*Bonifacio*, 2009] was sampled in central Kansas (Figure 6.2). A transect was established radiating from the CAFO edge (0 m) to 5 downwind sites (30, 130, 230, 330 m, and

1.6 km from the CAFO edge). The average wind direction during the summer in at the CAFO site is from the south and southeast [*Bonifacio,* 2009]. The CAFO passive sampling was conducted from 8/6/10 to 8/21/10.

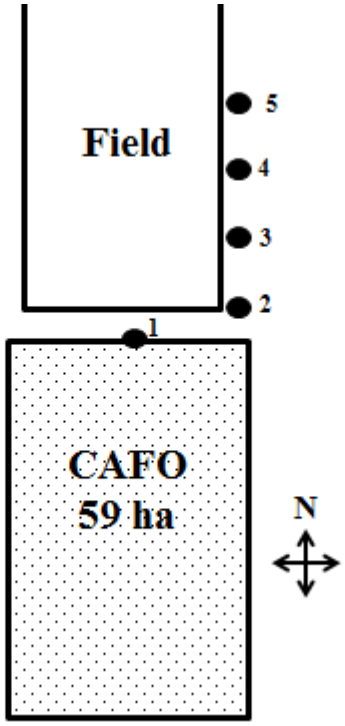

Figure 6.3: Diagram of concentrated animal feeding operation. Not to scale.

Bald Head Island dune transect

Bald Head Island, NC, USA is a barrier island off the east coast of the U.S. in which the primary transportation is electric golf carts, thus minimizing fossil fuel combustion emissions. A transect (4 sites) was established on the western part of the island from the edged of the maritime forest across a dune to the edge of the beach. Ogawa NO_2 passive samplers were deployed from 8/1/11 to 9/10/11.

6.3 RESULTS AND DISCUSSION

6.3.1 NO_2 and HNO_3 collection for isotope analysis

Ogawa samplers were deployed in duplicate (4 sample filters, 2 per sampler) at seven sampling sites to obtain standard deviation among sample filters. The standard deviation for $\delta^{15}N$ and $\delta^{18}O$ was 0.7‰ and 1.5‰, respectively. HNO_3 samplers were not tested for deviation in this study due to a lack of available samplers during field sampling. Elliott et al. [2009] report the standard deviation among HNO_3 samplers as a range from 0 to 0.3‰ and 0.3 to 1.0‰ for $\delta^{15}N$ and $\delta^{18}O$, respectively.

6.3.2 Conventionally managed cornfield transect

Tables 6.2 and 6.3 summarize [NO_2], [HNO_3], $\delta^{15}N$-NO_2, $\delta^{18}O$-NO_2, $\delta^{15}N$-HNO_3, and $\delta^{18}O$-HNO_3 data at the conventionally managed cornfield.

NO_2 concentration, $\delta^{15}N$-NO_2

NO_2 concentration over the four sampling sessions ranged from 1.7 to 6.1 ppb with a mean of 4.6 $\pm$ 1.1 ppb. Mean NO_2 concentrations after the 35lb N/ac and 120 lb N/ac fertilizer application were 4.1 and 5.0 ppb, respectively. This 22% increase in [NO_2] following the higher fertilization rate was expected since soil N availability in the soil increases rates of nitrification and denitrification wherein NO is released as a byproduct during these reactions. Differences in concentration between fertilization events may have been influenced by different sample exposure lengths (29 and 33 days following 35 and 120 lb N/ac applications, respectively) where the longer deployment time would include a more 'typical' ambient NO_2 concentrations.

$\delta^{15}N\text{-}NO_2$ values over the four sampling sessions ranged from -25.6 to -2.0‰ with a mean of -16.7 $\pm$ 7.3‰ and mean values at each site were not significantly different from site to site (ANOVA, p =0.96) (Figure 6.4). Mean $\delta^{15}N\text{-}NO_2$ values after the 35lb N/ac and 120 lb N/ac fertilizer application were -12.7 and -21.0‰, respectively. It is assumed that the two major local sources to the transect are vehicle emissions from upwind roadways and soil emissions from the fertilized field. The higher $\delta^{15}N\text{-}NO_2$ values during the sampling sessions after the 35 lb N/ac application indicates a smaller contribution from soil NO_x since vehicle emissions should be relatively consistent through time.

The mean $\delta^{15}N\text{-}NO_2$ values at sites upwind (UW), 1-4, ranged from -17.5 to -18.3‰ and indicated soil NO_x emissions as the primary NO_2 source. These low values suggest that a majority of vehicle NO_2 is deposited close to the roadway rather than transported over the cornfield. The mean $\delta^{15}N\text{-}NO_2$ values in the riparian zone at sites 5 and 6 were -15.5 and -12.8‰, respectively. This could indicate mixing with 'background' ambient NO_2, but could also indicate uptake of the lighter NO_2 by the riparian vegetation, as vegetation can assimilate NO_2 through the stomata [*Amman et al.,* 1999; *and refs therein*]. When the entirety of $\delta^{15}N$ and $\delta^{18}O\text{-}NO_2$ data from the cornfield transect is plotted with known isotopic values of NO_2 sources, the positions of the $\delta^{15}N$ data suggest a mixing between vehicle NO_2 and fertilized soil NO_2. Elevated $\delta^{18}O$ data relative to the source values indicate ^{18}O enrichment due to oxidation processes (Figure 6.5).

HNO_3 concentration, $\delta^{15}N\text{-}HNO_3$

HNO_3 concentration over the four sampling sessions ranged from 0.6 to7.7 $\mu g/m^3$ with a mean of 1.6 $\pm$ 1.3 $\mu g/m^3$. HNO_3 concentrations after the 35 lb N/ac and 120 lb N/ac fertilizer

application were 2.0 and 1.1 μg/m^3, respectively; a trend opposite to that of [NO_2]. This was unexpected because HNO_3 is an oxidation product of NO_2, but suggests that a non-local source of HNO_3 is being transported to the cornfield.

δ^{15}N-HNO_3 values over the four sampling sessions ranged from -10.8 to +2.9‰ with a mean of -4.4 $\pm$ 3.3‰ (Figure 6.6) and mean δ^{15}N values at each site were not significantly different from site to site (ANOVA, p = 0.75). Mean δ^{15}N-HNO_3 were higher after the 35 lb N applications than the 120 lb N applications (-2.4 and -6.3‰, respectively) which was also true for the δ^{15}N-NO_2 values suggesting a similar emission source. To further bolster this hypothesis, δ^{15}N-HNO_3 values were significantly correlated with corresponding δ^{15}N-NO_2 values obtained at each site during each sampling session, again suggesting a similar emission source (R^2=0.41, p=0.0009) (Figure 6.7). This suggests a portion of HNO_3 is from locally oxidized NO_2 while the remaining portion was transported from varying regional sources. When δ^{15}N-HNO_3 data are plotted with NO_2 isotopic source signatures (Figure 6.5), the values fall between the δ^{15}N-NO_2 values of the two local sources, fertilized soil and vehicles. The high δ^{18}O values obtained through oxidation cause the majority of the HNO_3 isotope data to fall within the range of previously reported dry deposition [*Elliott, et al.*, 2009].

Table 6.2: NO_2 concentration, $\delta^{15}N$-NO_2, and $\delta^{18}O$-NO_2 at the BARC cornfield transect

	Session 1 35 lbs N/ac			Session 2 120 lbs N/ac			Session 3 35 lbs N/ac			Session 4 120 lbs N/ac		
Site	$[NO_2]$ (ppb)	$\delta^{15}N$ (‰)	$\delta^{18}O$ (‰)	$[NO_2]$ (ppb)	$\delta^{15}N$ (‰)	$\delta^{18}O$ (‰)	$[NO_2]$ (ppb)	$\delta^{15}N$ (‰)	$\delta^{18}O$ (‰)	$[NO_2]$ (ppb)	$\delta^{15}N$ (‰)	$\delta^{18}O$ (‰)
UW	3.5	-4.7	5.7	6.0	-25.5	22.6	4.5	-16.4	29.3	4.4	-23.9	28.7
1	2.9	-8.2	12.2	2.7	NA	NA	4.7	-19.9	28.1	4.4	-25.6	19.9
2	3.7	-2.0	3.8	1.7	-23.2	9.2	4.5	-22.4	30.3	5.8	-22.5	21.0
2	4.6	-9.5	16.3	4.6	-19.0	9.3	4.2	-21.6	27.7	5.9	-20.6	18.4
4	3.4	-8.0	5.4	4.5	-17.1	17.4	3.6	-23.0	26.2	5.8	-25.0	13.7
5	4.3	-5.7	8.1	6.1	-16.0	25.5	4.2	-19.7	30.6	6.0	-20.6	21.6
6	4.3	-4.1	9.5	5.8	-14.1	29.6	5.6	-13.0	22.7	6.0	-20.0	25.9

Table 6.3: HNO_3 concentration, $\delta^{15}N$- HNO_3, and $\delta^{18}O$- HNO_3 at the BARC cornfield transect

	Session 1 35 lbs N/ac			Session 2 120 lbs N/ac			Session 3 35 lbs N/ac			Session 4 120 lbs N/ac		
Site	$[HNO_3]$ ($\mu g/m^3$)	$\delta^{15}N$ (‰)	$\delta^{18}O$ (‰)	$[HNO_3]$ ($\mu g/m^3$)	$\delta^{15}N$ (‰)	$\delta^{18}O$ (‰)	$[HNO_3]$ ($\mu g/m^3$)	$\delta^{15}N$ (‰)	$\delta^{18}O$ (‰)	$[HNO_3]$ ($\mu g/m^3$)	$\delta^{15}N$ (‰)	$\delta^{18}O$ (‰)
UW	1.6	-0.4	59.8	1.0	-2.1	52.8	0.9	-4.9	67.7	0.9	-5.5	68.5
1	7.7	2.9	22.8	NA	NA	NA	1.8	NA	NA	1.2	-7.1	62.4
2	1.9	-4.7	56.1	1.1	-7.5	53.3	1.5	-3.9	59.0	1.0	-8.7	61.3
2	1.8	-2.2	53.3	2.3	-4.3	47.4	1.5	NA	NA	1.1	-9.5	61.3
4	1.5	NA	NA	1.6	-1.7	39.4	1.9	-4.9	63.2	1.0	-10.8	63.3
5	1.4	-2.3	54.9	0.9	-5.7	61.8	1.7	-4.0	63.8	1.1	-4.7	64.3
6	1.8	0.5	48.0	0.6	NA	NA	0.7	-2.8	59.5	0.5	-7.7	71.6

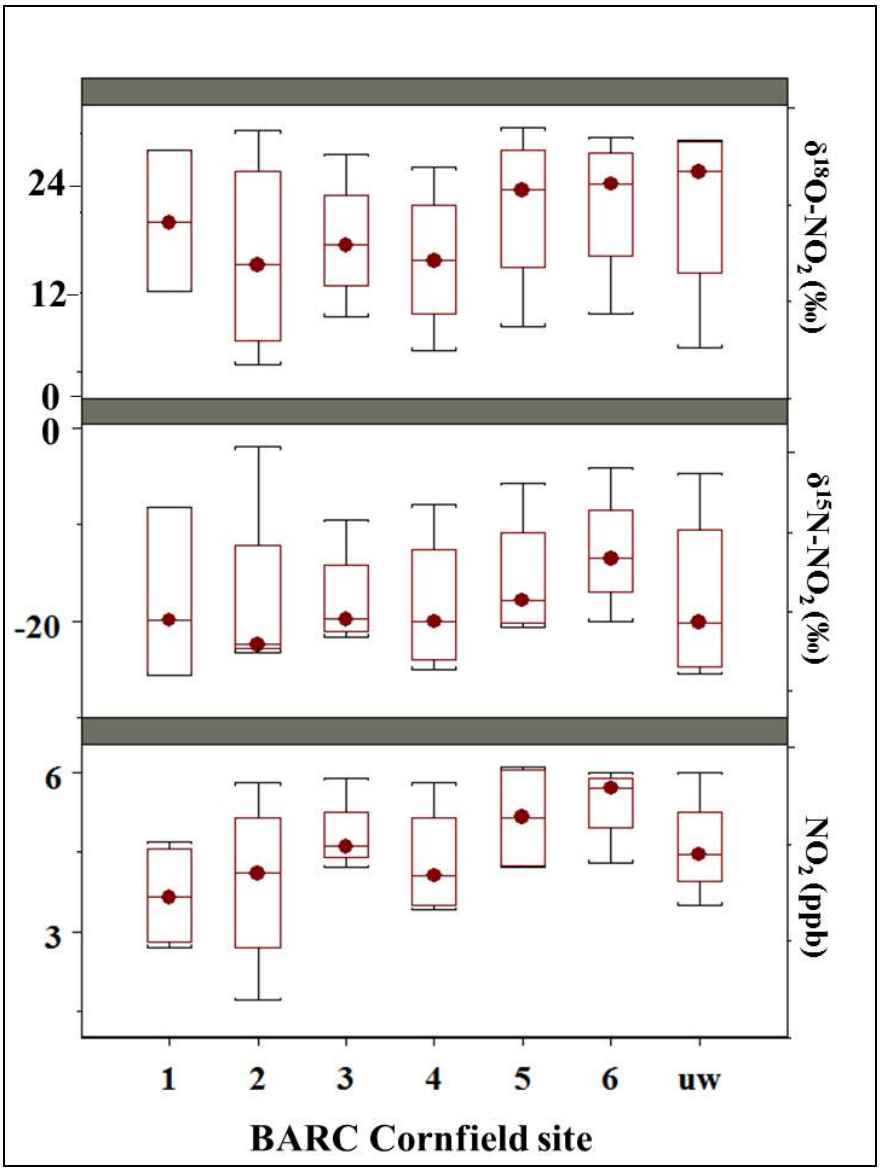

Figure 6.4: Box plots of δ^{15}N-NO_2, δ^{18}O-NO_2 and [NO_2] for all BARC cornfield sampling sessions.

.

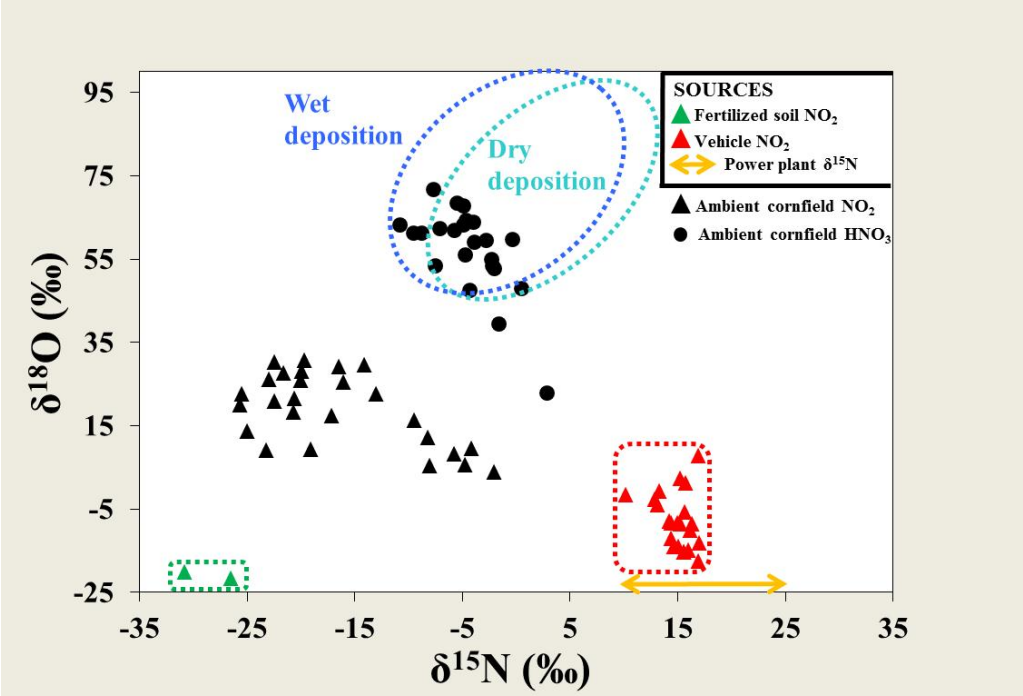

Figure 6.5: $\delta^{15}N$ and $\delta^{18}O$ of NO_2 and HNO_3 at the BARC cornfield transect plotted with NO_2 isotope source signatures.

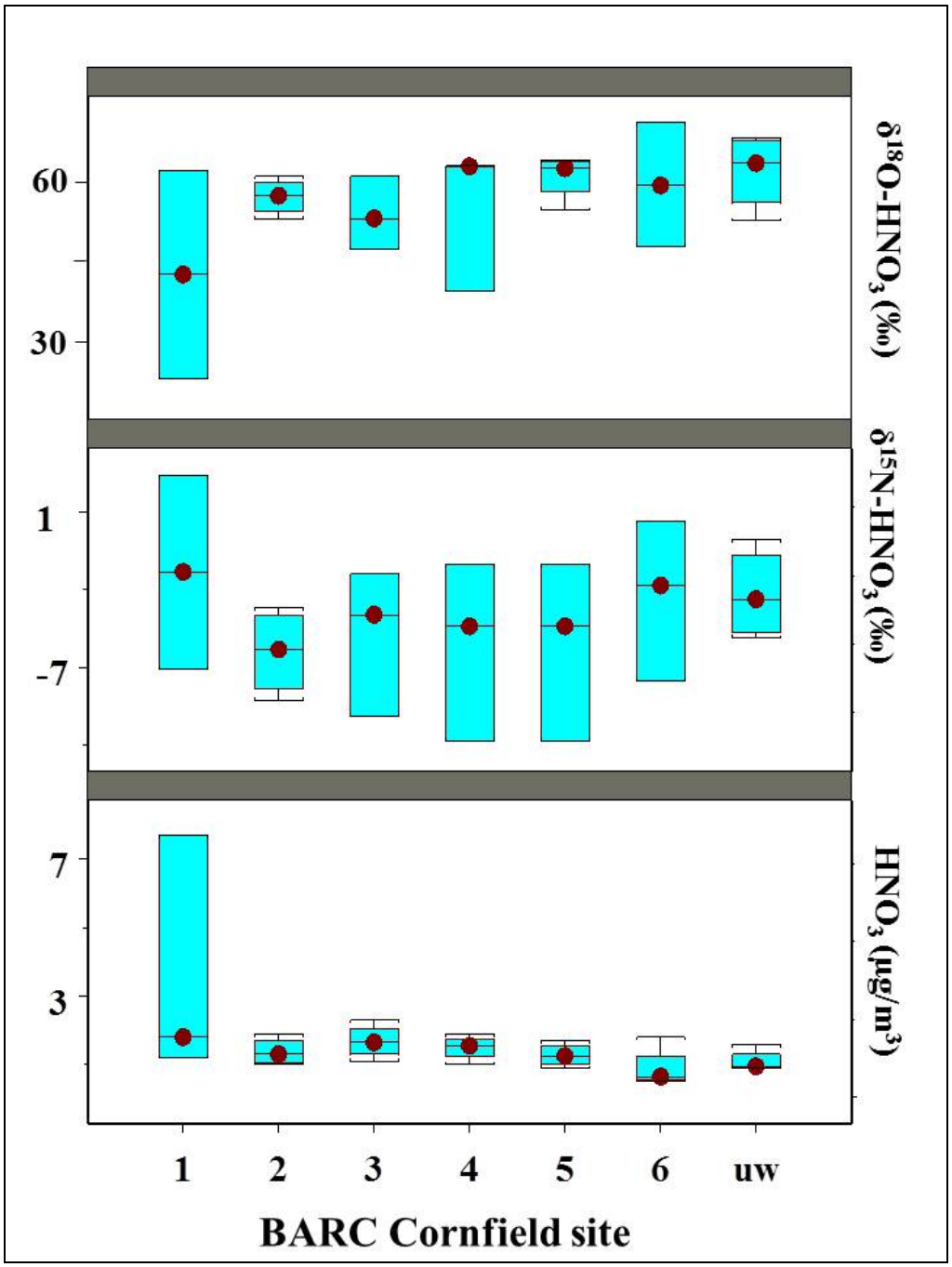

Figure 6.6: Box plot of δ^{15}N-HNO_3, δ^{18}N-HNO_3 and [HNO_3] for all BARC cornfield sampling sessions.

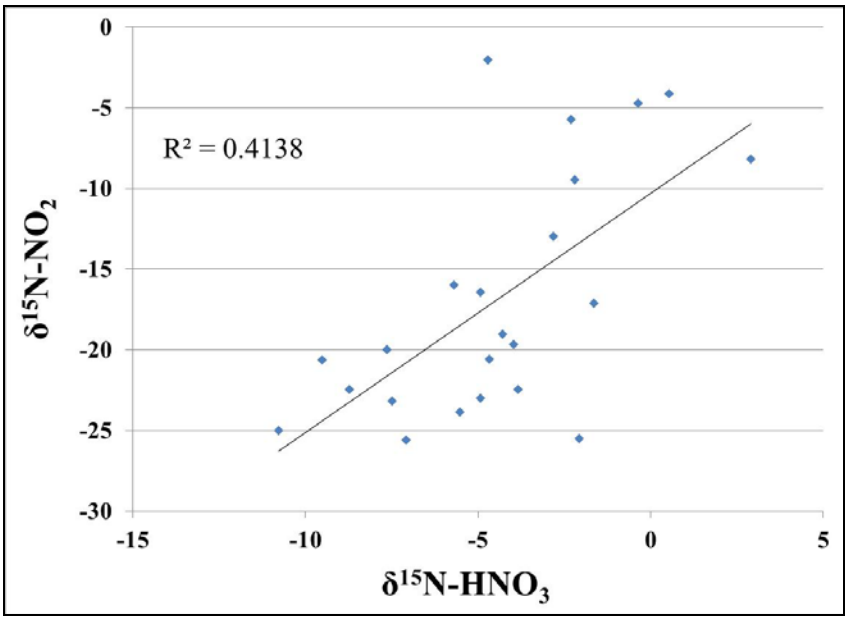

Figure 6.7: δ^{15}N-HNO_3 vs. δ^{15}N-NO_2 for each BARC cornfield sampling session.

Predicting % NO_2 source contribution at a conventionally managed cornfield

To predict % NO_2 source contribution to the ambient air [NO_2] at a conventionally managed cornfield, an isotope mixing model was developed.

$$\delta^{15}\text{N-NO}_{2\text{obs}} = f_{\text{vehicle}}*(\delta^{15}\text{N-NO}_{2\text{ vehicle}}) + (1-f_{\text{vehicle}})*(\delta^{15}\text{N-NO}_{2\text{ soil emission}}) \qquad (2)$$

It is assumed that the two main contributors to [NO_2] at the field site are vehicle exhaust and emissions from fertilized soils. The range of δ^{15}N-NO_2 values for vehicle emissions (+10.2 to +17.0‰) used in the mixing models was from the δ^{15}N-NO_2 values from a moderately trafficked tunnel [*Chapter 6*]. The range of δ^{15}N-NO_2 values from fertilized soil emissions NO_2 (-30.8 to -26.5‰) used in the mixing models was from the δ^{15}N-NO_2 values obtained from samples in soil flux chambers at this site [*Chapter 6*]. The relative contributions (%) of NO_x emissions from vehicle and fertilized soils are estimated for each cornfield transect sampling event (Figure 6.8).

The percent contribution is reported as the maximum likelihood estimation (MLE) from Monte Carlo simulations (n =1000) for each data point at each site. The average MLE amount of vehicle NO_2 contribution to the air over the cornfield (sites 1-4) after the 35 lb N/ac and 120 lb N/ac fertilizer application was 34 and 18%, respectively. These results suggest that ambient air over a crop field adjacent to commuter or highly trafficked roadway receives a majority of the NO_2 in ambient air from soil emissions. This demonstrates that while nationally, fossil fuel combustion is the significant source of NO_x, locally other NO_x sources can be significant.

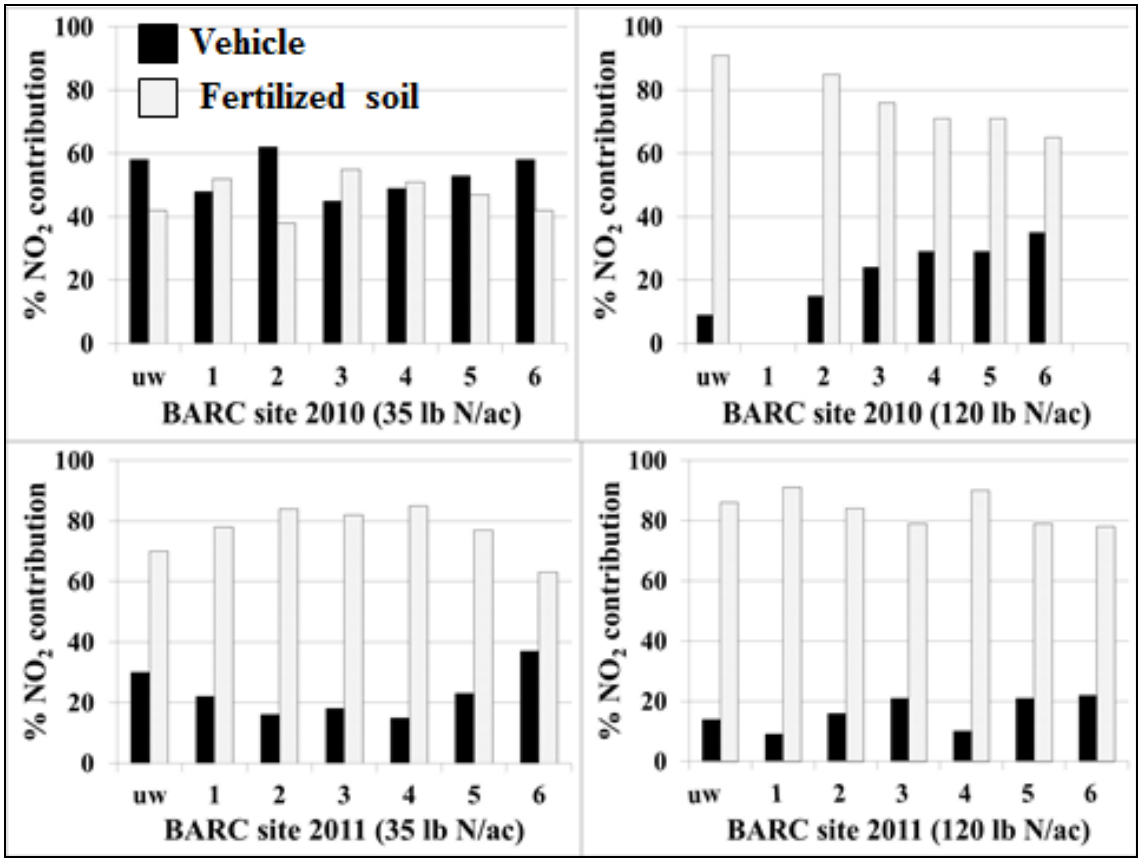

Figure 6.8: Percent NO_2 contribution from vehicle exhaust and fertilized soil emissions after each fertilizer application. Contribution maximum likelihood estimations were obtained using Monte Carlo simulations.

6.3.3 CAFO [NO_2], [HNO_3], $\delta^{15}N$

NO_2 concentrations range from to 1.6 to 5.1 ppb with a mean of 3.2 $\pm$ 1.2 ppb and HNO_3 range from to 1.2 to 5.1 $\mu g/m^3$ with a mean of 2.8 $\pm$ 2.0 $\mu g/m^3$. Neither NO_2 nor HNO_3 show a concentration gradient with distance from CAFO.

$\delta^{15}N$-NO_2 values range from to -29.0 to -8.5‰ with a mean of -16.5 $\pm$ 7.5‰ and $\delta^{15}N$-HNO_3 values range from to -7.7 to +1.5‰ with a mean of -1.6 $\pm$ 3.3‰. Both $\delta^{15}N$ values of NO_2 and HNO_3 increase with distance from the CAFO, likely due to isotopically light NO_2 emitted during microbial activity in the livestock waste. These emissions have similarly low $\delta^{15}N$ values to those from fertilized soil. As emissions are transported away from the CAFO, isotopically depleted $\delta^{15}N$-NO_2 from livestock waste mixes mix with 'background' $\delta^{15}N$ values causing a net increase in $\delta^{15}N$-NO_2 with distance. While the lowest $\delta^{15}N$-NO_2 value was obtained from site 1 at the CAFO, the lowest $\delta^{15}N$-HNO_3 value was at site 2, 30 m downwind of the CAFO. The low $\delta^{15}N$-HNO_3 value at site 2 could be from the NO_2 from the livestock emissions being transported before oxidation to HNO_3. This suggests that the NO_2 may be traveling up to 30 m before significant oxidation to HNO_3. Future studies using isotopes of NO_2 and HNO_3 can be used to investigate residence times and transport.

Table 6.4: NO_2 concentration, HNO_3 concentration, $\delta^{15}N$ and $\delta^{18}O$ of NO_2 and HNO_3 at the CAFO transect.

Distance from CAFO (m)	$[NO_2]$ (ppb)	$\delta^{15}N$ (‰)	$\delta^{18}O$ (‰)	$[HNO_3]$ ($\mu g/m^3$)	$\delta^{15}N$ (‰)	$\delta^{18}O$ (‰)
0	3.3	-29.0	13.3	1.2	-2.4	54.4
30	3.8	-22.0	20.9	1.2	-7.7	50.7
130	2.2	-12.1	19.3	5.6	-0.5	20.2
230	2.9	-13.8	18.8	2.8	-1.1	48.7
330	5.1	-13.8	19.3	5.0	0.5	18.5
1600	1.6	-8.5	0.5	1.2	1.5	28.2

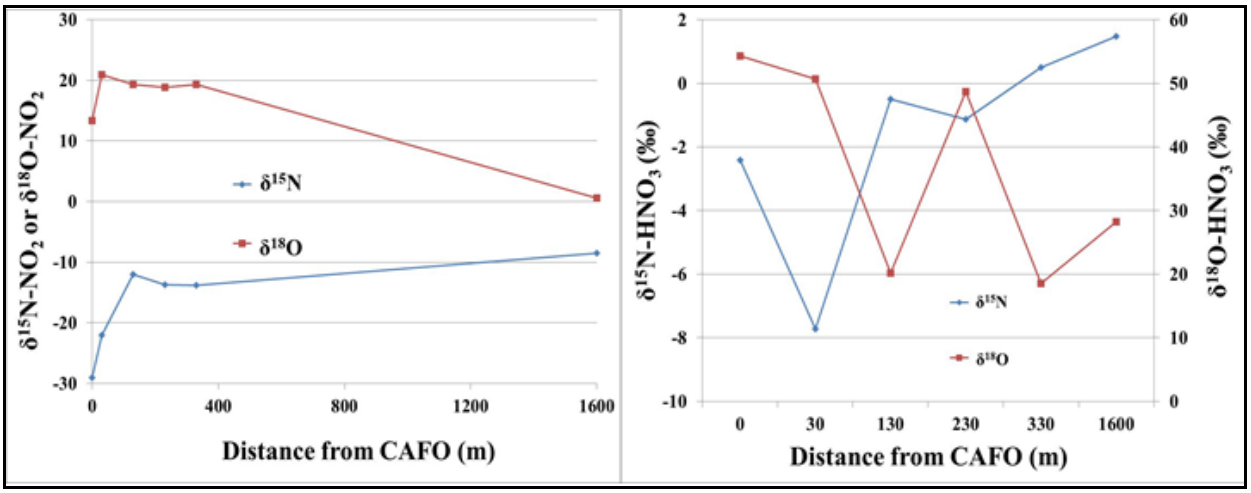

Figure 6.9: $\delta^{15}N$-NO_2 and $\delta^{18}O$-NO_2 values at the CAFO.

6.3.4 Bald Head Island $[NO_2]$, $\delta^{15}N$ and $\delta^{18}O$

NO_2 concentrations at the Bald Head Island dune transect ranged from 0.8 to 1.6 ppb with a mean of 1.2 $\pm$ 0.4 ppb and there was no concentration gradient across the dunes. $\delta^{15}N$-NO_2 values at Bald Head Island ranged from -3.3 to -1.2‰ with a mean of -2.2 $\pm$ 0.9‰. The barrier island has minimal NO_2 from fossil fuel combustion as only electric golf carts are used as transportation. Thus it is expected that the primary NO_2 source is lightning as lightning is estimated to produce 70% of the NO_x below 500 mbar over the North Atlantic Ocean during the summer (Levy et al., 1996). Lightning $\delta^{15}N$-NO_x is reported as -0.5 to 1.4‰ [*Hoering, 1957*], a value close to that of the mean (-2.2‰) at the island transect. The slightly lower mean $\delta^{15}N$ value reported at the transect could be due to mixing with fertilized soil emissions from a golf course located at the opposite end of the island (~2 miles NW). Although this is a limited data set (n=4), a significant correlation (R^2 = 0.96, p = 0.02) is observed between $\delta^{18}O$ and $\delta^{15}N$ of NO_2 and suggests a potential relationship between oxidation processes and resulting $\delta^{15}N$ values.

Table 6.5: NO_2 concentration, $\delta^{15}N$ and $\delta^{18}O$ of NO_2 at the Bald Head Island transect.

Site	[NO_2] (ppb)	$\delta^{15}N$ (‰)	$\delta^{18}O$ (‰)
1	1.0	-3.3	50.4
2	1.6	-1.9	20.5
3	0.8	-1.2	14.7
4	1.4	-2.4	30.9

Figure 6.10: Bald Head Island transect with observed $\delta^{15}N$ values. Transect sites are represented by yellow dots.

6.4 CONCLUSION

U.S. air quality regulations have reduced NO_x emissions from fossil fuel combustion but other NO_x emissions sources can be locally significant and are difficult to quantify. Quantification of NO_x contributions from individual sources and understanding subsequent transport are important first steps for the continuing reduction of NO_x emissions. To provide an additional tool for this quantification, we sampled ambient NO_x across various land-use types to demonstrate how the stable isotopic composition of NO_x can be used to characterize the transport

of NO_x emissions across landscapes. We have shown that by sampling NO_2 and it oxidation products simultaneously, inferences can be made to atmospheric residence time and transport. At a sampling transect where we assume two major NO_x sources, we use ambient $\delta^{15}N\text{-}NO_2$ values to predict % source contributions to a landscape. These source contribution estimates can aid in determining NO_x emission abatement techniques at a local scales.

7.0 THE AGRICULTURAL HISTORY OF HUMAN-NITROGEN INTERACTIONS AS RECORDED IN THE NITROGEN ISOTOPIC COMPOSITION OF ICE CORE NITRATE

7.1 INTRODUCTION

Nitrogen oxide (= NO + NO_2) emissions can have detrimental effects on the environment and human heath [*Galloway et al.,* 2004]. While the atmospheric lifetime of NO_x can be less than 24 hours and is mainly lost to HNO_3 formation and aerosol uptake [*Lamsal et al.,* 2010] the HNO_3 formation product has a lifetime of up to 5 days allowing it to be transported and deposited over long distances [*McElroy et al.,* 2002]. Thus, HNO_3 formation and transport can deposit NO_y products far from the point of emission [*Elliott et al.,* 2007]. As a consequence, targeted emission reductions in Europe and the U.S. aim to ameliorate associated environmental and human health impacts. For example, recently the U.S. EPA strengthened the health-based National Ambient Air Quality Standard for NO_x [*EPA,* 2010] and the European Commission's Thematic Strategy on Air Pollution [2005] has objectives of reducing year 2000 levels of NO_x emissions by 60% before 2020. While the primary source of NO_x is fossil fuel combustion

(vehicles, power plants), there are significant natural NO_x sources including lightning, biomass burning and biogenic emissions produced during nitrification and denitrification reactions in soils. Given the short lifetime of NO_x and the heterogeneity of sources in space and time, NO_x emissions inventories are notoriously difficult to evaluate. As a consequence, emission inventories from area sources, such as lightning and soil emissions, are subject to large uncertainties. For instance, Holland et al. [1999] report a global soil NO_x emission range of 4–21 Tg N yr^{-1} and recent studies have reported a lightning-produced NO_x range of 1 to 20 Tg yr^{-1} [*Schumann et al.,* 2007].

Recent advances in characterizing nitrogen isotope ratios of NO_x sources ($\delta^{15}N\text{-}NO_x$) can be used to help constrain emission inventories. Recent studies report power plant and vehicle emissions $\delta^{15}N\text{-}NO_x$ values of +10 to +20 ‰ and +3.7 to +5.7‰, respectively [*Felix et al.,* 2012; *Ammann et al.,* 1999; *Pearson et al.,* 2000; *Redling et al.,* submitted]. In comparison, biogenic soil emissions have lower $\delta^{15}N\text{-}NO_x$ values (-19.9 to -48.9‰) [*Li et al.,* 2008]. These relatively large differences in $\delta^{15}N\text{-}NO_x$ values allow the use of isotope mixing models to clarify NO_x source apportionment in gases, aerosols, and resulting nitrate deposition. For example, $\delta^{15}N\text{-}NO_3$ in precipitation across the Northeastern U.S. is strongly correlated with NO_x emissions from electricity generating units within 400 km of rainwater monitoring sites (Elliott et al., 2007).

Prior investigations suggest nitrate isotopes in ice cores also record temporal changes in NO_x source contributions. Hastings et al. [2009] report a clear change in $\delta^{15}N\text{-}NO_3$ in a Greenland ice core over the last 255 years and suggest changes in NO_x sources that contribute to HNO_3 formation over time. Here, we present evidence that 20th century increases in fertilizer use prompted higher fluxes of biogenic NO_x from soils; and these changes are recorded as negative $\delta^{15}N\text{-}NO_3$ excursions in a Summit, Greenland ice core (72.5°N, 38.4°W). We

reconstruct historical rates of fertilizer application and biomass burning, isotopically characterize NO_x emitted from conventionally fertilized agricultural fields, and develop a multiple source mixing model to constrain modern and historic NO_x emission fluxes.

7.2 METHODS

The reconstructed record of $\delta^{15}N\text{-}NO_3$ values in a Summit, Greenland ice core is compared with historic land use records, biomass burning and fertilizer application data, and $\delta^{15}N\text{-}NO_x$ source characterization data to investigate sources of NO_x to a remote location in Greenland. Approximate $\delta^{15}N\text{-}NO_x$ source values were generally derived from literature values and supplemented with biogenic NO_x emissions characterized below [*Felix et al.,* 2012; *Ammann et al.,* 1999; *Pearson et al.,* 2000; *Redling et al., submitted; Li et al.,* 2008].

7.2.1 Reconstruction of agricultural history and air mass trajectories

Fertilizer consumption data (1850 to 1890 decadal, 1891 to 2005 annual) and farmland acreage data (1850 to 1910 decadal, 1911 to 2005 annual) was obtained from U.S. Department of Commerce reports [*US Department of Commerce, 1975; US Department of Commerce Census 1970-2010*]. Biomass burning data (billion btu produced commercial and residential sector) was obtained from U.S. EIA [2010]. Evidence for biomass burning sourced NO_x contributing to $\delta^{15}N\text{-}NO_3$ was obtained by comparing $\delta^{15}N$ values with a record of black carbon and vanillic acid concentrations in a Central Greenland ice core [*McConnell et al.,* 2007]. North American CO_2 emissions [*Marland et al.,* 2008] were correlated with $\delta^{15}N\text{-}NO_3$ to infer contributions from

fossil fuel combustion NO_x.

Given patterns in air mass trajectories, fertilizer consumption data for the European Union [*Fertilizers Europe,* 2010] was not considered explicitly in this interpretation of the $\delta^{15}N$-NO_3 ice core data. Specifically, the primary air masses (85%) traveling over Greenland during the spring fertilizer application period originate in the American Midwest [*Kahl et al.,* 1997]. This is the case for 700 hPa back trajectory; the closest to the actual altitude of Summit, Greenland [*Kahl et al.,* 1997].

7.2.2 Assumptions in reconstructing emissions contributions to NO_3 deposition in Greenland

A $\delta^{15}N$-NO_x mixing model equation was created using the $\delta^{15}N$ value of combined biomass burning/fossil fuel NO_x emissions and the $\delta^{15}N$ value of biogenic NO_x, such that $\delta^{15}N$-NO_x ice core = $(1-f_{biogenic}) * (\delta_{biomass\ burn/fossil\ fuel}) + (f_{biogenic} * \delta_{biogenic})$. From 1750 to 1850, we assume the NO_x source contributing to ice core $\delta^{15}N$-NO_3 values is biomass burning. From 1850 to 1920, we assume that the main sources of NO_x contributing to ice core $\delta^{15}N$-NO_3 values are biomass burning and fossil fuel. This results in an average $\delta^{15}N$-NO_3 value of 9.5‰ and a $\delta^{15}N$-NO_x value of 12.4‰ ($\delta^{15}N$-NO_3 values from Hastings et al. [2009] and $\delta^{15}NO_x$ values calculated as follows: $\delta^{15}N$-$NO_2 = (\delta^{15}N$-$HNO_3 + (1000*(1-0.9971)))$ [*Freyer et al.,* 1991].

The biogenic $\delta^{15}N$-NO_x value was obtained from Li and Wang [2008] who reported a biogenic $\delta^{15}N$-NO range from urea fertilized soil of -20 to -49 ‰ (urea fertilizer $\delta^{15}N$ = 1.3‰). This range is attributable to lower $\delta^{15}N$-NO released after initial fertilizer application because the lighter ^{14}N of NO will be preferentially utilized by the soil bacteria. The heavier ^{15}N will be used more readily as the residual fertilizer pool becomes ^{15}N enriched. This range also suggests that

the biogenic $\delta^{15}N\text{-}NO_x$ value may be dependent on the $\delta^{15}N$ value of the fertilizer applied. Since fertilizer is made from air (N_2 = 0‰), commercial fertilizer $\delta^{15}N$ values tend deviate slightly around 0 ± 2‰ [*Bateman et al.,* 2007]. NO_x produced from lightning is not considered separately, as annual contributions are assumed to be constant over the ice core record.

7.2.3 Characterization of the $\delta^{15}N\text{-}NO_x$ value of biogenic NO_x

To constrain the large range of biogenic $\delta^{15}N\text{-}NO_x$ reported by the Li and Wang [2008] laboratory study, we collected biogenic NO_2 at a heavily instrumented conventionally managed cornfield at the Beltsville Agricultural Research Center in Beltsville, MD. The cornfield is managed to represent conventionally managed agriculture in the U.S. fertilized with Urea/Ammonium/Nitrate (UAN). For this study, after a 120 lb N/acre UAN application, an Ogawa passive NO_2 sampler containing a glass fiber filter coated with triethanolamine was placed in a Teflon flux chamber deployed into the fertilized soil. The sampler was deployed in the chamber for one month. The resulting $\delta^{15}N\text{-}NO_2$ of -27‰ is within the range reported by Li and Wang but rather represents an integrated $\delta^{15}N$ value of biogenic NO_2 emissions over one month in an actual field setting. Given that this $\delta^{15}N\text{-}NO_2$ endmember represents an average $\delta^{15}N$ value from fertilized soil over time in a field setting, this value was used in the mixing model as a biogenic NO_x endmember.

7.3 RESULTS AND DISCUSION

Historic U.S. fertilizer application rates increase dramatically after the advent of the Haber-Bosch method in the early 20th century [*US Department of Commerce, 1975; US Department of Commerce Census 1970-2010*]. Fertilizer application rates from 1890 to 2005 are strongly, negatively correlated with ice core δ^{15}N-NO_3 for equivalent years (R^2 = 0.87, $p<0.0001$) (Figure 7.1a). This strong correlation, coupled with our observed δ^{15}N-NO_x values of biogenic soil emissions reported herein, indicate that the negative trends observed in ice core δ^{15}N may be attributable to the intensification of soil NO_x emissions stemming from widespread application of industrial fertilizers accelerating after 1920. Together, these findings suggest that temporal changes in ice core δ^{15}N-NO_3 values reflect shifting NO_x sources in the U.S. largely driven by the acceleration of industrial fertilizer application (Figure 7.2). Relative changes in potential contributions from three major NO_x sources (biomass burning, fossil fuel combustion, and biogenic soil emissions) mesh well with periods roughly as follows pre-Industrial Revolution, Industrial Revolution pre- Haber-Bosch process and post-Haber-Bosch process. This is followed by quantitative prediction of contributions from these individual sources using a mixing model.

From 1750 until the onset of the Industrial Revolution in 1850, biomass burning is the primary NO_x source contributing to δ^{15}N-NO_3 values. This is supported by a strong correlation between black carbon concentrations and vanillic acid data prior to 1850 in a prior Greenland ice core study [*McConnell et al.,* 2007]. These correlations suggests that conifer burning is the primary source of black carbon to Greenland [*McConnell et al.,* 2007]. If so, this indicates a biomass burning δ^{15}N-NO_3 end member value of 11.5 ‰ and δ^{15}N-NO_x value of 14.4‰ These

biomass burning $\delta^{15}N$ values fall within the range (+10.6 to +25.7‰) of $\delta^{15}N$ values of total nitrogen on aerosol particles collected from biomass burning plumes [*Hastings,* 2010].

From 1850 to 1920, the main NO_x sources contributing to $\delta^{15}N\text{-}NO_3$ ice core values are biomass burning and fossil fuel combustion, transitioning at the onset of the Industrial Revolution in 1850. Accordingly, correlations between North American CO_2 emissions [*Marland et al.,* 2008] and ice core $\delta^{15}N\text{-}NO_3$ values are significant between 1850 to 1920 ($p < 0.05$) but not prior to this time (not shown). This indicates that fossil fuel NO_x emission contributions to ice core $\delta^{15}N\text{-}NO_3$ values become important beginning in 1850. Data from this time period result in an average biomass/fossil fuel $\delta^{15}N\text{-}NO_3$ end member value of 9.5‰ and a $\delta^{15}NO_x$ value of 12.4‰. With increased fossil fuel burning, there is an overall decrease in $\delta^{15}N\text{-}NO_x$ of ~2 ‰ between 1850 and 1920. This decrease is corroborated by a recent study of $\delta^{15}N\text{-}NO_x$ values from power plants lacking selective catalytic reduction emission controls (+10‰) (Felix et al., 2012) and recent $\delta^{15}NO_x$ values reported for roadside vehicle emissions (+3.7 to +5.7) [*Ammann et al.,* 1999; *Pearson et al.,* 2000; *Redling et al. submitted*]. Combined, contributions from these $\delta^{15}N\text{-}NO_x$ source values would lower the pre-1850 $\delta^{15}N\text{-}NO_x$ value of 14.4 ‰.

Another possible explanation for the post 1850 decrease in $\delta^{15}N\text{-}NO_3$ is contribution from soil NO_x produced from cleared land following farmland increases from 293,561,000 to 841,202,000 acres between 1850 and 1900 in the U.S. However, from 1850 to 2002 the farmland acreage and ice core $\delta^{15}N\text{-}NO_3$ are weakly but significantly correlated ($R^2 = 0.31$) ($p = 0.01$) (Figure 7.1b) [*US Department of Commerce, 1975; US Department of Commerce Census 1970-2010*]. The relative weakness of this correlation suggests that the application of fertilizer, rather than the acreage of cleared land, drives the increase in soil NO_x emissions.

After 1920, the main emission sources of NO_x accounted for by the model are biogenic soil NO_x, biomass burning, and fossil fuel emissions. After 1920, widespread industrial fertilizer application began in the U.S. following the advent of the Haber Bosch method. Soil nutrient enrichment via fertilizer application can contribute to large pulses of biogenic soil NO_x [*Veldkamp et al.,* 1997]. For example, Hudman et al. [2010] report a 50% increase in soil NO_x over the agricultural Great Plain in June 2006 due to rainwater induced pulsing. Jaeglé et al [2005] suggest that during the summer in the northern mid-latitudes, soil NO_x emissions can reach half that of fossil fuel combustion sources.

The temporal constraints on ice core history allow for exploration of temporal linkages between agricultural history and NO_y deposition recorded in the ice core. For example, the greatest rate of negative change in $\delta^{15}N\text{-}NO_3$ values is from 1950 to 1980 (slope of -0.25‰/yr.) — a period coincident with the Green Revolution when farmers worldwide nearly tripled grain production [*Mann,* 1997]. As further example, higher $\delta^{15}N\text{-}NO_3$ values during the early 1930s can be linked to the Great Depression, a period of decreasing fertilizer use in the U.S. (Figure 7.2) [*US Department of Commerce*, 1975]. Lastly, higher $\delta^{15}N\text{-}NO_3$ values in the 1980s (1983 to 1990) can be attributed to the U.S. recession and heavy farm debt leading to less fertilizer application [*US Department of Commerce Census 1970-2010*]. Also during this time, European farming suffered due to the fall of Communism, resulting in a lack of state support and a decrease in European fertilizer application (Fertilizers Europe, 2010). While an increase in biomass burning could have contributed to higher $\delta^{15}N\text{-}NO_3$ values during this period, a weak correlation between $\delta^{15}N\text{-}NO_3$ ice core values and biomass burning is observed between 1949 and 2005 ($R^2 = 0.13$) ($p < 0.05$) (Figure 7.1c) [*U.S. Energy Information Administration,* 2009]. The relatively minor influence of biomass burning is further supported by Greenland ice cores

recording weakening correlations between black carbon and vanillic acid after 1951 [*McConnell et al.,* 2007].

Contemporary and historical NO_x source inventories are challenging to constrain, particularly estimates of biogenic NO_x source emissions. Large discrepancies exist between modeled estimates of soil biogenic NO_x emissions and estimates derived from remote sensing observations of tropospheric NO_2 column concentrations [*Hudman et al.,* 2010; *Jaegle et al.,* 2005]. In the following, we use ice core $\delta^{15}N\text{-}NO_3$ to constrain U.S. emission inventories of historic and contemporary soil NO_x. We couple ~yearly $\delta^{15}N\text{-}NO_3$ ice core measurements with an isotope mixing model that incorporates contributions from biomass burning/fossil fuels and soil biogenic NO_x (Figure 7.3):

Model results illustrate the ability of the $\delta^{15}N\text{-}NO_3$ values to aid in constraining contributions of biogenic NO_x emissions to deposition (Table A5). For instance, in 1996, using the 27‰ $\delta^{15}N\text{-}NO_x$ value reported herein, biogenic NO_x emissions contribute an estimated 25% of total NO_3^- deposited to the ice core from North America. This estimate is 4 times larger than the 6% of the NO_x inventory attributed by the U.S. EPA to U.S. biogenic NO_x emissions during this time period [*EPA,* 1998]. The apparent underestimate by emission inventories is supported by predictions of a biogenic soil NO_x contribution of ~10% by a recent "bottom-up" NO_x emission inventory for 2005-2006, produced using a global model of tropospheric chemistry (GEOS-Chem), [*Lamsal et al.,* 2010]. Our mixing model, estimates even a greater biogenic NO_x contributions to Greenland during 2005 of 21%. These mixing model estimates confirm remote sensing studies indicating historic biogenic NO_x emissions and associated NO_y deposition are underestimated. This underestimate has important implications for contemporary estimates of biogenic NO_x emissions to global reactive nitrogen budgets. The anomaly in the model between

1950 and 1960, when the fraction of biogenic NO_x peaks and U.S. fertilizer use does not, may be due to European Union (EU) nitrogen fertilizer use nearly tripling during this period of time (Figure 7.4) [*Fertilizers Europe,* 2010]. Although the predominant source of Greenland air masses originate from North America during the spring, a relatively smaller portion is also derived from the European continent, thus resulting in potential contributions of biogenic soil NO_x from EU air masses [*Kahl et al.,* 1997]. The offset between the modeled fraction of biogenic NO_x peaks and actual U.S. fertilizer consumption may result from ice core data that represents several years of deposition, rather than strictly annual increments. This may be resolved by analyzing annual or seasonal sections of the ice core, although post-depositional process may mask seasonal trends in the ice core $\delta^{15}N\text{-}NO_3$ values.

In addition, post- depositional processes in the surface snow such as photolysis of NO_3 or evaporative loss of HNO_3 [*Rothlisberger et al., 2002*] would lead to the snow NO_3 being enriched in ^{15}N and the resulting NO_x and HNO_3 released to the atmosphere being depleted in ^{15}N. The enrichment in the snow would be more prevalent during warmer temperatures and increased sunlight of spring and summer. This enrichment due to post-depositional processes may contribute to the seasonal trend of $\delta^{15}N\text{-}NO_3$ [*Hastings et al.,* 2003] found in Greenland surface snow that is opposite of that found in precipitation across the U.S. [*Elliott et al 2007, Elliott et al.,* 2009, *Elliott submitted*], and Julich, Germany [*Freyer,* 1978] with higher ^{15}N in winter and lower in spring and summer. Since the precipitation reaching Greenland is from air masses originating from the US and Europe it is expected that the $\delta^{15}N\text{-}NO_3$ values in this precipitation and Greenland snow would follow the same seasonal trend. The observed offset in seasonal trends provides insight into how post-depositional processes lead to isotopic fractionation and suggests that seasonal trends are masked in the ice core. Diffusion of NO_3

through the ice, especially during warmer temperatures [Thibert et al., 1998], may also confound the ability to investigate seasonal trends in $\delta^{15}N\text{-}NO_3$ values.

7.4 CONCLUSION

The primary finding of this work, that increases in 20th century commercial fertilizer use prompted an increase in biogenic soil NO_x emissions driving the steep negative $\delta^{15}N\text{-}NO_3$ trend recorded in the ice core, may also indicate that biogenic soil NO_x emissions contribute to decreasing $\delta^{15}N$ trends recently reported in sediment records from 25 remote Northern Hemisphere lakes [*Holtgrieve et al.*, 2011]. Moreover, a similar decreasing ^{15}N trend of N_2O in firn air samples from Antarctica has been observed and is attributed to increased microbial activity due to increasing commercial fertilizer use [*Park et al.*, 2012]. While it has been established that soil microbial activity is a major source of N_2O, our work indicates that soil microbial activity is a historically underestimated source of NO_x.

As global population growth and N fertilizer use continues to increase, it will become increasingly important to quantify biogenic NO_x source emissions contributions to environmental systems. Given that excess inputs of reactive nitrogen cause global air, water quality, and ecosystem impacts with important implications for human health, effective efforts to curb reactive nitrogen loading to the environment will utilize accurate emission inventories Nitrate isotopes in ice cores, coupled with newly constrained $\delta^{15}N\text{-}NO_x$ values for NO_x emission sources, provide a novel means for estimating contemporary and historic contributions from

individual NO_x emission sources to historical deposition. In regions with incomplete empirical records of biomass burning, fossil fuel combustion, and fertilizer consumption, $\delta^{15}N\text{-}NO_3$ ice core data can provide essential records for understanding the role of these evolving human activities on air quality, water quality, and ecosystem health.

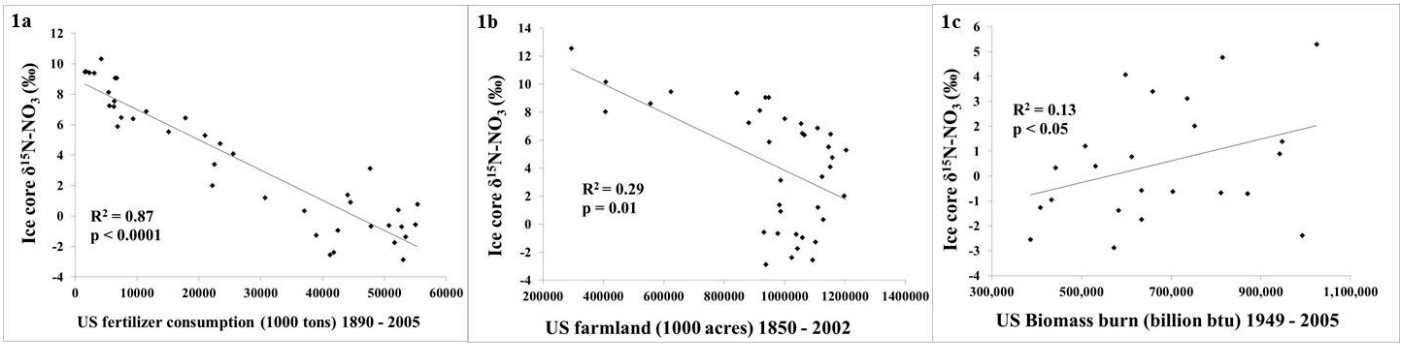

Figure 7.1: Ice core $\delta^{15}N\text{-}NO_3$ data correlations. $\delta^{15}N\text{-}NO_3$ values of Summit, Greenland ice core correlations with U.S. (a) U.S. fertilizer consumption, (b) U.S. farmland acreage, and (c) biomass burning [*US Department of Commerce,* 1975*; US Department of Commerce Census 1970-2010; US EIA,* 2010].

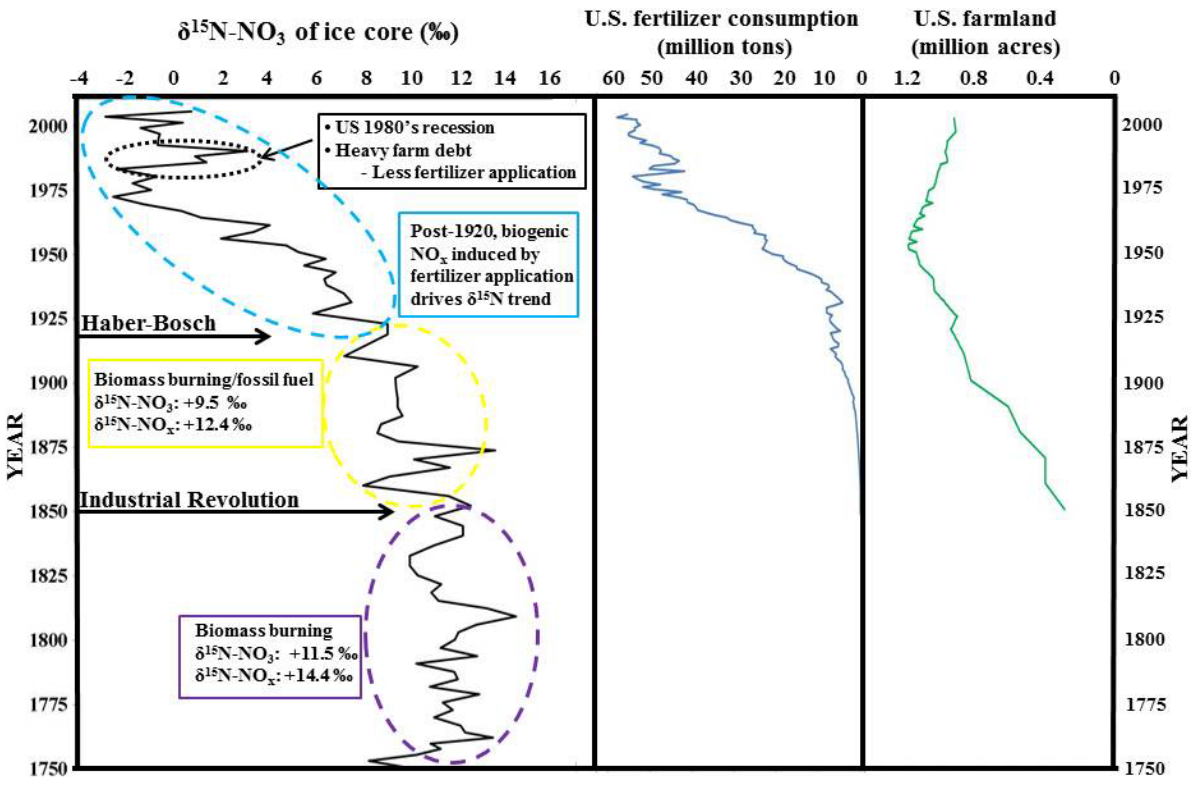

Figure 7.2: Ice core $\delta^{15}N\text{-}NO_3$, U.S. fertilizer consumption and U.S farmland versus time. Left: Ice core $\delta^{15}N\text{-}NO_3$ data versus time. Key periods in U.S. agricultural history leading to changes in NO_x emission sources and thus changes in $\delta^{15}N\text{-}NO_3$ (‰ vs. N_2) values are noted. Average $\delta^{15}N\text{-}NO_3$ and $\delta^{15}N\text{-}NO_x$ values are included for time periods when biomass burning and biomass burning/fossil fuels are the major NO_x emission sources contributing to ice core nitrate. Middle: Ice core $\delta^{15}N\text{-}NO_3$, U.S. fertilizer consumption (tons). Right: U.S. farmland (acres) versus time [*Hastings et al.*, 2009*; US Department of Commerce*, 1975*; US Department of Commerce Census 1970-2010*]

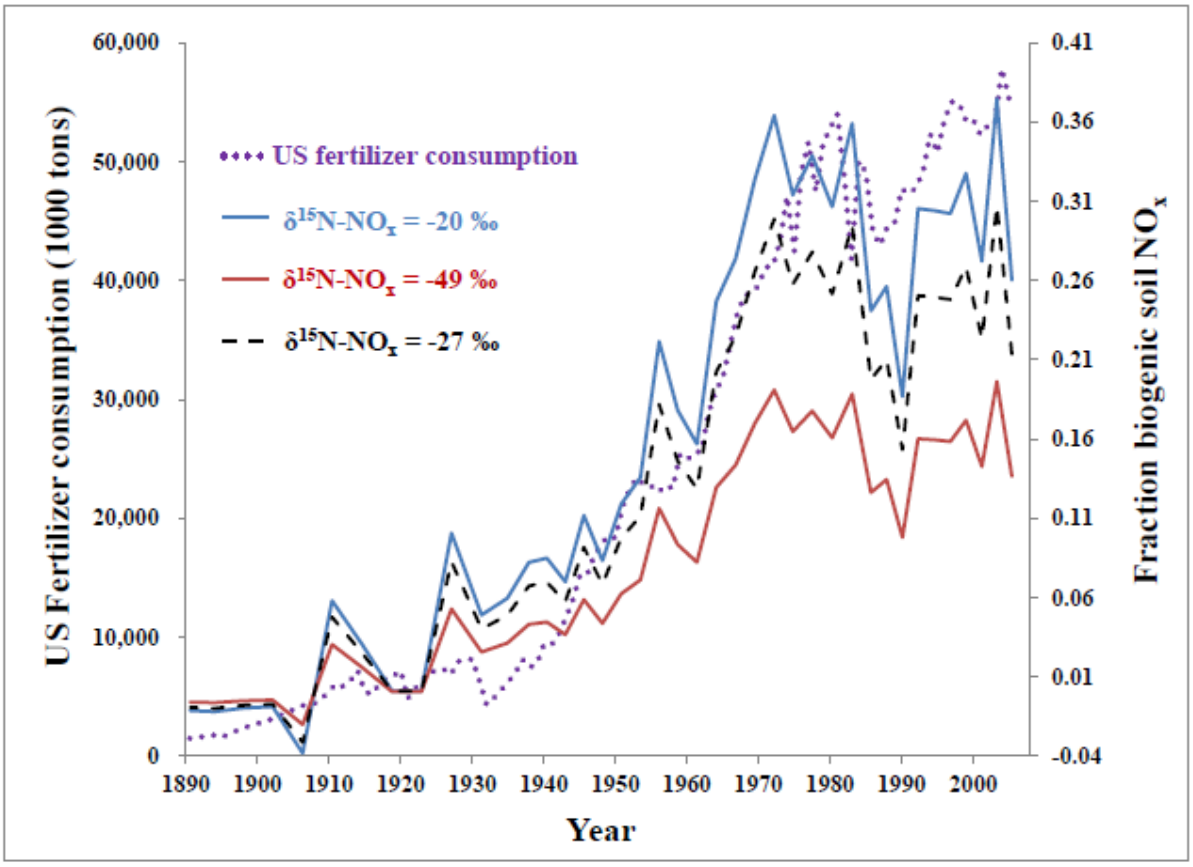

Figure 7.3: Predicted contributions of biogenic NO_x to Greenland ice core nitrate deposition relative to U.S. fertilizer consumption. The fraction of NO_x contributed by biogenic soil NO_x to the Summit, Greenland ice core is predicted using a two end-member mixing model wherein a $\delta^{15}N\text{-}NO_x$ value of +12‰ is used as a biomass burning/fossil fuel endmember in the mixing model and the biogenic soil NO_x endmember varies between -48.9 and -19.9‰. The blue, black-dashed, and red lines represent the fraction of biogenic soil NO_x contributing to the ice core when the -20‰, -27‰, and -49‰ end member is utilized, respectively. The purple dotted line represents actual U.S. fertilizer consumption.

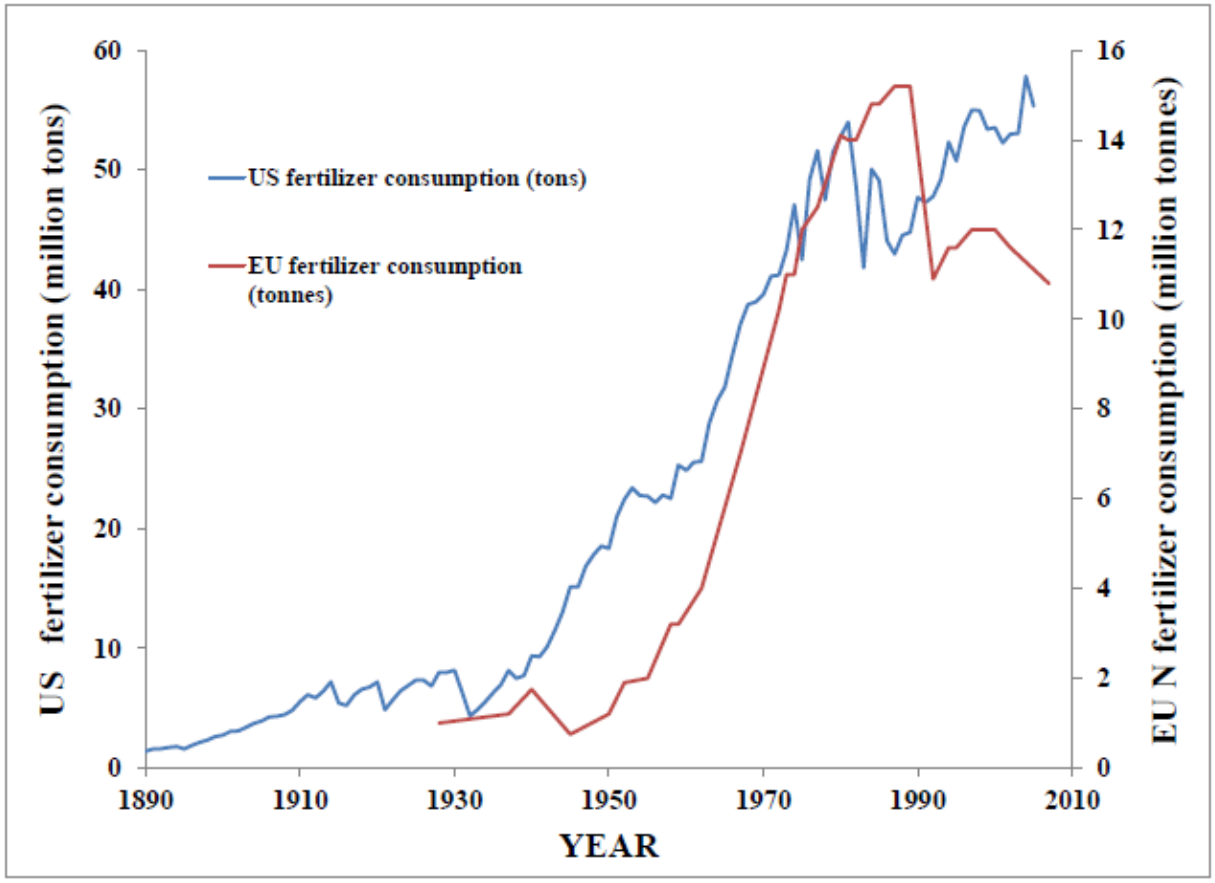

Figure 7.4: U.S. fertilizer consumption (1890 to 2005) and EU nitrogen fertilizer consumption (1928 to 2007). [*US Department of Commerce,* 1975*; US Department of Commerce Census 1970-2010; Fertilizers Europe,* 2010]

8.0 CONCLUSION

The adverse impacts to human and ecosystem health associated with excess Nr deposition are well documented. This has led to the accumulation of well constrained data and knowledge regarding the creation and consequences of N deposition. However, in comparison, large knowledge gaps exist when considering the transport and fate of N compounds in environmental systems [*Galloway et al.*, 2008]. For example, in the mid-1990s, the fate of only 35% of Nr emissions to the terrestrial biosphere were accounted for [*Galloway et al.*, 2004]. This illustrates the growing need for additional tools to aid in the quantification of Nr sources and transport.

To help address this knowledge gap, this dissertation presents a template for the use of stable isotopes to investigate Nr emission sources and transport. A comprehensive inventory of the isotopic composition of NH_3 and NO_x emissions was created to bolster the existing literature inventory. The created inventory shows a distinct difference between the isotopic compositions of NH_3 and NO_x emissions associated with fossil fuel combustion, agricultural activity and natural process. This inventory allowed for source identification and quantification when investigating isotopic composition of ambient atmospheric Nr concentrations across land-use types. This quantification can aid in determining Nr emission abatement techniques at a local scales. The isotopic composition of ambient NH_3 was

investigated at the regional scale in conjunction with the AMoN network, and the results provide proof-of-concept that the isotopic composition of NH_3 is a valuable tool for distinguishing potential spatial and temporal emission source contributions to varying regions in the U.S.

To assess the use of isotope composition to investigate Nr emission transport on a continental scale, nitrate isotopes in a Greenland ice core were examined. From the results of this study we demonstrated that nitrate isotopes in ice cores, coupled with newly constrained $\delta^{15}N\text{-}NO_x$ values for NO_x emission sources, provide a novel means for estimating contemporary and historic contributions from individual NO_x emission sources to deposition. In regions with incomplete empirical records of biomass burning, fossil fuel combustion, and fertilizer consumption, $\delta^{15}N\text{-}NO_3$ ice core data can provide essential records for understanding the role of these evolving human activities on air quality, water quality, and ecosystem health.

Since 1970, global human population has increased 78% while Nr creation has increased 120%. Global population is expected to increase from present levels (6.8 billion) to 9.3 billion by 2050 [*UN World Population Prospects: The 2010 Revision,* 2010*]* and this anticipated population expansion will be accompanied by greater demand for food and energy, and consequently, greater Nr as well. With the potential for growing Nr inputs to the environment, multiple Nr mitigation techniques must be considered. Galloway et al., [2008] suggests that a reduction of ~28% of Nr inputs to the environment is possible by using existing fossil fuel emission reduction technology and animal management strategies, increasing N uptake efficiency in crops, and providing access to sewage treatment for 3.2 billion people living in cities without access.

In future studies, we believe the isotope techniques that aid in Nr quantification techniques can also aid in assessing the efficacy of these suggested mitigation techniques. For

instance, we have shown that $\delta^{15}N\text{-}NO_x$ values emitted from power plants vary dependent on emission reduction technologies employed. This indicates that monitoring changes in $\delta^{15}N\text{-}NO_x$ and its oxidation products can be a valuable tool for assessing the effectiveness of SCR or SNCR technology for reducing power plant NO_x contributions to reactive nitrogen deposition. This concept may also apply to changing NO_x reduction technologies and efficiencies in vehicles, although further investigation is required.

For isotope techniques investigating Nr emission and mitigation to become increasingly viable, future work should be aimed at more extensively characterizing the stable isotopic compositions of Nr emission sources. Although we have contributed more data to the existing source signature inventory; the isotopic composition of soil NO_x, vehicle NO_x/NH_3, and power plant NO_x/NH_3 should continue to be measured, and the isotopic composition of biomass burning NO_x/NH_3 and soil NH_3 have yet to be directly measured. Isotopic fractionation of Nr emissions can occur after the point of emission through chemical reactions and subsequent depositional processes, thus masking the original isotopic source signature. Future efforts should be focused on characterizing these possible fractionation processes. Constraining these fractionation processes and isotopic source signatures associated with Nr emissions will decrease the uncertainty involved in using isotope techniques to quantify emission source contributions.

APPENDIX A: DATA TABLES

Table A1: $\delta^{15}N\text{-}NH_3$ data

Sample	$[NH_3]$ ($\mu g/m^3$)	$\delta^{15}N\text{-}NH_3$ (‰)
BARC1 1	2.5	-17.4
BARC1 2	3.9	-13.1
BARC1 3	3.0	-7.8
BARC1 4	1.9	-9.1
BARC1 5	1.4	-8.5
BARC1 6	1.4	-5.1
BARC1 UW	3.6	-1.3
BARC2 1	21.3	-38.5
BARC2 2	20.7	-39.4
BARC2 3	19.8	-41.4
BARC2 4	21.6	-36.3
BARC2 5	12.6	-33.3
BARC2 6	12.5	-27.9
BARC2 UW	9.2	-30.4
BARC3 1	4.8	-7.0
BARC3 2	1.3	-28.6
BARC3 3	3.9	-16.9
BARC3 4	4.6	-14.0
BARC3 5	1.5	-9.5
BARC3 6	9.1	-2.1
BARC3 UW	5.0	-12.3
BARC4 1	17.6	-31.7
BARC4 2	17.7	-45.3
BARC4 3	15.1	-44.9
BARC4 4	13.0	-48.0
BARC4 5	12.4	-41.1
BARC4 6	6.8	-25.6
BARC4 UW	9.3	-19.6
Dairy barn 1	165.6	-22.8
Dairy barn 2	128.2	-28.5

Sample	**[NH_3] (µg/m^3)**	**δ^{15}N-NH_3 (‰)**
Dairy barn 3	46.8	-21.7
Dairy barn 4	19.1	-17.7
KS3 1	109.3	-38.3
KS3 2	60.1	-19.9
KS3 3	60.4	-20.4
KS3 4	49.5	-14.3
KS3 5	51.0	-16.7
KS3 DW	26.9	-14.1
Konza 1		
Konza 2		
Konza 3		-4.9
Konza 4		
Konza 5		-8.8
BARC Poultry 1	NA	-36
BARC Poultry 2	NA	-56
BARC Dairy 1	NA	-23
BARC Dairy 2	NA	-27
Vehicle 5/10	NA	-4.6
Vehicle 6/10	NA	-2.2
Power plant A	NA	-11.3
Power plant B	NA	-14.6
AMoN 1_10 MI96	0.4	-6.5
AMoN 2_10 MI96	0.4	-15.3
AMoN 3_10 MI96	1.4	-21.9
AMoN 4_10 MI96	1.2	-23.8
AMoN 5_10 MI96	0.2	NA
AMoN 6_10 MI96	0.4	-15.2
AMoN 7_09 MI96	8.2	-5.4
AMoN 8_09 MI96	1.4	-4.7
AMoN 9_09 MI96	0.4	-21.1
AMoN 10_09 MI96	1.1	-14.8
AMoN 11_09 MI96	1.6	-18.6
AMoN 12_09 MI96	0.5	-10.2
AMoN 1_10 TX43	1.7	-29.2
AMoN 2_10 TX43	1.7	-29.2
AMoN 3_10 TX43	3.3	-42.4
AMoN 4_10 TX43	2.1	-22.2
AMoN 5_10 TX43	2.1	-23.0
AMoN 6_10 TX43	2.7	-19.0
AMoN 7_09 TX43	4.3	-7.5
AMoN 8_09 TX43	3.1	-22.2
AMoN 9_09 TX43	3.6	-4.4

Sample	$[NH_3]$ ($\mu g/m^3$)	$\delta^{15}N\text{-}NH_3$ (‰)
AMoN 10_09 TX43	0.8	-0.7
AMoN 11_09 TX43	0.9	-38.7
AMoN 12_09 TX43	2.9	-31.1
AMoN 1_10 OK99	2.8	-2.6
AMoN 2_10 OK99	0.5	-13.5
AMoN 3_10 OK99	1.0	-24.2
AMoN 4_10 OK99	1.4	-22.3
AMoN 5_10 OK99	0.1	-34.0
AMoN 6_10 OK99	0.8	-17.2
AMoN 7_09 OK99	NA	NA
AMoN 8_09 OK99	NA	NA
AMoN 9_09 OK99	NA	NA
AMoN 10_09 OK99	0.5	-4.7
AMoN 11_09 OK99	2.7	-8.1
AMoN 12_09 OK99	1.1	-19.9
AMoN 1_10 OH02	0.6	3.5
AMoN 2_10 OH02	0.0	NA
AMoN 3_10 OH02	1.0	-17.8
AMoN 4_10 OH02	1.2	-13.2
AMoN 5_10 OH02	0.7	-5.5
AMoN 6_10 OH02	1.1	-19.2
AMoN 7_09 OH02	0.7	-7.2
AMoN 8_09 OH02	0.6	-8.4
AMoN 9_09 OH02	1.2	-11.0
AMoN 10_09 OH02	0.2	-4.7
AMoN 11_09 OH02	0.0	NA
AMoN 12_09 OH02	0.6	-5.2
AMoN 1_10 IN99	0.0	NA
AMoN 2_10 IN99	0.5	7.1
AMoN 3_10 IN99	1.2	-23.4
AMoN 4_10 IN99	1.2	-27.9
AMoN 5_10 IN99	1.5	-24.3
AMoN 6_10 IN99	3.3	-20.7
AMoN 7_09 IN99	NA	NA
AMoN 8_09 IN99	NA	NA
AMoN 9_09 IN99	NA	NA
AMoN 10_09 IN99	0.5	-18.9
AMoN 11_09 IN99	0.9	-23.4
AMoN 12_09 IN99	1.4	-12.2
AMoN 1_10 SC05	0.2	-4.8
AMoN 2_10 SC05	0.6	-4.4
AMoN 3_10 SC05	1.1	-10.2

Sample	$[NH_3]$ ($\mu g/m^3$)	$\delta^{15}N\text{-}NH_3$ (‰)
AMoN 4_10 SC05	0.8	-5.3
AMoN 5_10 SC05	0.2	-3.9
AMoN 6_10 SC05	0.6	-2.2
AMoN 7_09 SC05	NA	NA
AMoN 8_09 SC05	NA	NA
AMoN 9_09 SC05	1.0	-2.4
AMoN 10_09 SC05	0.0	NA
AMoN 11_09 SC05	0.1	NA
AMoN 12_09 SC05	0.0	NA
AMoN 1_10 IL11	0.2	-10.7
AMoN 2_10 IL11	0.0	NA
AMoN 3_10 IL11	0.9	-28.4
AMoN 4_10 IL11	3.7	-19.6
AMoN 5_10 IL11	0.3	-17.1
AMoN 6_10 IL11	1.6	-18.5
AMoN 7_09 IL11	8.9	-10.1
AMoN 8_09 IL11	1.5	1.7
AMoN 9_09 IL11	1.2	-19.3
AMoN 10_09 IL11	0.2	-20.8
AMoN 11_09 IL11	2.6	-17.4
AMoN 12_09 IL11	0.6	-4.1
AMoN 1_10 KS24	1.0	-12.0
AMoN 2_10 KS24	3.2	-17.1
AMoN 3_10 KS24	2.4	-35.3
AMoN 4_10 KS24	2.0	-24.2
AMoN 5_10 KS24	3.4	-18.4
AMoN 6_10 KS24	3.2	-22.6
AMoN 7_09 KS24	13.0	-10.6
AMoN 8_09 KS24	5.7	-6.4
AMoN 9_09 KS24	6.3	-11.1
AMoN 10_09 KS24	2.1	-17.0
AMoN 11_09 KS24	2.9	-4.1
AMoN 12_09 KS24	1.8	-19.5
AMoN 1_10 NC35	1.2	-12.4
AMoN 2_10 NC35	NA	NA
AMoN 3_10 NC35	NA	NA
AMoN 4_10 NC35	NA	NA
AMoN 5_10 NC35	NA	NA
AMoN 6_10 NC35	NA	NA
AMoN 7_09 NC35	NA	NA
AMoN 8_09 NC35	5.1	-13.6
AMoN 9_09 NC35	5.3	-18.4

Sample	**[NH_3] (µg/m^3)**	**δ^{15}N-NH_3 (‰)**
AMoN 10_09 NC35	2.7	-22.1
AMoN 11_09 NC35	4.0	-12.4
AMoN 12_09 NC35	2.7	-25.0

Table A2: $\delta^{15}N\text{-}NO_2$ and $\delta^{18}O\text{-}NO_2$ data

Sample	$[NO_2]$ (ppb)	$\delta^{15}N\text{-}NO_2$ (‰)	$\delta^{18}O\text{-}NO_2$ (‰)
BARC1 1	3.5	-4.7	5.7
BARC1 2	2.9	-8.2	12.2
BARC1 3	3.7	-2.0	3.8
BARC1 4	4.6	-9.5	16.3
BARC1 5	3.4	-8.0	5.4
BARC1 6	4.3	-5.7	8.1
BARC1 UW	4.3	-4.1	9.5
BARC2 1	6.0	-25.5	22.6
BARC2 2	2.7	NA	NA
BARC2 3	1.7	-23.2	9.2
BARC2 4	4.6	-19.0	9.3
BARC2 5	4.5	-17.1	17.4
BARC2 6	6.1	-16.0	25.5
BARC2 UW	5.8	-14.1	29.6
BARC3 1	4.5	-16.4	29.3
BARC3 2	4.7	-19.9	28.1
BARC3 3	4.5	-22.4	30.3
BARC3 4	4.2	-21.6	27.7
BARC3 5	3.6	-23.0	26.2
BARC3 6	4.2	-19.7	30.6
BARC3 UW	5.6	-13.0	22.7
BARC4 1	4.4	-23.9	28.7
BARC4 2	4.4	-25.6	19.9
BARC4 3	5.8	-22.5	21.0
BARC4 4	5.9	-20.6	18.4
BARC4 5	5.8	-25.0	13.7
BARC4 6	6.0	-20.6	21.6
BARC4 UW	6.0	-20.0	25.9
KS3 1	3.3	-29.0	13.3
KS3 2	3.8	-22.0	20.9
KS3 3	2.2	-12.1	19.3
KS3 4	2.9	-13.8	18.8
KS3 5	5.1	-13.8	19.3
KS3 DW	1.6	-8.5	0.5
Konza 1			
Konza 2		-8.4	5.1
Konza 3			
Konza 4		-4.8	55.5
Konza 5			
Poultry		-8.5	31.9

Dairy		-20.4	37.8
BHI 1	1.0	-3.3	50.4
BHI 2	1.6	-1.9	20.5
BHI 3	0.8	-1.2	14.7
BHI 4	1.4	-2.4	30.9
Port of VA		-6.6	24.2
BARC2 flux chamber		-26.5	-21.5
BARC3 flux chamber		-30.8	-20.2
SHT in 5_10	Saturated	16.9	-17.5
SHT in 6_10	Saturated	15.6	-15.3
SHT in 7_10	Saturated	15.6	-15.2
SHT in 8_10	Saturated	17.0	-13.1
SHT in 9_10	Saturated	16.0	-14.9
SHT in 11_12_10	Saturated	15.1	-14.0
SHT in 1_11	Saturated	15.0	-8.4
SHT in 1_11 10 day		16.4	-8.5
SHT in 2_11	Saturated	14.4	-12.1
SHT in 3_11	Saturated	14.6	-13.9
SHT in 4_11	Saturated	16.2	-10.0
SHT in 5_11	Saturated	15.3	-8.5
SHT out 1_11	Saturated	15.6	-5.8
SHT out 3_11	Saturated	14.2	-7.8
SHT out 5_11	Saturated	14.4	-8.4
SHT out 7_19 to 7_28_11 out	59.1	10.2	-1.7
SHT out 11_7 to 11_11_11 1m out	52.8	13.1	-4.1
SHT out 11_7 to 11_11_11 2m out	50.3	12.8	-2.7
SHT out 11_7 to 11_11_11 3m out	46.8	13.3	-0.7
SHT out 11_11 to 11_14_11 1m out	40.4	16.9	7.8
SHT out 11_11 to 11_14_11 2m out	36.4	15.8	1.3
SHT out 11_11 to 11_14_11 3m out	31.8	15.3	2.5

Table A3: $\delta^{15}N\text{-}HNO_3$ and $\delta^{18}O\text{-}HNO_3$ data

Sample	$[HNO_3]$ ($\mu g/m^3$)	$\delta^{15}N\text{-}HNO_3$ (‰)	$\delta^{18}O\text{-}HNO_3$ (‰)
BARC1 1	2.9	-8.2	12.2
BARC1 2	3.7	-2.0	3.8
BARC1 3	4.6	-9.5	16.3
BARC1 4	3.4	-8.0	5.4
BARC1 5	4.3	-5.7	8.1
BARC1 6	4.3	-4.1	9.5
BARC1 UW	3.5	-4.7	5.7
BARC2 1	2.7	NA	NA
BARC2 2	1.7	-23.2	9.2
BARC2 3	4.6	-19.0	9.3
BARC2 4	4.5	-17.1	17.4
BARC2 5	6.1	-16.0	25.5
BARC2 6	5.8	-14.1	29.6
BARC2 UW	6.0	-25.5	22.6
BARC3 1	4.7	-19.9	28.1
BARC3 2	4.5	-22.4	30.3
BARC3 3	4.2	-21.6	27.7
BARC3 4	3.6	-23.0	26.2
BARC3 5	4.2	-19.7	30.6
BARC3 6	5.6	-13.0	22.7
BARC3 UW	4.5	-16.4	29.3
BARC4 1	4.4	-25.6	19.9
BARC4 2	5.8	-22.5	21.0
BARC4 3	5.9	-20.6	18.4
BARC4 4	5.8	-25.0	13.7
BARC4 5	6.0	-20.6	21.6
BARC4 6	6.0	-20.0	25.9
BARC4 UW	4.4	-23.9	28.7
KS3 1	1.2	-2.4	54.4
KS3 2	1.2	-7.7	50.7
KS3 3	5.6	-0.5	20.2
KS3 4	2.8	-1.1	48.7
KS3 5	5.0	0.5	18.5
KS3 DW	1.2	1.5	28.2
Konza 1	0.7	-7.1	61.1
Konza 2	6.8	1.3	19.5
Konza 3	8.6	2.7	19.2
Konza 4	6.9	2.1	17.7
Konza 5	0.5		
SHT in 5_10	0.6	9.6	9.4

SHT in 6_10	1.3	2.7	46.7
SHT in 10_10	0.2	4.6	35.6
SHT in 11_12_10	0.3	11.1	28.2
SHT in 1_11	0.4	9.1	34.1
SHT in 1_11 10 day	1.0	9.9	11.5
SHT in 2_11	0.4	8.3	30.2
SHT in 3_11	0.5	7.1	38.1
SHT in 4_11	0.5	6.5	46.8
SHT in 5_11	0.6	4.1	45.7
SHT out 1_11	0.5	4.8	48.9
SHT out 2_11	0.4	6.2	43.5
SHT out 3_11	1.2	5.2	45.3
SHT out 4_11	0.8	3.7	47.7
SHT out 5_11	1.0	0.8	45.3

Table A4: Eluent concentrations and isotopic analysis from SCR- , SNCR-, OFA-, and LNB-equipped EGU samples. Standard deviations (Std. dev.) reported are deviations of replicate analysis of individual samples for the number of replicates indicated (N).

Sample	Plant and Technology	Nitrate (ppm)	Nitrite (ppm)	Mean $\delta^{15}N\text{-}NO_3/NO_2$ (‰)	*Std. dev. of N (‰)	N (number of replicates)
H_2SO_4 Grab 1	A SCR/LNB	8.9	0	20.6	0.7	3
H_2SO_4 Grab 2	A SCR/LNB	10.8	0	21.0	1.0	3
H_2SO_4 Grab 3	A SCR/LNB	4.2	0	20.9	1.0	4
H_2SO_4 Grab 4	A SCR/LNB	8.1	0	15.5	1.0	4
H_2SO_4 Grab 5	A SCR/LNB	16.7	0	19.3	1.0	4
Mean		*9.7*	*0*	*19.5*	*1.0*	
H_2SO_4 Grab 1	B OFA/LNB	35.2	0	9.2	0.3	4
H_2SO_4 Grab 2	B OFA/LNB	25.1	0	9.0	0.1	4
H_2SO_4 Grab 3	B OFA/LNB	22.9	0	10.4	-	2
H_2SO_4 Grab 4	B OFA/LNB	25.7	0	10.5	0.3	3
Mean		*27.2*	*0*	*9.8*	*0.2*	
NaOH Grab 5	B OFA/LNB	22.3	NA	11.0	0.7	3
NaOH Grab 6	B OFA/LNB	14.6	NA	11.5	-	2
NaOH Grab 7	B OFA/LNB	19.6	NA	9.6	0.9	3
NaOH Grab 8	B OFA/LNB	19.9	NA	11.7	0.5	3
Mean		*19.1*	NA	*11.0*	*0.7*	
TEA Grab 9	B OFA/LNB	19.0	NA	10.2	0.8	3
TEA Grab 10	B OFA/LNB	8.3	NA	10.7	0.4	3
TEA Grab 11	B OFA/LNB	10.0	NA	10.0	-	1
TEA Grab 12	B OFA/LNB	10.3	NA	9.5	-	2
Mean		*11.9*	NA	*10.1*	*0.6*	
H_2SO_4 Grab 1	C SCR/OFA/LNB	5.0	0	15.5	-	1
H_2SO_4 Grab 2	C SCR/OFA/LNB	3.4	0	25.6	-	1
H_2SO_4 Grab 3	C SCR/OFA/LNB	4.0	0	18.4	-	2
Mean		*4.1*	*0*	*19.8*	-	
H_2SO_4 Grab 4	C SNCR/OFA/LNB	26.4	0	13.6	-	2
H_2SO_4 Grab 5	C SNCR/OFA/LNB	18.3	0	13.9	-	2
H_2SO_4 Grab 6	C SNCR/OFA/LNB	29.7	0	15.1	0.7	3
Mean		*24.8*	*0*	*14.2*	-	
H_2SO_4 Grab 7	C OFA/LNB	31.8	0	12.6	-	2
H_2SO_4 Grab 8	C OFA/LNB	31.0	0	12.1	-	2
H_2SO_4 Grab 9	C OFA/LNB	30.3	0	11.8	1.0	3
Mean		*31.0*	*0*	*12.2*	-	
H_2SO_4 Grab 1	D SCR	12.6	0	18.9	-	2
H_2SO_4 Grab 2	D SCR	12.7	0	19.1	-	2
H_2SO_4 Grab 3	D SCR	12.8	0	19.2	-	2
H_2SO_4 Grab 4	D SCR	12.9	0	19.3	-	2
H_2SO_4 Grab 5	D SCR	12.8	0	19.2	-	2
H_2SO_4 Grab 6	D SCR	12.4	0	18.7	-	2
H_2SO_4 Grab 7	D SCR	13.3	0	18.9	-	2
H_2SO_4 Grab 8	D SCR	13.7	0	20.4	-	2
Mean		*12.9*	*0*	*19.3*	-	

Table A5: NH_3 sources accounted for in CMU NH_3 inventory

Livestock waste					
Dairy deep pit confinement	Dairy deep pit storage	Dairy deep pit land app	Dairy dry lot confinement	Dairy dry lot storage	Dairy dry lot land app
Dairy flush confinement	Dairy flush storage	Dairy flush land app	Dairy scrape confinement	Dairy scrape storage	Dairy scrape land app
Dairy composite	Beef dry lot confinement	Beef dry lot storage	Beef dry lot land app	Beef pasture confinement	Beef composite
Swine deep pit confinement	Swine deep pit land app	Swine lagoon confinement	Swine lagoon storage	Swine lagoon land app	Swine outdoor confinement
Swine composite	Poultry broilers confinement	Poultry broilers storage	Poultry broilers land app	Poultry layers dry confinement	Poultry layers dry land app
Poultry layers wet confinement	Poultry layers wet storage	Poultry layers wet land app	Poultry turkeys confinement	Poultry turkeys storage	Poultry turkeys land app
Poultry composite	horses	sheep	goats	geese	ducks
Fertilizer					
mix	Anhydrous ammonia	Aqueous ammonia	Ammonium nitrate	Ammonium sulfate	Ammonium thiosulfate
Calcium ammonium nitrate	Nitrogen solutions	urea	Diammonium phosphate	Monoammonium phosphate	Liquid ammonium polyphosphate
Potassium nitrate					
Vehicle					
Cars	Trucks				
Industry					
All industry					

Table A6: Mixing model estimates of biogenic NO_x emission contributions to ice core nitrate

Year (ice core date)	Ice core $\delta^{15}N$-NO_3	% biogenic NO_x (-20 ‰)	% biogenic NO_x (-27 ‰)	% biogenic NO_x (-49 ‰)
2005.4	0.77	26	21	14
2003.3	-2.88	37	31	20
2001.2	0.39	27	22	14
1999	-1.38	33	27	17
1996.8	-0.57	30	25	16
1994.6	-0.63	30	25	16
1992.3	-0.67	31	25	16
1990.1	3.12	19	15	10
1987.9	0.9	26	21	13
1985.7	1.39	24	20	13
1983.1	-2.39	36	29	19
1980.3	-0.71	31	25	16
1977.5	-1.74	34	28	18
1974.8	-0.95	31	26	16
1972.2	-2.55	36	30	19
1969.5	-1.26	32	27	17
1966.8	0.34	27	22	14
1964.1	1.2	25	20	13
1961.4	4.08	16	13	8
1958.7	3.4	18	15	9
1956.1	2.01	22	18	12
1953.5	4.76	14	11	7
1950.8	5.29	12	10	6
1948.2	6.43	8	7	4
1945.6	5.52	11	9	6
1943	6.86	7	6	4
1940.4	6.38	9	7	4
1937.9	6.47	8	7	4
1934.9	7.19	6	5	3
1931.3	7.53	5	4	3
1927.1	5.88	10	8	5
1922.9	9.06	0	0	0
1918.8	9.06	0	0	0
1914.6	8.12	3	3	2
1910.4	7.24	6	5	3
1906.3	10.32	-4	-3	-2
1902.1	9.38	-1	-1	0
1898	9.41	-1	-1	-1

1894	9.48	-1	-1	-1
1890.6	9.46	-1	-1	-1

BIBLIOGRAPHY

AMoN Ammonia monitoring network (2012), http://nadp.sws.uiuc.edu/AMoN/sites/data/

Aneja, V.P., P.A. Roelle, G.C. Murray, J. Southerland, J.W. Erisman, D. Fowler, W.A.H. Asman, and N. Patni (2001), Atmospheric nitrogen compounds: II. Emissions, transport, transformation, deposition, and assessment. *Atmos. Environ.* 35 :1903–1911

Ammann, M., R. Siegwolf, F. Pichlmayer, M. Suter, M. Saurer, and C. Brunold (1999), Estimating the uptake of traffic-derived NO_2 from ^{15}N abundance in Norway spruce needles, *Oecologia*,*118*(2), 124-131.

Baggs EM (2008), A review of stable isotope techniques for N_2O source partitioning in soils: recent progress, remaining challenges and future considerations. *Rapid Commun Mass Spectrom 22***:** 1664–1672

Bateman, A.S., Kelly, S.D (2007), Fertilizer nitrogen isotope signatures. *Isotopes in Environmental and Health Studies*, 43(3): 237–247. doi: 10.1080/10256010701550732.

Bouwman et al. (1997), A global high-resolution emission inventory for ammonia. *Global Biogeochemical Cycles*, vol. 11, no. 4, pages 561-587,

Bonifacio, H. F. (2009), Particulate matter emissions from commercial beef cattle feedlots in Kansas. MS thesis. Manhattan, Kans.: Kansas State University.

Bradley M.J. and Jones B.M. (2002), Reducing global NOx emissions: promoting the development of advanced energy and transportation technologies. *Ambio* 31: 141–149.

Bytnerowicz, A., et al. (2005), Passive sampler for monitoring ambient nitric acid (HNO3) and nitrous acid (HNO2) concentrations, *Atmos. Environ.*, 39(14), 2655–2660, doi:10.1016/j.atmosenv.2005.01.018.

Cape, J.N., Tang, Y.S., van Dijk, N., Love, L., Sutton, M.A., Palmer, S.C.F., (2004), Concentrations of ammonia and nitrogen dioxide at roadside verges, and their contribution to nitrogen deposition. *Environ. Pollut*. 132, 469–478.

Cape JN, Jones MR, Leith ID, Sheppard LJ, van Dijk N, Sutton MA, Fowler D (2008), Estimate of annual NH_3 dry deposition to a fumigated ombrotrophic bog using concentration-dependent deposition velocities. *Atmospheric Environment* 42 6637-6646.

Chimka, C.T., Galloway, J.N., Cosby, B.J. (1997), Ammonia and the Chesapeake Bay Airshed. Chesapeake Bay Program. *Scientific and Technical Advisory Committee*, Annapolis, MD, Publication 97-1.

Davidson EA, David MB, Galloway JN, Goodale CL, Haeuber R, Harrison JA, Howarth RW, Jaynes DB, Lowrance RR, Nolan BT, Peel JL, Pinder RW, Porter E, Snyder CS, Townsend AR, Ward MH (2012), Excess nitrogen in the U.S. environment: Trends, risks, and solutions. *Issues Ecol. Report* 15.

Eaton, A.D., Franson, M.H.,n(2005), Standard method for the examination of water and wasterwater. 21 ed. American Public Health Association. Port City Press. Baltimore, MD.

Elliott, E.M., Kendall, C., Boyer, E.W., Burns, D.A., Lear, G., Golden, H.E., Harlan, K., Bytnerowicz, A., Butler, T.J., Glatz, R., (2009), Dual nitrate isotopes in dry deposition: utility for partitioning NOx source contributions to landscape nitrogen deposition. *J. Geophys. Res.* 114 (G04020). doi:10.1029/2008JG000889.

Elliott EM, Kendall C, Wankel SD, Burns DA, Boyer EW, Harlin K, Bain DJ, Butler TJ. (2007), Nitrogen isotopes as indicators of NO_x source contributions to atmospheric nitrate deposition across the Midwestern and northeastern United States. *Environmental Science & Technology* 41: 7661–7667.

Erisman JW, Bleeker A, Galloway JN, Sutton MS, 2007. Reduced nitrogen in ecology and the environment. Environ Pollut 150:140–149.

EIA, (2012), http://www.eia.gov/totalenergy/data/monthly/#electricity, August 2012

EPA, (1999) EPA NO_x technical bulletin 1999

EPA, (2010), Determination of Nitrogen Oxide Emissions from Stationary Sources http://www.epa.gov/ttn/emc/promgate/m-07b.pdf.

European Environment Agency (2010), European Environment Agency 2010. Air Quality Modelling and Assessment Unit, 22 November 2010, V3 Guidance on modelling the concentration and deposition of ammonia emitted from intensive farming

Felix, J.D., Elliott, E.M., Shaw, S. (2012), Nitrogen isotopic composition of coal-fired power plant NO_x: Influence of emission controls and implications for global emission inventories. *Environmental Science and Technology*.

Fertilizers Europe. Annual Forecast 2009. (2010), www.fetilizerseurope.com January 2010

Frank DA, Evans RD, Tracey BF. (2004), The role of ammonia volatilization in controlling the natural ^{15}N abundance of a grazed grassland. *Biogeochemistry* 68:169–178

Fowler, D., Sutton, M.A., Smith, R.I., Pitcairn, C.E.R., Coyle, M., Campbell, G. and Stedman, J., (1998), Regional mass budgets of oxidized and reduced nitrogen and their relative contribution to the nitrogen inputs of sensitive ecosystems. *Environmental Pollution*, 102, pp. 337–342.

Freyer, H. D. (1978), Seasonal trends of NH_4^+ and NO_3^- nitrogen isotope composition in rain collected at Jülich, Germany. *Tellus*, 30, 83–92.

Freyer, H.D. (1991) Seasonal variation of 15N/14N ratios in atmospheric nitrate species. *Tellus*, 43B, 30–44.

Galloway, J. N., F. Dentener, D. Capone, C. Cleveland, P. Green, E. Holland, D. Karl, A. Michaels, J. Porter, A. Townsend, and C. Vörösmarty 2004. Nitrogen cycles: past, present, and future, Biogeochemistry, 70, 153-226

Golden, H. E., et al. (2008), Simple approaches for measuring dry atmospheric nitrogen deposition to watersheds, *Water Resour. Res.*, 44, W00D02, doi:10.1029/2008WR006952.

Gormly, J. R., and Spalding, (1979), R.E. Sources and concentrations of nitrate-nitrogen in ground water of the central Platte region, Nebraska. *Ground Water* 17: 291-301.

Hastings, M.G., Steig, E.J. & Sigman, D.M. (2004), Seasonal variations in N and O isotopes of nitrate in snow at Summit, Greenland: Implications for the study of nitrate in snow and ice cores. *Journal Of Geophysical Research-Atmospheres*, 109

Hastings, M. G., Jarvis, J. C., and Steig, E. J., (2009), Anthropogenic impacts on nitrogen isotopes of ice-core nitrate, *Science*, 324, 1288, doi:10.1126/science.1170510.

Hastings, M. G., (2010), Evaluating source, chemistry and climate change based upon the isotopic composition of nitrate in ice cores *IOP Conf. Ser.: Earth Environ. Sci. 9*

Hastings, M. G., Sigman, D. M., and Lipschultz, F., (2003), Isotopic evidence for source changes of nitrate in rain at Bermuda, J. Geophys. Res., 108(D24), 4790,doi:10.1029/2003JD003789.

Heaton, T. H. E. (1987), $^{15}N/^{14}N$ ratios of nitrate and ammonium in rain at Pretoria, South Africa *Atmospheric Environment*, 21, 843–852.

Heaton, T. H. E. (1990), $^{15}N/^{14}N$ ratios of NO_x from vehicle engines and coal-fired power 770 stations, *Tellus, 42B*, 304-307.

Heeb, N. V., Saxer, C. J., Forss, A.-M., and Bruhlmann, S. (2008), Trends of NO-, NO2-, and NH3- emissions from gasoline-fueled Euro- 3- to Euro-4-passenger cars, *Atmos. Environ*., 42, 2543–2554,

Hoering, T. (1957), The Isotopic Composition of the Ammonia and the Nitrate Ion in Rain, 774 *Geochimica et Cosmochimica Acta*, *12*(1-2), 97-102.

Holland, E.A., Dentener, F.J., Braswell, H.B., Sulzman, J.M. (1999), Contemporary and Pre-Industrial Global Reactive Nitrogen Budgets. *Biogeochemistry* Vol. 46, No. 1/3, (Jul., 1999) pp. 7-43

Holtgrieve, G.W. D. E. Schindler, W. O. Hobbs, P. R. Leavitt, E. J. Ward, L. Bunting, G. Chen, B. P. Finney, I. Gregory-Eaves, S. Holmgren, M. J. Lisac, P. J. Lisi, K. Nydick, L. A. Rogers, J. E. Saros, D. T. Selbie, M. D. Shapley, P. B. Walsh and A. P. Wolfe, (2011), A coherent signature of anthropogenic nitrogen deposition to remote watersheds of the northern hemisphere. *Science* 334, 1545 DOI: 10.1126/science.1212267

Hudman, R.C., Russell, A., Valin, L., Cohen, R. (2010), Interannual variability in soil nitric oxide emissions over the United States as viewed from space, *Atmos. Chem. Phys.*, doi:10.5194/acp-10-9943-2010.

Hristov, A. N., Zaman, S., Vander Pol, M., Ndegwa, P., Campbell, L. and Silva, S. (2009), Nitrogen losses from dairy manure estimated through nitrogen mass balance or using markers. J. *Environ. Qual*. 38:2438 _2448.

Hristov, A.N., Hanigan, M.D., Cole, N.A., Todd, R.W., McAllister, T.A., Ndegwa, P.M., Rotz, A. (2011), Review: ammonia emissions from dairy farms and beef feedlots. *Can. J. Anim. Sci. 91*, 1-35.

Jaeglé, L., L. Steinberger, R.V. Martin, and K. Chance, (2005), Global partitioning of NOx sources using satellite observations: Relative roles of fossil fuel combustion, biomass burning and soil emissions, *Faraday Discussions*, 130, 407-433, doi:10.1039/b502128f.

Jickells, T. D., Kelly, S. D., Baker, A. R., Biswas, K., Dennis, P. F., Spokes, L. J., Witt, M., Yeatman, S. (2003), Isotopic evidence for a marine ammonia source. *Geophysical Research Letters*, 30(7), 1374, doi: 10.1029/2002GL016728.

Kahl, J. D. W., Martinez D. A., Kuhns H.,. Davidson C. I,. Jaffrezo J. L, and Harris J. M. (1997), Air mass trajectories to Summit, Greenland: A 44-year climatology and some episodic events, *J. Geophys. Res.*, 102, 26,861– 26,875,

Kean, A.J.; Harley, R.A., Littlejohn, D., Kendall, G.R. (2000), On Road Measurement of Ammonia and Other Motor Vehicle Exhaust Emissions; *Environmental Science and Technology* 34: 3535-3539.

Konza, (2012), www.konza.ksu.edu/, August 2012

Kirchner, M., Jakobi, G., Feicht, E. Bernhardt, M. and Fiscer, A. (2005), 'Elevated NH_3 and NO_2 air concentrations and nitroden deposition rates in the vicinity of a highway in Southern Bavaria.', *Atmospheric Environment* 39, 4531–4542.

Lamsal, L. N., Martin, R. V., van Donkelaar, A., Celarier, V., Bucsela, E. J., Boersma, K. F., Dirksen, R., Luo, C., and Wang, Y (2010), Indirect validation of tropospheric nitrogen dioxide retrieved from the OMI satellite instrument: Insight into the seasonal variation of nitrogen oxides at northern midlatitudes, *J. Geophys. Res*., 115, D05302, doi:10.1029/2009JD013351.

Lehmann, C.M.B., V.C. Bowersox, and S.M. Larson (2005), Spatial and Temporal Trends of Precipitation Chemistry in the United States, 1985-2002. *Environmental Pollution*, 135:347-361.

Levy, H., II, et al., (1996), A global three-dimensional time-dependent lightning source of tropospheric NOx, *J. Geophys. Res.*, 101, 22,911 – 22,922,

Li, B.S. Lollar, H. Li, U.G. Wortmann, G. Lacrampe-Couloume., (2012), Ammonium stability and nitrogen isotope fractionations for NH4 –NH3(aq)–NH_3(gas) systems at 20–70 C and pH of 2–13: Applications to habitability and nitrogen cycling in low-temperature hydrothermal systems. *Geochimica et Cosmochimica Acta* 84 280–296

Li, D., and X. Wang (2008), Nitrogen isotopic signature of soil-released nitric oxide (NO) after fertilizer application, *Atmospheric Environment*. *42*, 4747-4754.

Mann, C. Reseeding the green revolution. (1997), *Science*. 277:1038–1043

Marland G., T. A. Boden, R. J. Andres, (2008), Trends: A Compendium of Data on Global Change (Oak Ridge National Laboratory, U.S. Department of Energy, Oak Ridge, TN.

Maryland Department of Transportation data (2011)

Matsumoto, Rie1; Umezawa, Natsumi; Karaushi, Masafumi; Yonemochi, Shin-Ichi; Sakamoto, Kazuhiko (2006), Comparison of Ammonium Deposition Flux at Roadside and at an Agricultural Area for Long-Term Monitoring: Emission of Ammonia from Vehicles *Water, Air, and Soil Pollution*, Volume 173, Numbers 1-4, pp. 355-371

Maw, S., Johnson, C., Lewis, A., McQuaid, J., (2002),A note on the emission of nitrogen oxides from silage in opened bunker silos. *Environmental Monitoring and Assessment* 74**:** 209–215,

McConnell, J. R., Edwards, R., Kok, G., Flanner, M., Zender, C., Saltzman, E., Banta, J., Pasteris, D., Carter, M., and Kahl, J. (2007), 20th-century industrial black carbon emissions altered arctic climate forcing. *Science* 317**,** 1381–1384

McElroy, M.B, (2002), The atmospheric environment: effects of human activity, Princeton University Press, Princeton, New Jersey.

Michalski, G., Scott Z., Kabiling M. and Thiemens M.. (2003), First measurements and modeling of Delta O-17 in atmospheric nitrate, *Geophys. Res. Lett*., 30(16), 1870, doi:10.1029/2003GL017015.

Moore, H., (1977), The isotopic composition of ammonia, nitrogen dioxide, and nitrate in the atmosphere. *Atmos. Environment. 11*, 1239-1243.

Nonomura, M., Hobo, T., Kobayashi, E., Murayama, T,Satoda, M. (1996), Ion chromatographic determination of nitrogen monoxide and nitrogen dioxide after collection in absorption bottles. *Journal of Chromatography.* 739 301-306

Ogawa (2006), Ogawa NO, NO_2, NO_x and SO_2 Sampling Protocol. Edition 6. June 2006

Park, S., Croteau P., Boering K. A., Etheridge D. M., Ferretti D., Fraser P. J., (2012), Trends and seasonal cycles in the isotopic composition of nitrous oxidesince 1940, *Nature Geosci.*, **5**, 261 – 265, doi: 10.1038/NGEO1421.

Pearson, J., Wells, D. M.; Seller, K. J., Bennett, A., Soares, A., Woodall, J., Ingrouille, M. J. **(**2000), Traffic exposure increases natural ^{15}N and heavy metal concentrations in mosses. *New Phytol. 147*, 317-326.

Perrino, C., Catrambone, M., Di Menno Di Bucchianino, A. and Allegrini, I. (2002), Gaseous ammonia in the urban area of Roma, Italy and its relationship with traffic emissions *Atmospheric Environment*, 36, 5385–5394

Pérez, T., S. E. Trumbore, S. C. Tyler, E. A. Davidson, M. Keller, and P. B. de Camargo (2000), Isotopic variability of N_2O emissions from tropical forest soils. Global Biogeochem. Cycles 14:525-535.

Pope III, C. A. and Dockery, D. W (2006), Health Effects of Fine Particulate Air Pollution: Lines that Connect, J. AirWaste Manage., 56, 709–742,

Pulchaski Sather, M.E., Walker, J.T., Lelunann, C.M.B., Gay, D.A., Mathew, J., Robarge, W.P., (2011), Passive ammonia monitoring in the United States: Comparing three different sampling devices *J. Environ. Monit*., 13, 3156

Rabalais, N.N., Turner, R.E., Scavia, D. (2002), Beyond science into policy: Gulf of Mexico hypoxia and the Mississippi River. *Bioscience* 52, 129–142.

Röthlisberger, R., Hutterli, M. A., Sommer, S., Wolff, E. W., and Mulvaney, R., (2002), Nitrate in Greenland and Antarctic ice cores: a detailed description of post-depositional processes. *Ann. Glaciol*. 35, 209–216

Redling, K.M.; Elliott, E.M. (2009), "Isotopic Investigation of Reactive Nitrogen Deposition Along a Highway Road Gradient." *Submitted Biogeochemistry*

Reis, S., Pinder, R. W., Zhang, M., Lijie, G., and Sutton, M. A. (2009), Reactive nitrogen in atmospheric emission inventories, *Atmos. Chem. Phys.*, 9, 7657–7677

Roadman, M., J. Scudlark, J. Meisinger, and W. Ullman (2003), Validation of Ogawa passive samplers for the determination of gaseous ammonia concentrations in agricultural settings, *Atmospheric Environment*, 37, 2317-2325.

Rogers, P.C., Moore, K. & Ryel, R. (2009), Aspen succession and nitrogen loading: a case for epiphytic lichens as bioindicators in the Rocky Mountains, USA. *Journal of Vegetation Science*, 20: 498–510.

Sather, M.E., Mathew, J., Nguyen, N., Lay, J., Golod, G., Vet, R., Cotie, J. and Geasland, F. (2008), Baseline Ambient Gaseous Ammonia Concentrations in the Four Corners Area and Eastern Oklahoma, USA. *J. Environ. Monit.* 10: 1319–1325.

Savarino, J., Kaiser, J., Morin, S., Sigman, D., Thiemens (2007), Nitrogen and oxygen isotopic constraints on the origin of atmospheric nitrate in coastal Antarctica, *Atmos. Chem. Phys*., 7(8), 1925–1945.

Schulz, H., Gehre, M., Hofmann, D. and Jung, K (2001), Nitrogen isotope ratios in pine bark as an indicator of N emissions from anthropogenic sources, Environmental Monitoring and Assessment, 69: 283–297

Schumann, U., Huntrieser, H. (2007), The global lightning-induced nitrogen oxides source. *Atmos. Chem*. Phys. 7, 3823–3907.

Shearer, G., and D. H. Kohl. (1988), Nitrogen isotopic fractionation and 18O exchange in relation to the mechanism of denitrification of nitrite by *Pseudomonas stutzeri*. J. Biol. Chem. 263:13231–13245.

Siefert, R.L., Scudlark, J.R., Potter, A.G., Simonsen, K.A., Savidge, K.B. (2004), Characterization of atmospheric ammonia emissions from a commercial chicken house on the Delmarva Peninsula. *Environmental Science and Technology*. 38(10): 2769-2778.

Sigman, D. M.,. Casciotti, K. L., Andreani, M., Barford, C., Galanter, M., Bohlke, J. K. (2001), A bacterial method for the nitrogen isotopic analysis of nitrate in seawater and freshwater, *Anal. Chem.*, 73(17), 4145 – 4153

Skinner, R.A., Ineson P, Jones HE, Sleep D, Theobald M., (2006), Sampling systems for isotope-ratio mass spectrometry of atmospheric ammonia. *Rapid com. Ms.* 20: 81–88

Skinner, R.A., Ineson, P., Hicks, W.K., Jones, H.E., Sleep, D., Leith, I.D., Sheppard, L.J., (2004), Correlating the spatial distribution of atmospheric ammonia with δ15N at an ammonia release site. *Water, Air, and Soil Pollution*, Focus 4: 219–228.

Smil, V. (2001), *Enriching the Earth*. MIT Press, Cambridge, Massachusetts. 640 pp.

Sutton M.A., Dragosits, U., Hellsten, S., Place, C.J., Dore, A.J., Tang, Y.S., van Dijk, N., Love, L., Fournier N., Vieno, M., Weston, K.J., Smith R.I., Coyle, M., Roy, D., Hall, J., and Fowler, D (2004), Ammonia Emission and Deposition in Scotland and Its Potential Environmental Impacts. *The Scientific World Journal*, 4, 795–810 ISSN 1537-744X; DOI 10.1100/tsw.2004.130

Srivastava, R.K., Hall, R.E., Khan, S., Culligan, K., Lani, B.W.., (2005), Nitrogen oxides emission control options for coal-fired electric utility boilers. *Journal of the Air & Waste Management Association*. 55, 1367.

Tang, Y.S., Cape, J.N., Sutton, M.A., (2001), Development and types of passive samplers for monitoring atmospheric NO_2 and NH_3 concentrations. *The Scientific World* 1, 513-529.

Tang, Y.S., van Dijk, N., Sutton, M.A. (2009), Operation Manual for the CEH ALPHA (Adapted Low-cost Passive High Absorption) sampler. Centre for Ecology & Hydrology Edinburgh Research Station Bush Estate, Penicuik, Midlothian, EH26 0QB, Scotland.

Thibert E and Domine F (1998), Thermodynamics and kinetics of the solid solution of HNO_3 in ice. *Journal of Physics, Chemistry and Biology* 102: 4432–4439.

Townsend, A. R., & Howarth, R. W. (2010), Fixing the global nitrogen problem. *Scientific American*, 302, 64e71.

UK National Ammonia Monitoring Network (2009), Centre for Ecology & Hydrology (CEH). SID 5 Research Final Report.

UN World Population Prospects: The 2010 Revision (2010)

USDA, (2012), OPE3 website, (http://hydrolab.arsusda.gov/ope3/ October 2012

US Department of Commerce 1975. (1975), Historical Statistics of the United States: Colonial times to 1970. Washington, DC.

US Department of Commerce Census 1970-2010. (2010), http://www.census.gov/ March 2010.

US Department of Commerce 1975. (1975), Historical Statistics of the United States: Colonial

U.S. Energy Information Administration / Annual Energy Review 2009. (2009), Table 10.2a Renewable Energy Consumption: Residential and Commercial Sectors, 194 9-2009 DOE/EIA-0384 (August 2010).

US EPA. National air pollutant emission trends, 1900 – 1998

US EPA. (2010), EPA Primary National Ambient Air Quality Standards for Nitrogen Dioxide; Final Rule Federal Register / Vol. 75, No. 26 / Tuesday, February 9, 2010 / Rules and Regulations.

US EPA TRI. *www.epa.gov/TRI/ October 2012.*

Walker, J.T., Aneja, V.P., Dickey, D.A., (2000), Atmospheric transport and wet deposition of ammonium in North Carolina. *Atmospheric Environment* 34, 3407–3418.

Walker, J. T., Robarge,W. P.,Wu, Y., and Meyers, (2006), Measurement of bi-directional ammonia fluxes over soybean using the modified Bowen-ratio technique, *Agric. For. Meteorol*., 138, 54–68.

Walker, J., Spence, P., Kimbrougha, S., and Robarge, W (2008), Inferential model estimates of ammonia dry deposition in the vicinity of a swine production facility, *Atmos. Environ*., 42, 3407–3418,

Wilburn, R. T., and Wright, T.L (2004), SCR ammonia slip distribution in coal plant effluents and dependence on SO3. *Power Plant Chemistry*, 6 (5) 295- 304.

Zhang, L., Altabet, M. A., Wu, T., and O. Hadas (2007), Sensitive measurement of NH4+ 15N/14N (δ15NH4+) at natural abundance levels in fresh and saltwaters. *Anal. Chem*. 79: 5297-5303.